AD NUMBER

AD806835

NEW LIMITATION CHANGE

TO

Approved for public release, distribution unlimited

FROM

Distribution: No foreign.

AUTHORITY

AFRPL ltr., 27 Oct 1971

AFRPL-TR-67-33

INVESTIGATION AND EVALUATION OF MOTOR INSULATION FOR MULTIPLE RESTART APPLICATION

First Phase Report

W. Bradley
Aerojet-General Corporation

TECHNICAL REPORT AFRPL-TR-67-33

January 1967

Rocket Propulsion Laboratory
Research and Technology Division
Air Force Systems Command
Edwards, California

Report AFRPL-TR-67-33

This document is subject to special export controls and each transmittal for Foreign Governments or Foreign Nationals may be made only with prior approval of AFRPL (RPPR-STINFO), Edwards, California 93523.

When U.S. Government drawings, specifications, or other data are used for any purpose other than a definitely related Government procurement operation, the Government thereby incurs no responsibility nor any obligation whatsoever, and the fact that the Government may have formulated, furnished, or in any way supplied the said drawings, specifications, or other data, is not to be regarded by implication or otherwise, or in any manner licensing the holder or any other person or corporation, or sell any patented invention that may in any way be related thereto.

Report AFRPL-TR-67-33

INVESTIGATION AND EVALUATION OF MOTOR INSULATION FOR MULTIPLE RESTART APPLICATION

First Phase Report

W. Bradley

Period Covered: 2 May 1966 through 15 January 1967

AEROJET-GENERAL CORPORATION 5817T
A SUBSIDIARY OF THE GENERAL TIRE & RUBBER COMPANY

FOREWORD

This technical phase report covers all work performed under Contract AF 04(611)-11609 from 2 May 1966 to 15 January 1967. The manuscript was released on 23 January 1967 for publication as a RTD Technical Report.

This contract with the Research and Technology Operations of the Aerojet-General Corporation, Sacramento, California, is being accomplished under the technical direction of Lt. R. Schoner (RPMC), Air Force Flight Test Center, Rocket Propulsion Laboratory, Edwards Air Force Base, California, 93523.

W. Bradley is the project manager for this program. Contributions in the area of material properties were made by A. A. Stenersen and Dr. J. DeAcetis. The experimental work pertaining to the pyrolysis of the virgin materials was conducted by Dr. G. R. Tichelaar and L. M. Wurzer. Design and fabrication of the Correlation Motors was coordinated by J. Nicholson. Work relating to the effect of heat soaking and thermal cycling on insulation-case bonds was conducted by S. Orchon.

Publication of this report does not constitute Air Force approval of the report's findings or conclusions. It is published only for the exchange and stimulation of ideas.

ABSTRACT

The primary purpose of this program is to investigate the properties and behavior of elastomeric insulation materials during multiple restart conditions and the influence of these properties on materials performance.

During the first phase of work, tests were conducted to determine the thermal, chemical, physical, and structural properties of five representative materials for correlation at a later date with motor performance. Designs, test firings, and performance analyses were completed for the three correlation motors (single pulse, two pulse, and three pulse). The effects of heat soaking and thermal cycling on the lap shear strengths of insulation-case bonds were determined.

TABLE OF CONTENTS

APPENDIXES

FIGURE LIST

FIGURE LIST (cont.)

FIGURE LIST (cont.)

FIGURE LIST (cont.)

FIGURE LIST (cont.)

FIGURE LIST (cont.)

FIGURE LIST (cont.)

APPENDIX I FIGURE LIST

APPENDIX II FIGURE LIST

BLANK PAGE

SECTION I

INTRODUCTION

This program was initiated under the sponsorship of the Air Force Rocket Propulsion Laboratory. The primary objective was to investigate the properties and behavior of elastomeric insulation during transient (heating and cooling) and steady-state heating conditions, and the influence of these properties on materials performance. A second objective was to develop a technique for predicting insulation performance for any stop-start duty cycle.

The program was divided into the following three phases of work:

Phase I, Laboratory Investigations
Phase II, Analytical Study
Phase III, Verification Testing

The purpose of Phase I, Laboratory Investigations, was to (1) determine the properties of elastomeric insulation that exert the greatest influence on performance; (2) establish which available compositions exhibit the best performance; and (3) determine what insulation ingredients affect performance.

The purpose of Phase II, Analytical Study, was to develop an analytical technique for predicting insulation performance in a multistart environment.

The purpose of Phase III, Verification Testing, was to verify the performance predicted for the best materials determined in Phase I by test firing three motors.

The initial work on this program was described in Quarterly Report AFRPL-TR-66-246. The reporting schedule has since been revised to phase-type reports. This report, the first phase report, covers the tasks completed from 2 May 1966 to 15 January 1967. It contains some of the work reported in the first quarterly to provide clarity.

SECTION II

SUMMARY

This report presents the results of progress made during the period from 2 May 1966 to 15 June 1967, under Contract AF 04(611)-11609 and includes the following:

A. PROPERTIES OF MATERIALS

The 15 commercially available elastomeric insulation materials listed in Figure 1 were selected for evaluation in the program. Thermal, chemical, physical, and structural properties have been determined on five representative materials (GenGard V-44, GenGard V-62, 40SA40, SMR 81-8 and 9790 V1-126K). Three material conditions were investigated: virgin, heat-soaked virgin, and char formed at high pressure and high temperature. These data will be correlated at a later date with motor performance to determine the properties that most significantly affect performance. These properties will then be determined on the remaining ten materials.

B. CORRELATION MOTOR FIRINGS

Three correlation motors--a single pulse (34.7 sec), a two pulse (17.7 and 17.1 sec) and a three pulse (10.7, 10.9 and 10.6 sec)--were successfully test fired using end burning, cartridge-loaded ANB 3066 propellant and a nominal operating pressure of 700 psi. The resulting data indicated that, of the five materials tested (V-44, V-62, 40SA40, SMR 81-8 and 9790 V1-126K), the V-62 and 9790 V1-126K performed the best in the single pulse motor. In the multipulse motor, the V-62 performed the best at the lower mass flux levels while V-44 was the best at the higher mass flux levels. The three motor firings also demonstrated that the five materials had higher ablation and regression rates in the multipulse firings than in the single pulse.

C. EFFECT OF HEAT SOAKING AND THERMAL CYCLING IN INSULATION-CASE BONDS

Lap shear testing was conducted on five insulation-adhesive combinations to evaluate insulation-case bond integrity under heat soaking and thermal cycling environments. Heat soaked specimens were subjected to 5- and 30-min soak periods at 250°F while the thermal cycling specimens were subjected to single and ten cycles of -65 to 250 to -65°F. In general, no significant difference in strength was noted as a result of heat soak or thermal cycling. However, the strengths of the thermal cycled specimens were considerably lower when tested at 250°F than when tested at -65°F.

SECTION III

TECHNICAL DISCUSSION

The scope of the work discussed in this report includes: (1) determining the thermal, chemical, physical, and structural properties of five elastomeric insulation materials; (2) conducting three pulse motor test firings for the purpose of obtaining performance data that can be correlated against properties; and (3) determining the effect of heat soaking and thermal cycling on insulation-case bonds.

A. PROPERTIES OF FIVE MATERIALS (TASK A, PHASE I)

1. Materials Selection

Commercially available elastomeric insulation materials have been reviewed for use in the program. Fifteen materials were selected for evaluation, reflecting present experience in large solid rocket boosters, operational solid rockets, and developmental controllable rocket motors. These 15 materials were divided into five general composition groups, as shown in Figure 1. One material from each group was selected for investigation in this task. These materials, which are considered to be representative of their groups, are as follows:

Material Class	Material Designation	Supplier
NBR	Gen-Gard V-44	General Tire & Rubber
SBR	Gen-Gard V-62	General Tire & Rubber
Urethane	40SA40	American Polytherm
Butyl	SMR 81-8	Stoner Rubber Co.
EPR	9790V1-126K	General Tire & Rubber

2. Determination of Properties of Representative Materials

a. Properties and Specimen Conditions

The properties determined on the five representative materials are shown in Figure 2. Specimens were prepared in the following three conditions:

(1) Virgin material, as-received.

(2) Virgin material after exposure to a simulated heat-soak temperature at ambient pressure to represent the soak period after each of the first two pulses.

(3) Char formed by a high pressure, high heat-flux exposure of virgin material.

Material Code	Elastomer	Filler	Supplier
NBR Class			
Gen-Gard V-44	Butadiene-Acrylonitrile	Asbestos-Silica	General Tire & Rubber Co.
H-356	NBR-Phenolic	Inorganic Hydrate	B. F. Goodrich
MX-4737	NBR-Phenolic	Silica	Fiberite Corp.
US 3800 (Mod)	Low Temperature NBR-Phenolic	Boric Acid	U. S. Rubber Co.
Gen-Gard V-50	Low-Temperature NBR	Silica-Asbestos	General Tire & Rubber Co.
Gen-Gard V-51	Low-Temperature NBR	Silica	General Tire & Rubber Co.
Gen-Gard V-61	Epoxy-Polysulfide NBR	Asbestos	General Tire & Rubber Co.
850-18C	PBAN-Epoxy (Trowelable)	Asbestos Carbon Black Potassium-Titanate Antimony-Trioxide	Aerojet-General Corp.
SBR Class			
Gen-Gard V-62	SBR-Phenolic	Silica	General Tire & Rubber Co.
Urethane Class			
40SA 2	Urethane	Silica Potassium-Titanate	American Polytherm Co.
40SA 40	Urethane	Silica Potassium-Titanate	American Polytherm Co.
Butyl Class			
SMR 81-8	Butyl	Asbestos-Silica	Stoner Rubber Co.
SMR 31-15	Butyl	Asbestos Potassium-Titanate Silica	Stoner Rubber Co.
EPR Class			
9790VI-126K	Ethylene-Propylene	Silica	General Tire & Rubber Co.
USR 3804	Ethylene-Propylene	Silica	U. S. Rubber Co.

Figure 1. Prospective Elastomeric Materials

Virgin Material

Kinetic Studies (TGA)

Differential Thermal Analysis (DTA)

Density

Thermal Conductivity

Heat Capacity

Heat of Combustion

Pyrolysis Gases

Regression Rates

Tensile Strength and Elongation

Virgin Material Heat Soaked

Kinetic Studies (TGA)

Differential Thermal Analysis (DTA)

Density

Thermal Conductivity

Heat Capacity

Heat of Combustion

Pyrolysis Gases

Weight Loss

Tensile Strength and Elongation

Char Layers

Density

Permeability

Pore Spectra

Thermal Conductivity

Heat Capacity

Thermal Expansion

Emissivity

Reflectivity

Shear Strength

Compressive Strength

Tensile Strength

Degradation Products

Density

Heat Capacity

Thermal Conductivity

Viscosity

Heat of Cracking

Heat of Formation

Figure 2. Properties to be Investigated

III, A, Properties of Five Materials (Task A, Phase I) (cont.)

b. Testing of Virgin and Heat-Soaked Virgin Material

In this task, the effect of heat soak on the properties of the virgin material was originally scheduled for determination after heat soaking at a temperature of 500°F for 5 and 30 min under ambient pressure conditions. Preliminary heat-soak tests were conducted using samples of the five types of materials (V-44, V-62, 40SA40, SMR 81-8, and 9790 V1-126K) and indications were that the 500°F temperature was too high. After 30 min of this temperature, there was excessive swelling of the SMR 81-8 material (see Figure 3). The 40SA40 samples became soft and mushy. To determine the exact maximum temperature/soak time criteria that each material could withstand and still be considered as heat-soaked virgin material would have required more program effort and time than considered warranted. Therefore, a decision was made on the basis of the results of the above tests and thermogravimetric (TGA) data to use a 400°F heat-soak temperature for periods of 5 and 30 min in the program. This is the temperature at which weight loss was first noted during the TGA tests, indicating decomposition initiation.

A discussion of the test procedures used in determining the thermal, chemical, physical, and structural properties is given in Appendix I; the results are discussed as follows:

(1) Kinetic Studies (TGA)

The results of TGA tests are shown in Figures 4 through 8. In general, no noticeable effect is seen between virgin and heat-soaked materials. In the case of 40SA40, further analysis and study will be required to justify the behavior of the material heat soaked for 30 minutes, as opposed to the other two 40SA40 material types. As mentioned above, the TGA test results were also used to select a heat-soak temperature for use in the program. A review of the curves indicates that decomposition was essentially initiated at 200°C (400°F).

Apparent chemical kinetic rate equations have been derived (Figure 9) for the virgin and heat-soaked virgin materials (complete composite materials), based upon the linear heating rate to the sample undergoing thermal decomposition and the characteristic shape of each sigmoid TGA curve. The derivation of these rate equations involved the determination of the activation energy, frequency factor, and order of reaction from each particular TGA curve. These apparent rate constants will be used in the analytical model studies in Phase II of the program.

To determine the dependence of heating rates on the degradation of polymeric substances, a thermogravimetric analysis was made on V-44 at 10°C/min, as opposed to the original 20°C/min. Analysis of the 10°C/min data indicates that approximately the same kinetic rate constants were obtained

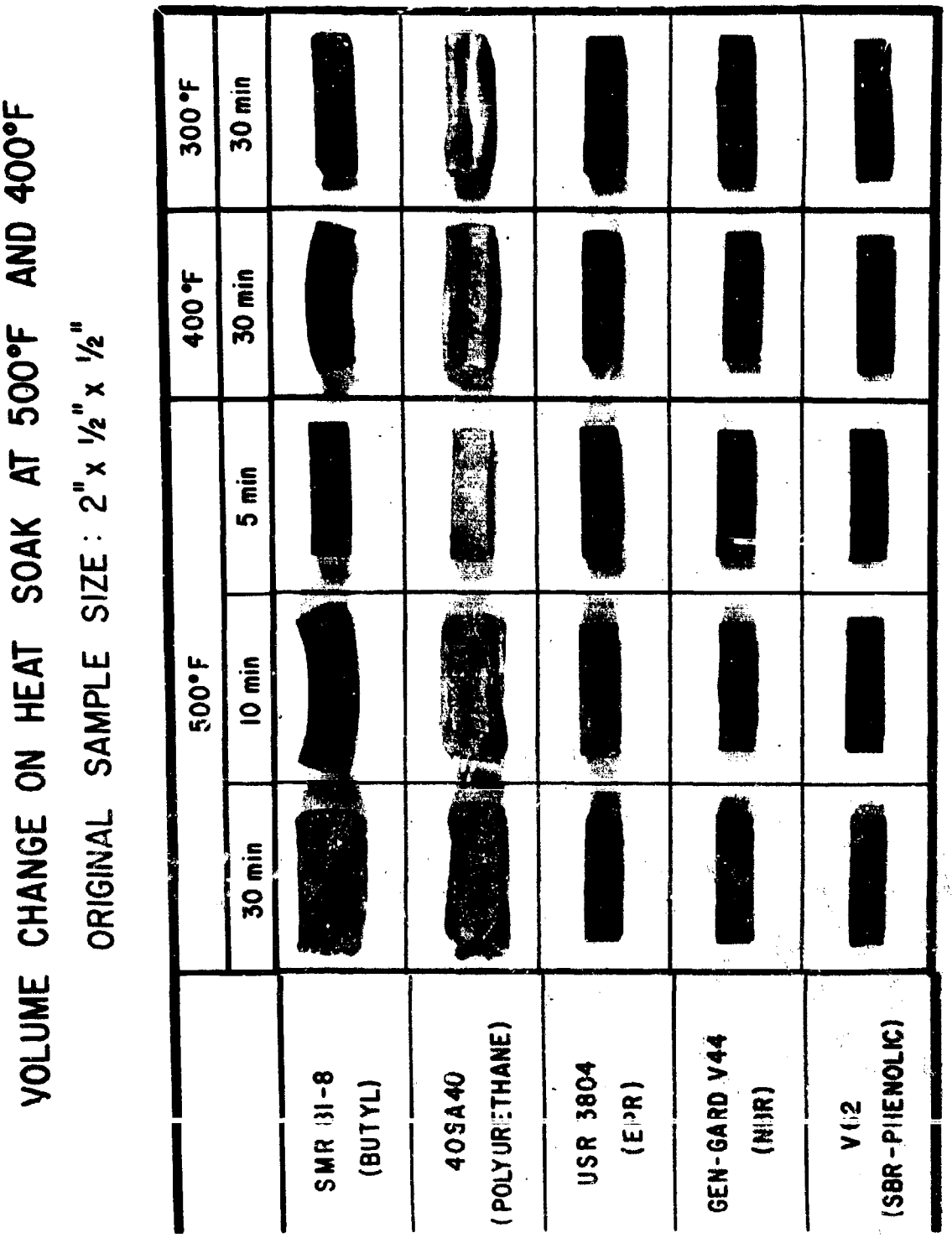

Figure 3. Volume Change on Heat Soak at 500 and 400°F

This Page Intentionally Left Blank

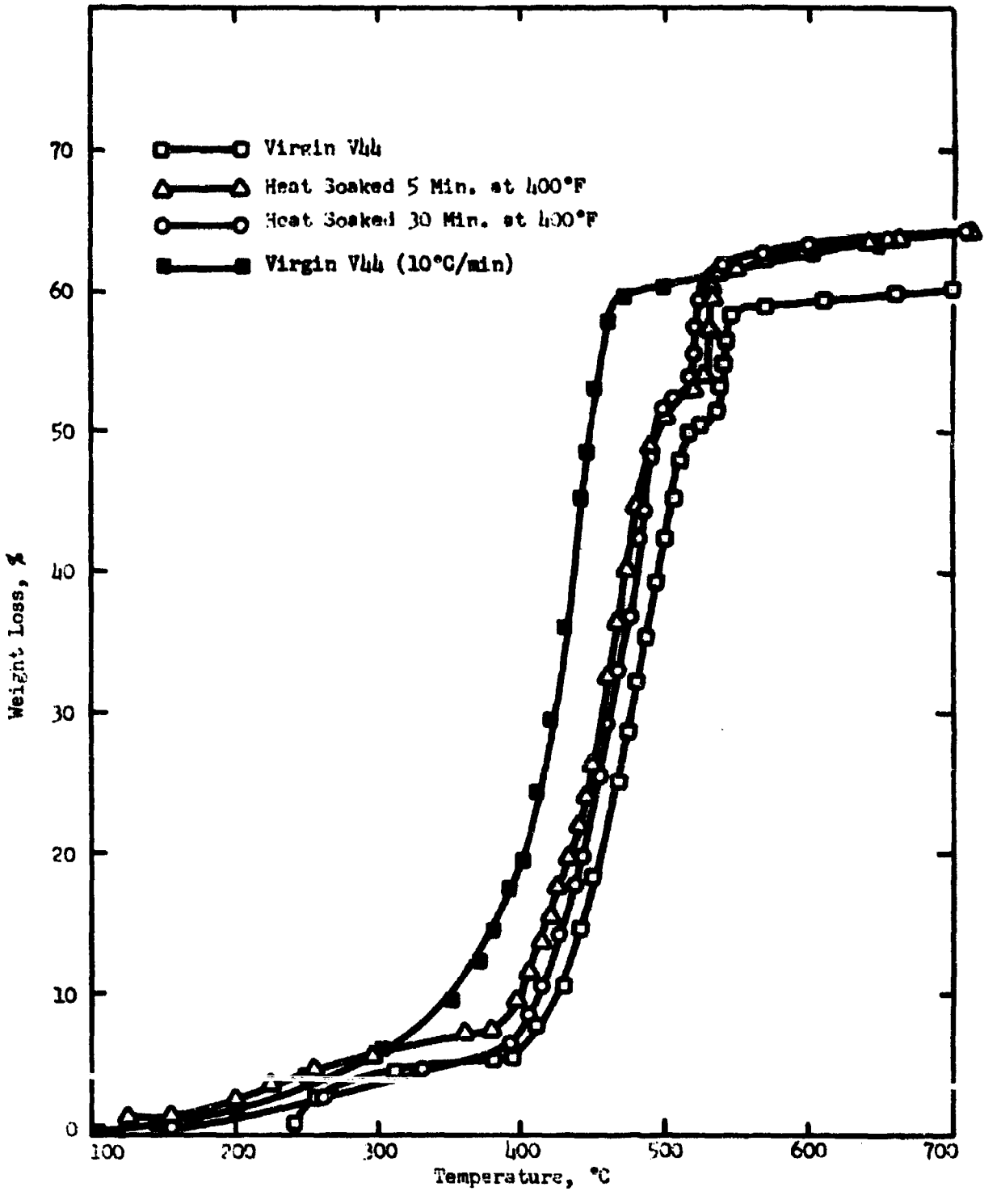

Figure 4. Thermogravimetric Analysis of V-44; Heating Rate: 20°C/min

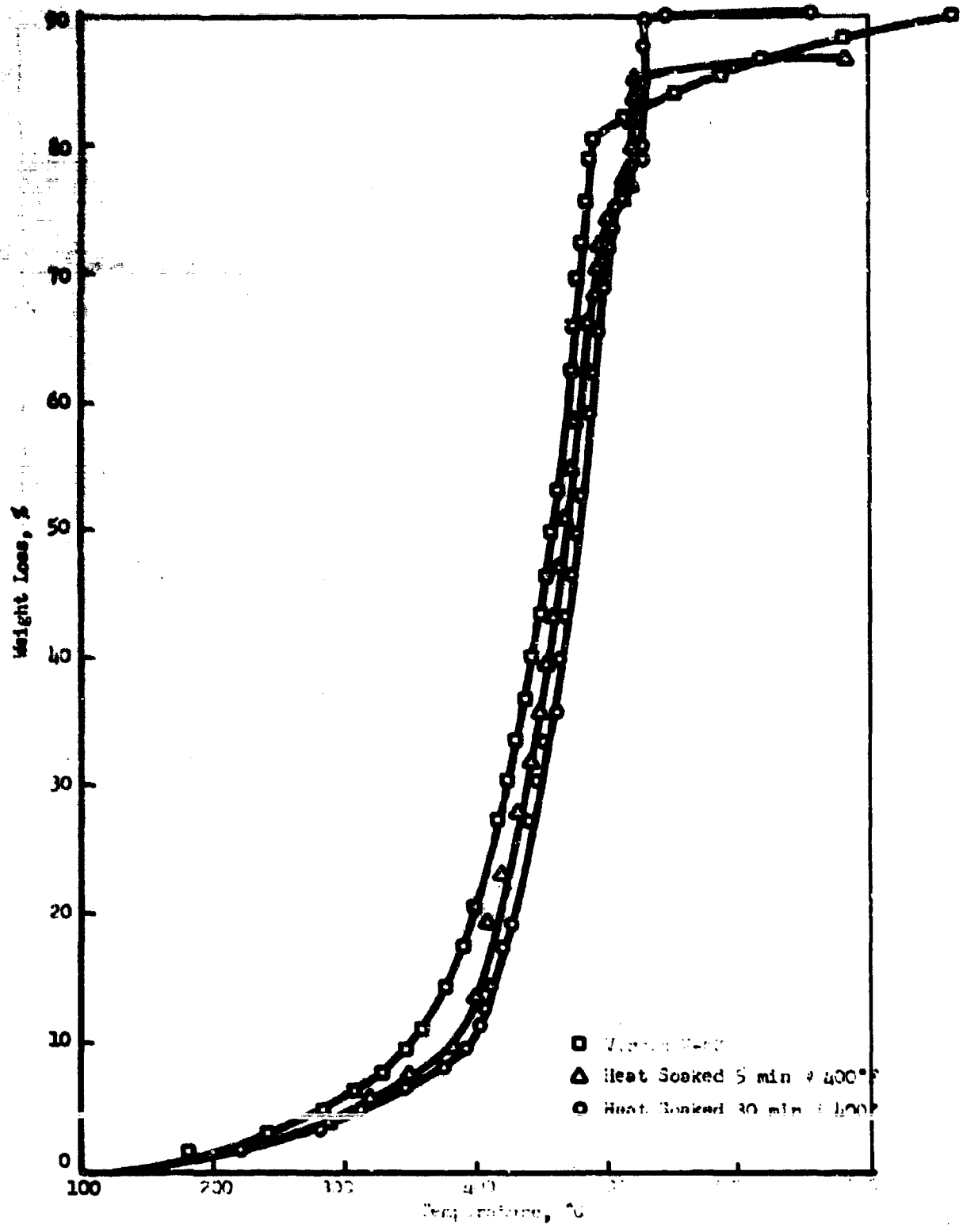

Figure 5. Thermogravimetric Analysis of V-62

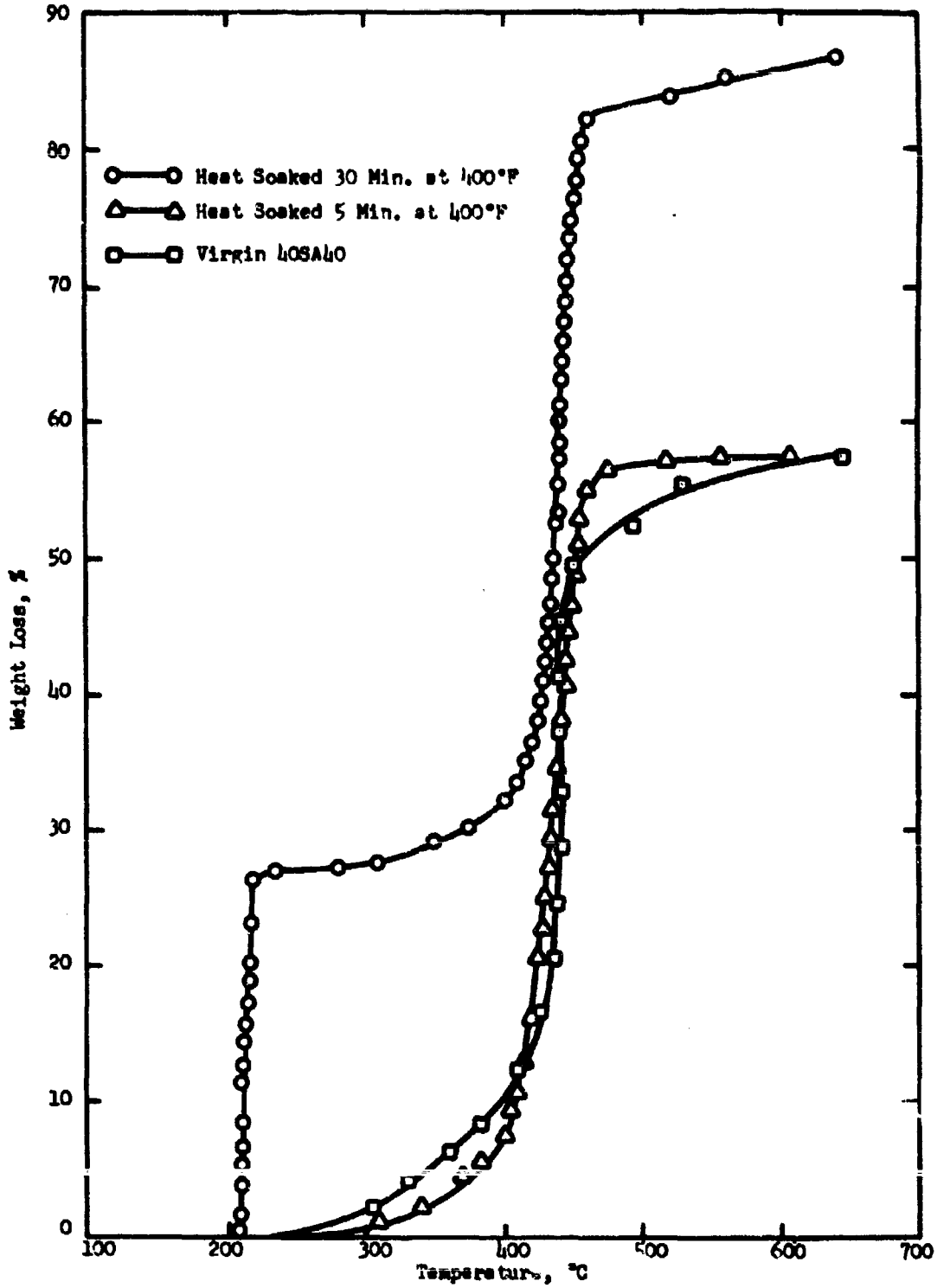

Figure 6. Thermogravimetric Analysis of 40SA40; Heating Rate: 20°C/min

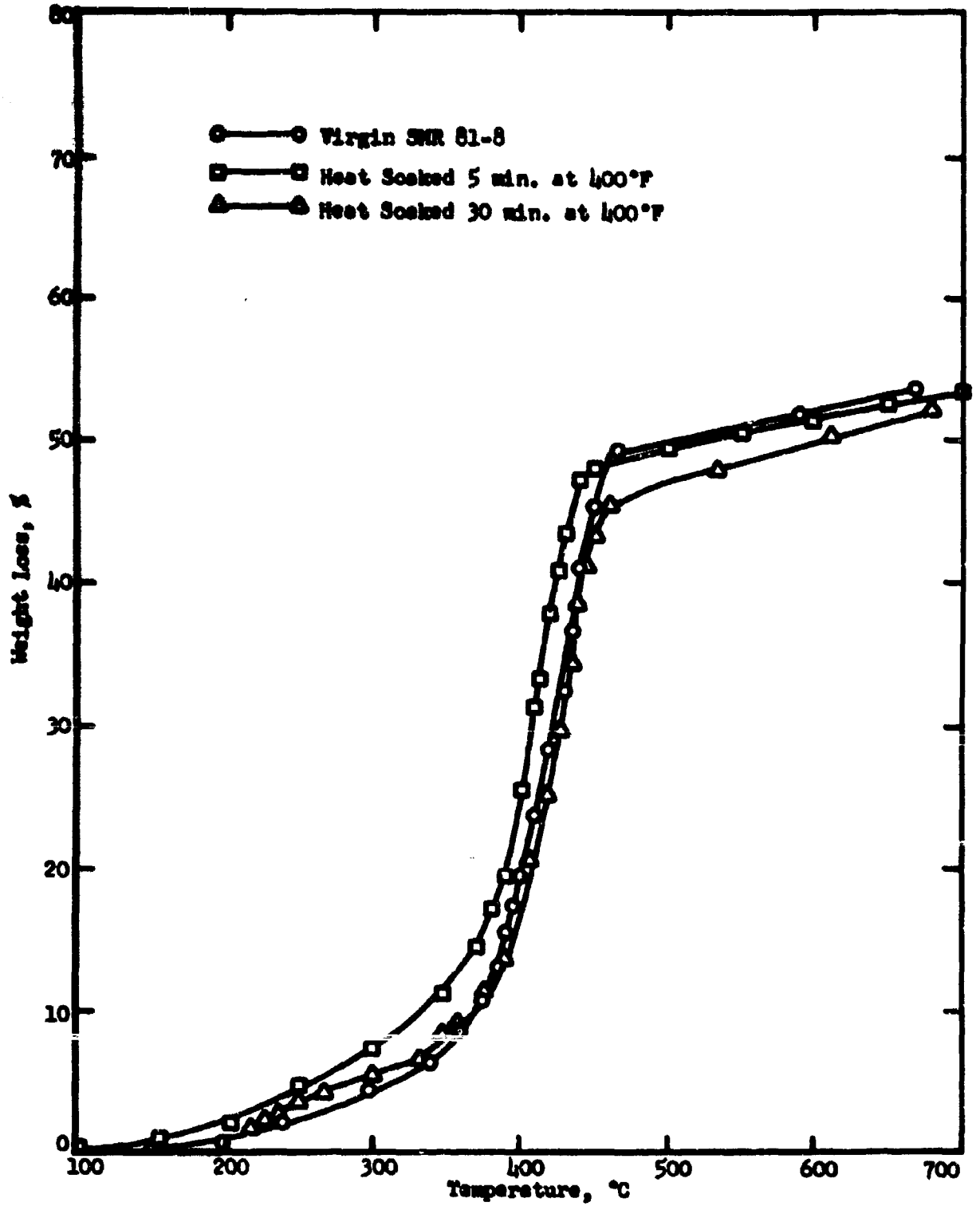

Figure 7. Thermogravimetric Analysis of SMR 81-8; Heating Rate: 20°C/min

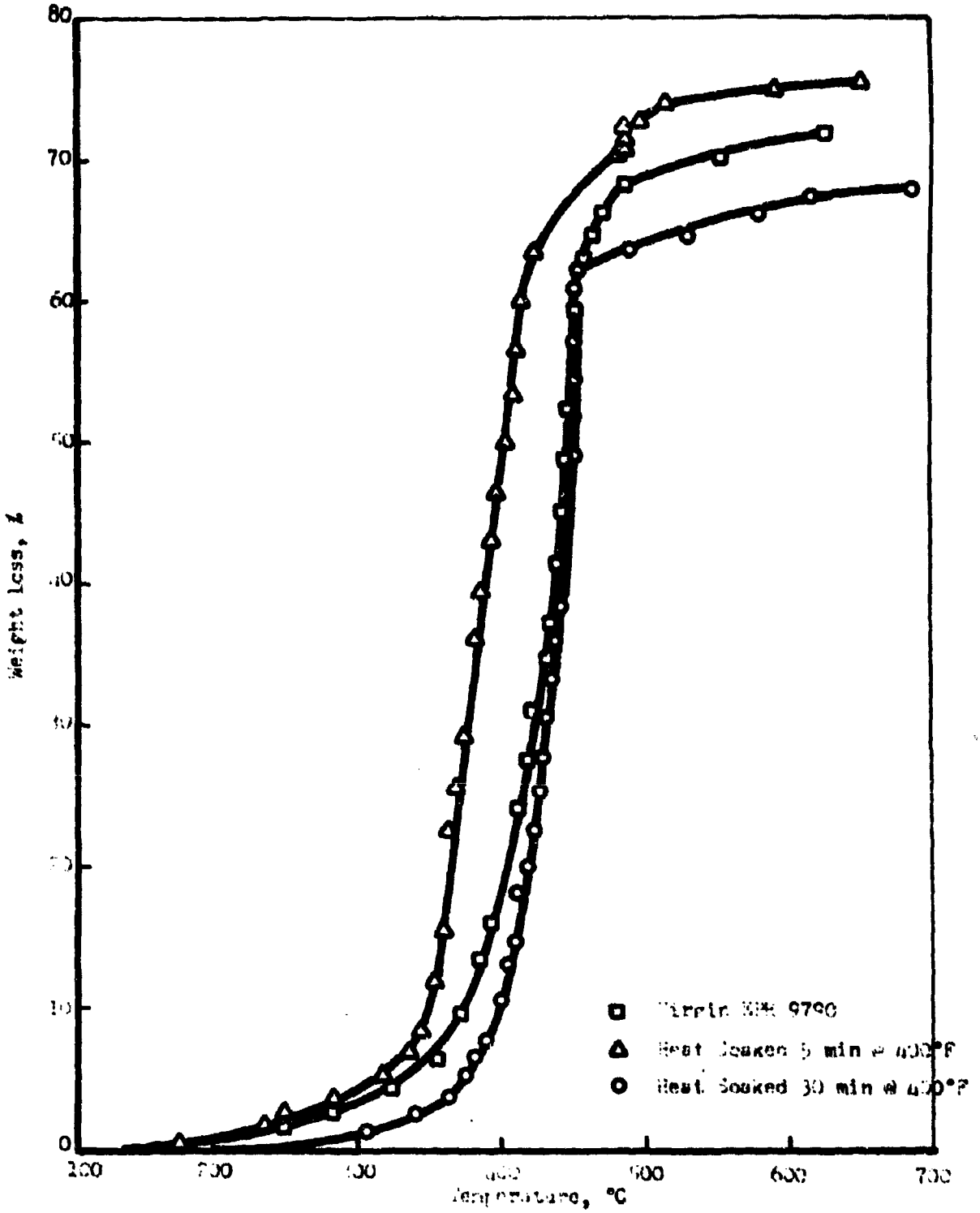

Figure 8. Thermogravimetric Analysis of EPR 9790VI-126K

Material *	Order of Reaction, n	Frequency Factor, A, min^{-1}	Activation Energy, H_a, kcal/gr-mole	Specific Rate Equation r, g/min
Virgin				
V44**	0.912	8.98×10^8	30	$W^{0.912}(8.98 \times 10^8) \exp\left(\frac{-30280}{RT}\right)$
V44	1.155	4.56×10^8	31.76	$W^{1.155}(4.56 \times 10^8) \exp\left(\frac{-31760}{RT}\right)$
9790 V1-126K	1.82	7.26×10^8	32.53	$W^{1.82}(7.26 \times 10^8) \exp\left(\frac{-32530}{RT}\right)$
V-62	1.27	5.12×10^8	31.25	$W^{1.27}(5.12 \times 10^8) \exp\left(\frac{-31250}{RT}\right)$
40SA40	1.12	5.75×10^{62}	203.24	$W^{1.12}(5.75 \times 10^{62}) \exp\left(\frac{-203240}{RT}\right)$
SMR 81-8	1.33	1.064×10^{10}	32.98	$W^{1.33}(1.06 \times 10^{10}) \exp\left(\frac{-32980}{RT}\right)$
5 min Heat Soaked at 400°F				
V44	1.42	2.07×10^9	33.91	$W^{1.42}(2.07 \times 10^9) \exp\left(\frac{-33910}{RT}\right)$
9790 V1-126K	2.15	2.54×10^{12}	41.91	$W^{2.15}(2.54 \times 10^{12}) \exp\left(\frac{-41910}{RT}\right)$
V-62	1.59	6.48×10^{10}	39.41	$W^{1.59}(6.48 \times 10^{10}) \exp\left(\frac{-39410}{RT}\right)$
40SA40	0.94	8.41×10^{15}	51.65	$W^{0.94}(8.41 \times 10^{15}) \exp\left(\frac{-51650}{RT}\right)$
SMR 81-8	1.02	1.57×10^9	29.73	$W^{1.02}(1.57 \times 10^9) \exp\left(\frac{-29730}{RT}\right)$

Figure 9. Apparent Chemical Kinetic Rate Constants of Virgin Material

Material*	Order of Reaction, n	Frequency Factor, A, min^{-1}	Activation Energy, H_a, kcal/gm-mole	Specific Rate Equation r, g/min
30 Min. Heat Soaked at 400°F				
V44	1.19	6.68×10^{8}	31.83	$W^{1.19} (6.68 \times 10^{8}) \exp (\frac{-31830}{RT})$
9790 V1-126K	2.32	1.86×10^{17}	62.16	$W^{2.32} (1.86 \times 10^{17}) \exp (\frac{-62160}{RT})$
V-62	1.56	6.82×10^{8}	33.93	$W^{1.56} (6.82 \times 10^{8}) \exp (\frac{-33930}{RT})$
40SA40-Initial	1.97	1.62×10^{96}	213.9	$W^{1.97} (1.62 \times 10^{96}) \exp (\frac{-213900}{RT})$
40SA40-Primary	0.62	3.22×10^{12}	39.29	$W^{0.62} (3.22 \times 10^{12}) \exp (\frac{-39290}{RT})$
SMR 81-8	0.95	1.41×10^{8}	26.88	$W^{0.95} (1.41 \times 10^{8}) \exp (\frac{-26880}{RT})$

* Complete composite materials - heated at 20°C/min.

** Heated at 10°C/min - this test only.

Figure 9. Apparent Chemical Kinetic Rate Constants of Virgin Material

III, A, Properties of Five Materials (Task A, Phase I) (cont.)

(see Figure 9). The essential difference in the two TGA curves (Figure 4) is that at the lower heating rate, the decomposition range of V-44 is decreased approximately 50°C. Although this information is quite preliminary, some evidence is seen that perhaps even at higher heating rates, similar chemical kinetic rate constants may be observed.

(2) Differential Thermal Analysis (DTA)

The results of the DTA analyses are shown in Figure 10. From this figure, it is seen that, in general, decomposition of the materials produces slightly exothermic reactions over the temperature range of the test. Also, the materials exhibited an endothermic reaction in the temperature range of 400° to 500°C. No apparent test significance can be ascertained.

(3) Density

The density data for the virgin and heat-soaked virgin materials are tabulated in Figure 11 and graphically presented in Figures 12, 13, and 14. These data show that there was no significant effect of the heat soak on the density except in the case of the 40SA40 material when tested at elevated temperatures. These data also show that the SMR-81-8 is the heaviest and the V-62 the lightest material.

(4) Heat Capacity

The heat capacity data are tabulated in Figure 15 and graphically presented in Figure 16. These data show that V-62 and 9790VI-126K have the highest heat capacity, and that heat soaking has a significant effect on the heat capacity of the materials.

(5) Thermal Conductivity

Results of the thermal conductivity tests are shown in Figure 17 and graphically presented in Figure 18. These data were calculated using the following equation:

$$k = \alpha \rho C_p$$

where
- k = thermal conductivity, Btu-in./hr-ft-°F
- α = thermal diffusivity, ft^2/hr
- ρ = density, lb/ft^3
- C_p = specific heat, Btu/lb °F

The specific heats and densities values of the virgin materials were at the same conditions as the thermal diffusivity.

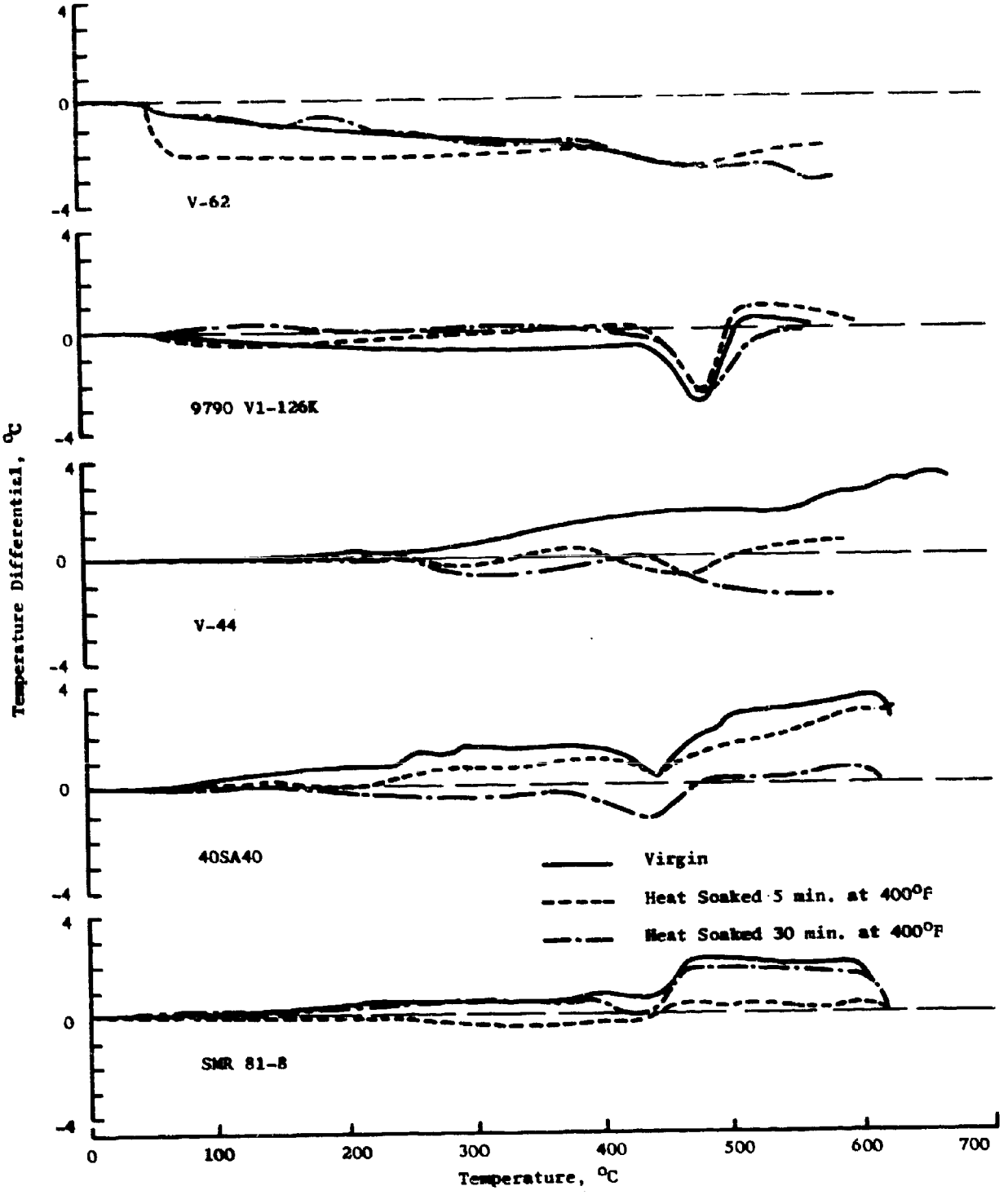

Figure 10. Differential Thermal Analysis

Material Condition		V44	V62	40SA40	SMR 81-8	9790-V1-126K
Virgin						
T_1, °F		100° - 1.267	102° - 1.063	100°-1.337	102°-1.353	102°- 1.091
		1.272	1.063	1.338	1.349	1.093
	Ave.	1.269	1.063	1.338	1.351	1.092
T_2, °F		249° - 1.203	246° - 0.996	242°-1.262	246°-1.286	250°-1.024
		1.204	0.994	1.264	1.288	1.025
	Ave.	1.204	0.995	1.263	1.287	1.025
T_3, °F		300° - 1.206	302° - 1.004	302°-1.266	300°-1.29[illegible]	300°- 1.011
		1.206	0.997	1.261	1.295	1.012
	Ave.	1.206	1.000	1.264	1.294	1.012
5 Min. Heat Soaked @ 400°F						
T_1, °F		100° - 1.276	102° - 1.062	101°-1.260	100°-1.355	102°- 1.091
		1.276	1.061	-	1.352	1.091
	Ave.	1.276	1.062	1.260	1.353	1.091
T_2, °F		249° - 1.201	244° - 0.995	239°-1.182	239°-1.284	250°- 1.024
		1.210	0.997	1.177	1.285	1.028
	Ave.	1.205	0.996	1.179	1.285	1.026
T_3, °F		300° - 1.212	302° - 1.001	295°-1.168	292°-1.291	299°- 1.013
		1.204	0.999	1.067	1.289	1.014
	Ave.	1.208	1.000	1.118	1.290	1.014
30 Min. Heat Soaked @ 400°F						
T_1, °F		100° - 1.272	102° - 1.062	100°-Too	102°-1.358	102°- 1.090
		1.281	1.063	porous to run	1.354	1.090
	Ave.	1.276	1.063		1.356	1.090
T_2, °F		249° - 1.213	248° - 0.997	239°-Melted	239°-1.288	250°- 1.027
		1.207	0.999		1.288	1.025
	Ave.	1.210	0.998		1.288	1.026
T_3, °F		300° - 1.214	302° - 1.004	295°-Melted	295°-1.291	298°- 1.018
		1.210	1.006		1.289	1.025
	Ave.	1.212	1.005		1.290	1.021

Figure 11. Density (gm/cc) of Virgin Materials

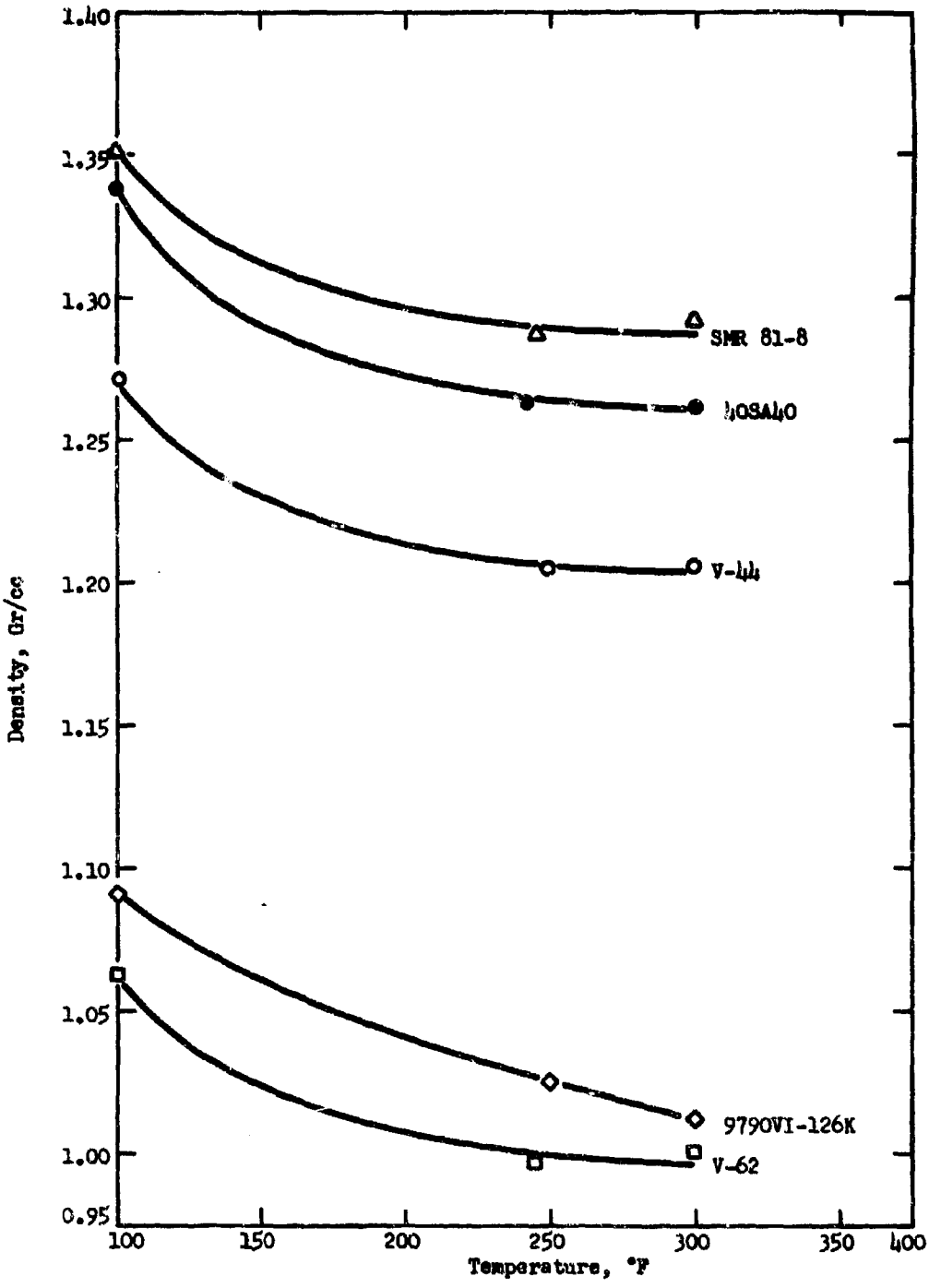

Figure 12. Density of Virgin Materials

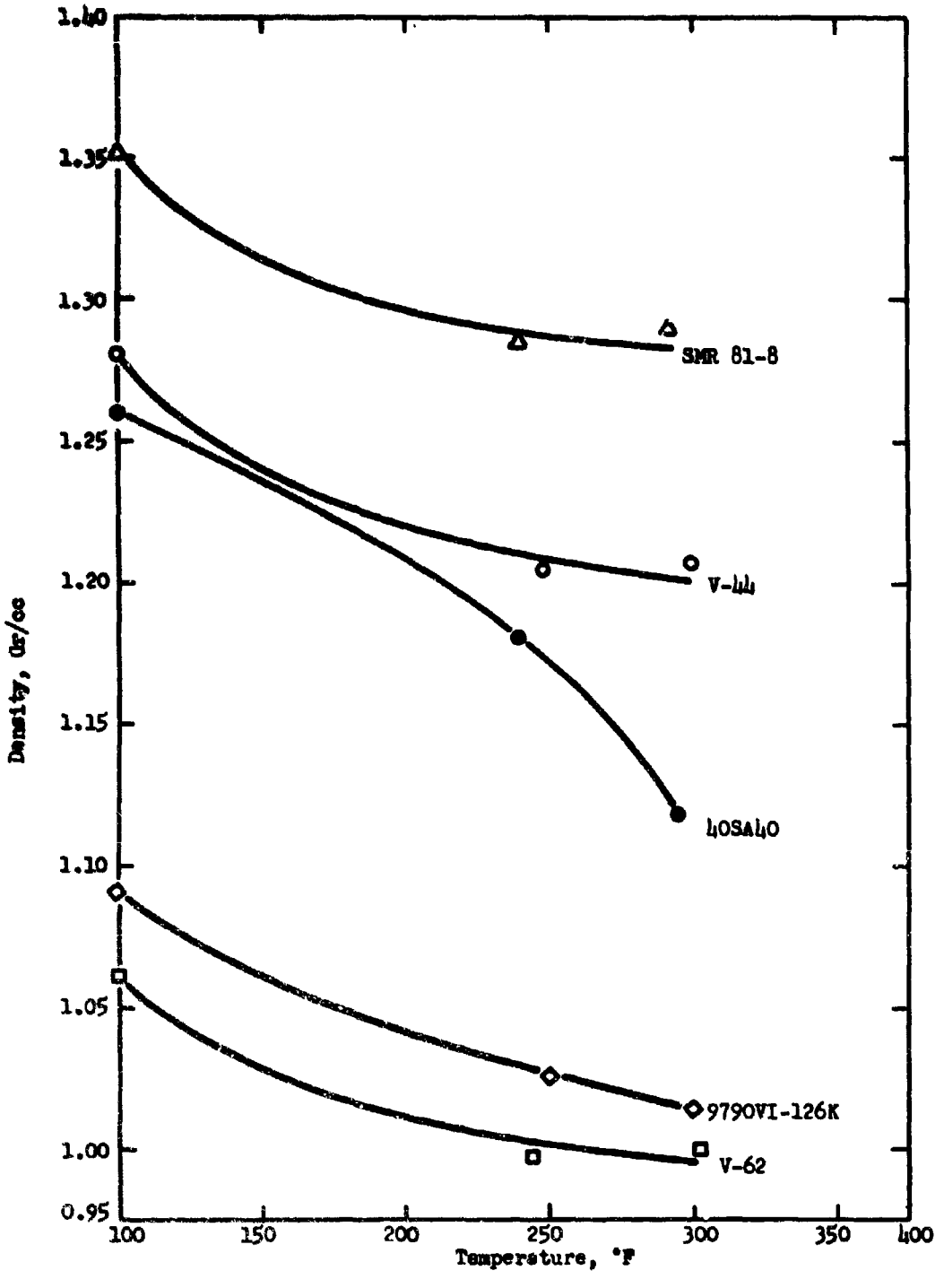

Figure 13. Density of Virgin Materials Heat-Soaked for 5 min at 400°F

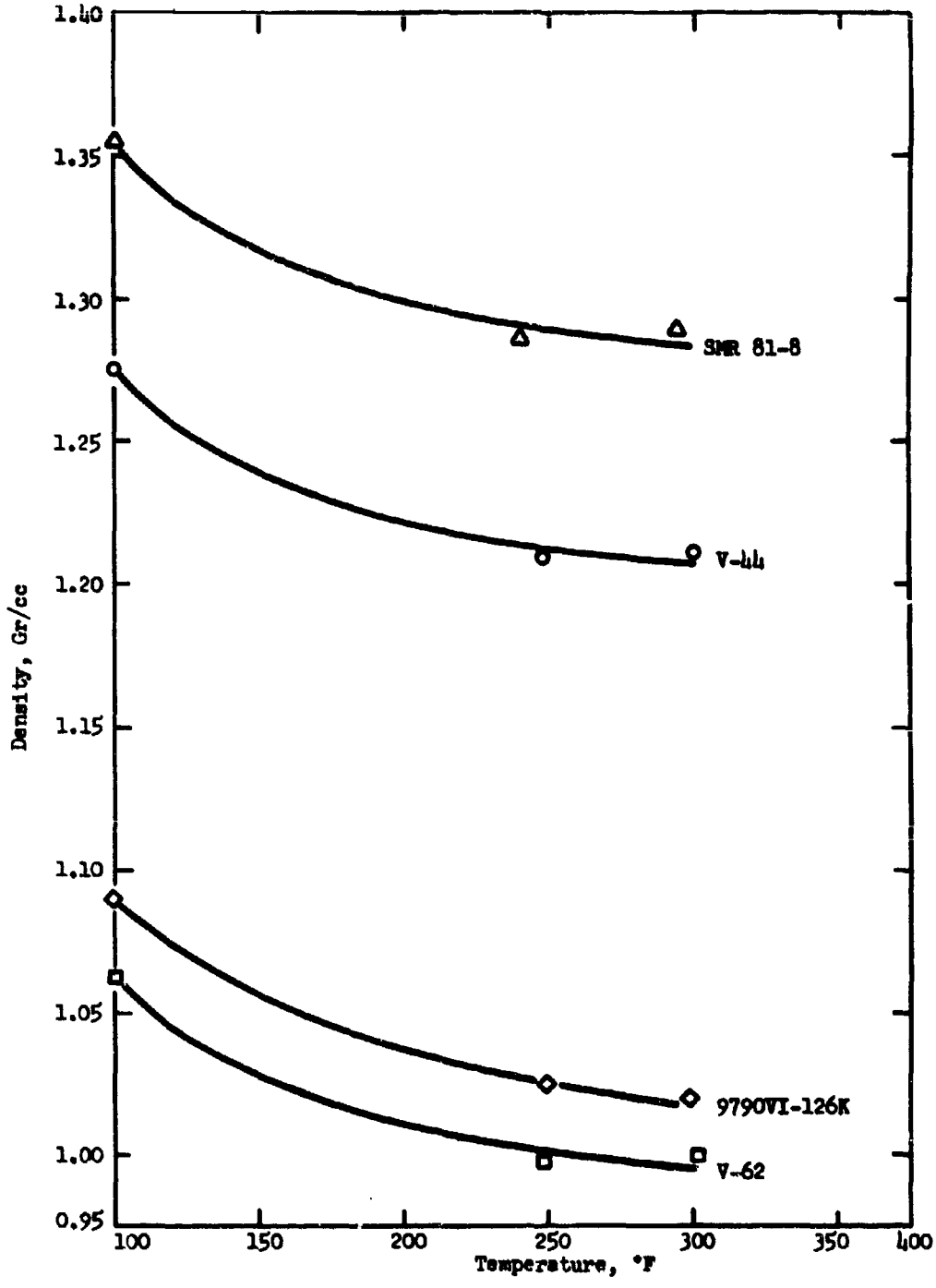

Figure 14. Density of Virgin Materials Heat-Soaked for 30 min at 400°F

Material Condition	V-44	V-62	40SA40	SMR 81-8	9790V1-126K
Virgin					
150°F	0.3987	0.4722	0.3134	0.3245	0.4594
	0.4290	0.4716	0.3084	0.3305	0.4595
Average	0.4139	0.4719	0.3110	0.3275	0.4595
250°F	0.4242	0.4622	0.3936	0.3925	0.4357
	0.4103	0.4486	0.3849	0.3938	0.4313
Average	0.4172	0.4554	0.3892	0.3931	0.4335
300°F	0.4386	0.4419	0.4032	0.4154	0.5088
	0.4203	0.4419	0.3962	0.4267	0.4939
					0.4886
Average	0.4294	0.4419	0.3998	0.4210	0.4971
5 min Heat Soak at 400°F					
150°F	0.3484	0.4679	0.3413	0.3500	0.4711
	0.3435	0.4654	0.3642	0.3776	0.4682
Average	0.3460	0.4666	0.3527	0.3638	0.4696
250°F	0.3450	0.4461	0.3368	0.3553	0.4329
	0.3201	0.4487	0.3358		0.4446
				0.3370	0.4388
Average	0.3326	0.4474	0.3363	0.3461	0.4388
300°F	0.3591	0.4433	0.3696	0.3738	0.4595
	0.3592	0.4593	0.3544	0.3579	0.4501
Average	0.3592	0.4513	0.3621	0.3658	0.4548
30 min Heat Soak at 400°F					
150°F	0.3494	---	Melted	0.2660	0.4681
	0.3731	0.4602		0.2730	0.4606
Average	0.3612	0.4602		0.2695	0.4643
250°F	0.3437	0.4455	Melted	0.2789	0.4517
	0.3734	0.4622		0.2954	0.4496
Average	0.3586	0.4538		0.2872	0.4506
300°F	0.3641	0.4328	Melted	0.3364	0.4483
	0.3635	0.4390		0.3392	0.4885
Average	0.3637	0.4359		0.3379	0.4684

Figure 15. Heat Capacity of Virgin Materials (cal/gm/°C

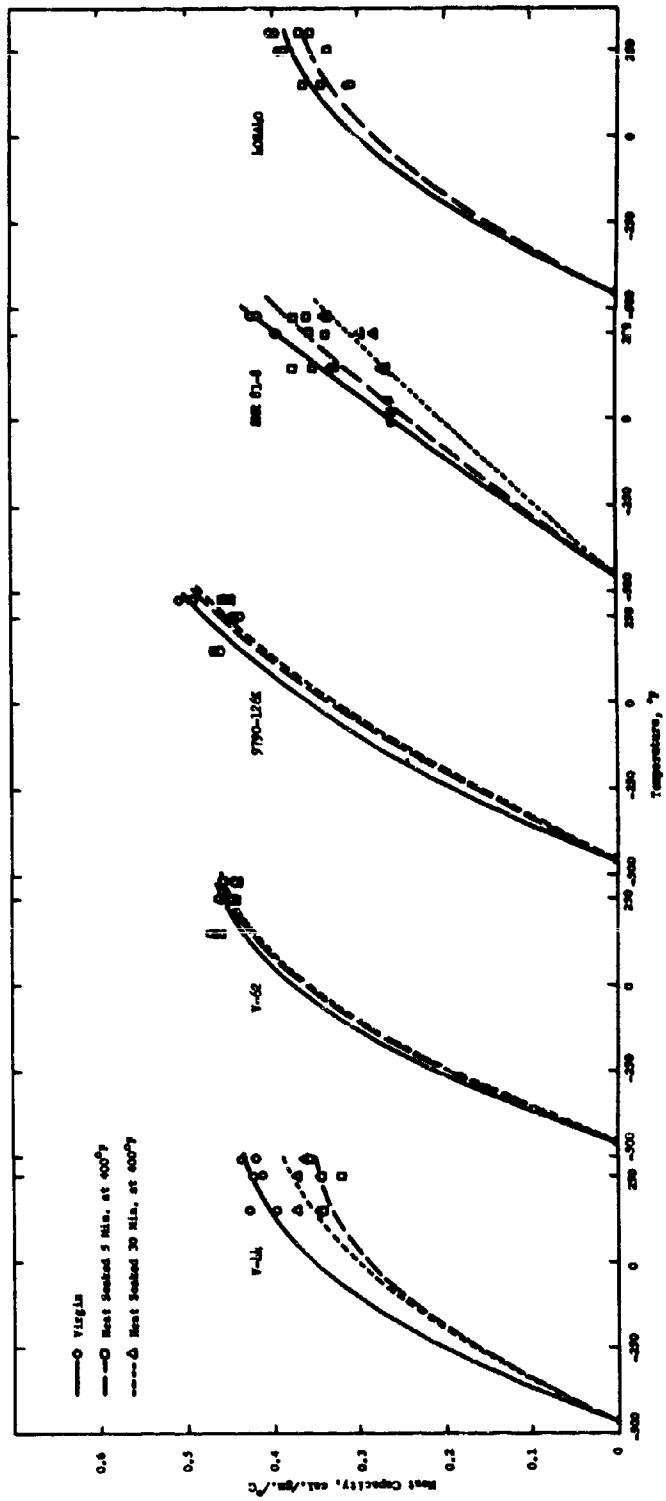

Figure 16. Heat Capacity of Virgin Materials

Material	Temperature, °F	Virgin	Heat-Soaked** 5 min	Heat Soaked 30 min
V-44	RT	1.815	1.267	1.198
	150	2.165	1.081	1.464
	250	1.789	1.058	1.400
V-62	RT	1.348	1.203	1.078
	150	1.084	1.140	1.156
	250	1.090	1.070	1.213
40SA40	RT	2.060	1.514	---
	150	1.980	1.45[illegible]	---
	250	1.935	1.818	---
SMR 81-8	RT	1.157	1.113	0.921
	150	1.421	1.305	1.112
	250	1.450	1.310	1.140
9790V1-126K	RT	1.390	1.108	0.971
	150	1.230	1.350	1.242
	250	1.156	1.191	1.151

*Btu-in./hr-ft^2-°F
**Heat-soaked at 400°F

Figure 17. Thermal Conductivity* of Virgin Materials

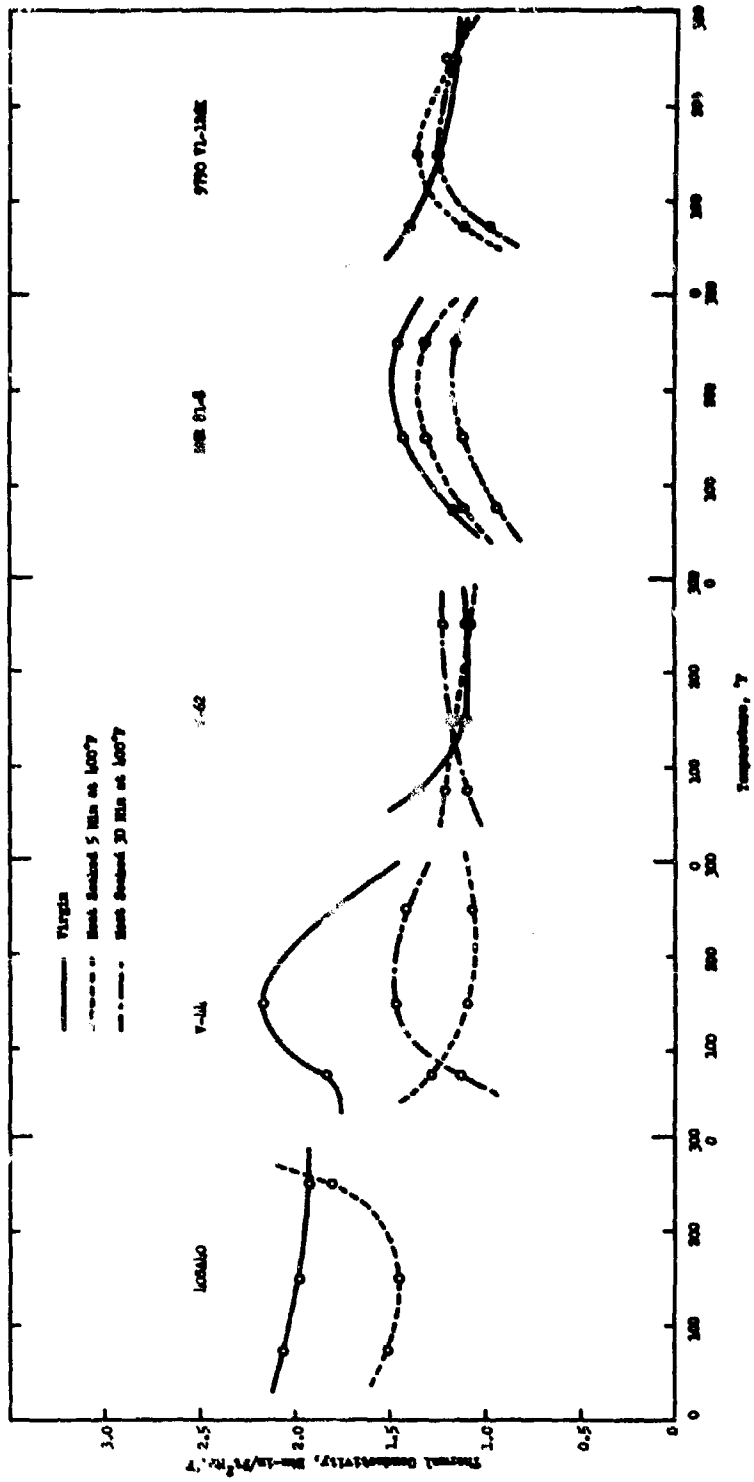

Figure 18. Thermal Conductivity of Virgin Materials

III, A, Properties of Five Materials (Task A, Phase I) (cont.)

The thermal conductivity of the virgin materials, in all cases except for the V-44 and SMR 81-8 materials, decreased with temperature. The thermal conductivity of the heat soaked materials generally increased with temperature and were approximately the same order of magnitude as those for the virgin material. Only in the cases of the 40SA40 and V44 materials were there appreciable differences. The highest conductivity was obtained on the V44 and 40SA40 virgin materials (approximately 2 Btu-in./hr-ft^2-°F). The heat-soaked materials had conductivity values between 1 and 1.5 Btu-in./hr-ft^2-°F.

(6) Heat of Combustion

The heat of combustion test results are given in Figure 19. V-62 has the highest heat of combustion. There appears to be no significant change because of heat soaking.

(7) Tensile Strength and Elongation

The tensile strength and ultimate elongation test results are given in Figure 20. Heat soaking has a significant effect on the tensile strength and elongation, particularly on materials heat soaked for 30 min. All levels, even the low values for the heat-soaked materials, should be satisfactory for the majority of start-stop applications.

(8) Weight Loss

The weight losses occurring during heat soak are shown in Figure 21. These data show that all weight losses are less than 1%. Effects of weight loss of this order on materials performance (regression and ablation rate) are expected to be insignificant.

The ingredients lost on heat soak at 400°F can be water, low molecular weight plasticizers, and other low-molecular weight binder constituents. Since V-44 normally loses from 0.5 to 1.0% water on heating at 300°F, it is apparent that the material lost in V-44 is primarily water. The ingredients lost in V-62, SMR 81-8, 40SA40, and 9790V1-126K on heat soak are also expected to be primarily water.

(9) Regression and Ablation Rates

Regression and ablation rates were determined for all 15 candidate materials rather than just the five representative materials for use in a later task when the best materials will be selected. These rates were obtained by means of plasma arc testing at heat flux levels of 50, 100, and 225 Btu/ft^2-sec using 1/2 diameter specimens, instrumented and shrouded, as discussed in Appendix I. The specimens were subjected to eight heating cycles (15 sec on, 15 sec off) to simulate a multipulse environment.

Material Condition	V-44	V-62	40SA40	SMR 81-8	2790V1-126K
Virgin					
			4750		
	5793	8671	4760	4869	7556
	5852	8596	4716	4863	7542
Average	5822	8633	4742	4866	7549
5 min Heat Soaked at 400°F					
	5794	8672	4790	4801	7552
	---	8719	4826	---	7560
Average	5794	8696	4808	4801	7556
30 min Heat Soaked at 400°F					
	5783	8680	4712	4802	7563
	5766	8689	4741	---	7559
Average	5774	8684	4726	4802	7561

Figure 19. Heat of Combustion of Virgin Materials

	Tensile Strength, psi/ Elongation, %/ Modulus, psi at 77°F				
	V-44	V-62	408A40	SMR 81-8	9790V3-126K
Virgin					
1	1331/430/-	634/750/1970	1091/130/4667	1075/340/2123	2070/800/5700
2	1406/450/1349	649/720/1712	1169/120/5649	673/370/1973	2089/810/4900
3	1610/520/1407	724/750/1684	1118/150/5466	1055/340/2503	1851/780/5300
Average	1446/467/1378	675/740/1789	1126/133/5261	934/350/2200	2003/797/5300
Heat-Soaked 5 min at 400°F					
1	1428/470/1333	542/660/1852	1446/ - /2478	463/490/2249	1431/1000+[1]/2600
2	1638/520/1311	493/650/1941	1768/ 17/1817	474/550/2275	1632/1000+ /2500
3	1463/430/1620	448/510/1858	1538/ 13/2538	628/230/3739	1597/1000+ /2800
Average	1510/473/1421	494/607/1550	1584/ 15/2278	522/423/2754	1553/1000+ /2633
Heat-Soaked 30 min at 400°F					
1	1530/150/2849	441/270/1833	396/ 10/1075	392/170/3412	1080/600/2500
2	1448/140/2396	433/280/1731	677/ 5/1531	304/500/2448	1132/620/1800
3	1508/270/2624	424/240/1868	412/ 5/1598	344/190/2312	1160/640/3500
Average	1495/170/2623	433/263/1811	495/ 7/1401	347/287/2724	1124/620/2600

(1) Specimens exceeded travel limit of Instron tester without breaking. Crosshead speed 20in./min.

Figure 20. Mechanical Properties of Virgin Materials

Material		5 min at 400°F(1) Original Weight, g	Final Weight, g	Weight Loss, g	Weight Loss, %	30 min at 400°F(1) Original Weight, g	Final Weight, g	Weight Loss, g	Weight Loss, %
V-44	1	171.28	170.36	0.82	0.478	169.22	167.84	1.38	0.815
	2	179.21	178.08	1.13	0.632	168.29	166.92	1.37	0.814
Average		175.25	174.22	0.975	0.555	168.75	167.38	1.375	0.8145
V-62	1	141.14	140.68	0.46	0.311	142.83	141.98	0.85	0.595
	2	141.18	140.70	0.48	0.326	140.32	139.40	0.92	0.662
Average		141.16	140.69	0.47	0.318	141.575	140.69	0.885	0.6285
40SA40	1	176.95	176.31	0.64	0.361	175.39	174.58	0.81	0.46
	2	174.31	173.76	0.55	0.315	179.83	179.16	0.67	0.37
Average		175.63	175.035	0.595	0.338	177.61	176.87	0.74	0.415
SMR 81-8	1	179.17	178.51	0.66	0.367	175.71	174.41	1.30	0.740
	2	176.66	175.95	0.71	0.402	177.69	176.37	1.32	0.743
Average		177.815	177.23	0.685	0.385	176.70	175.78	1.31	0.741
9790VI-1 126K	1	150.45	150.05	0.40	0.265	149.59	148.88	0.71	0.475
	2	150.88	150.48	0.40	0.265	150.28	149.56	0.72	0.460
Average		150.66	150.26	0.40	0.265	149.93	149.22	0.715	0.468

(1) 4 in. by 4 in. by ½ in. specimens.
Approximately 20 min required to bring center of specimens up to 400°F.

Figure 21. Weight Loss on Heat-Soak at 400°F

III, A, Properties of Five Materials (Task A, Phase I) (cont.)

Although plasma arc test results do not generally show the same ablation rates encountered in motor firings because reduced surface regression takes place and other degrees of simulation are not close enough, they do provide good qualitative results. In multicycle firings another factor is encountered in comparisor to single pulses; that is the potential loss of char at the initiation of every pulse. With the particular type of specimens used during plasma testing, the char was essentially kept in position by the shrouding. With these considerations in mind, the test results are shown in Figure 22 and further presented in Figures 23 through 25. These data show that, based on plasma arc testing, the four best materials at three heat flux levels would be: (1) V-62, N356, MX 4737 and USR 3804 at a heat flux of 50 Btu/ft^2-sec; (2) N356, USR 3800, MX 4737, and V-62 at 100 Btu/ft^2-sec; and (3) V-62, N356, USR 3800, and USR 3804 at 225 Btu/ft^2-sec.

Temperature-time data were also obtained on the 15 materials at three different thermocouple depths and at the three heat flux levels. These data are shown in Figures 1 through 15 of Appendix II. In order to present more readily comparable data, the above results have been standardized for thermocouple depths of 0.070 and 0.120 and plotted in the form shown in Figures 26 through 30. A dotted line has been added, passing through the average temperature for each cycle and the materials below that line should be among the best candidates.

Each plasma arc specimen was visually examined for type of char, retention of char at the char-virgin interface, and condition of virgin material at interface. As indicated in Figure 31, only in the cases of the N356, MX 4737, 850-15C, USR 3800, 40SA2, and V61 materials was the char-virgin interface intact. In these instances, the plasma arc results should be more quantitatively correct than for those where the interface separated.

c. Determination of Degradation Products

The degradation products of the pyrolyzed virgin materials as determined by mass spectrographic techniques are shown in Figure 32. The temperature used for the pyrolysis was 550°C, as determined from previous thermogravimetric analysis of the virgin materials. Several experiments were run using atomic grade helium at 550°C in vacuum, 0.10 psig, 69.9 psig, 139.7 psig, and 349.3 psig to determine the shift in gas phase chemical composition, if any, with pressure. A pressure of 349.3 psig was determined to be the limiting pressure needed to cause no further measurable change in composition, as denoted by the mass spectrometer. It was also determined that no significant difference (within experimental accuracy and reproducibility) in chemical composition was obtained between the gaseous pyrolysis products obtained from the heat soaked materials and those from virgin pyrolysis products. An example of this comparison is shown in Figure 33 for SMR 81-8 materials.

Material	50 Btu/ft^2-sec Regression Rate[2] mils/sec	50 Btu/ft^2-sec Ablation Rate mils/sec	100 Btu/ft^2-sec Regression Rate mils/sec	100 Btu/ft^2-sec Ablation Rate mils/sec	225 Btu/ft^2-sec Regression Rate mils/sec	225 Btu/ft^2-sec Ablation Rate mils/sec
V44	0.01	1.31	2.00	3.50	2.94	3.68
	0.25	1.29	1.50	2.20	2.67	3.30
Average	0.13	1.30	1.75	2.85	2.80	3.99
9790VI-126K	0.04	1.29	1.37	2.27	2.29	3.56
	0.16	1.37	1.25	2.11	2.50	3.60
Average	0.10	1.33	1.31	2.19	2.40	3.58
V62	-0.21[3]	0.40	1.49	2.56	1.85	2.68
	-0.13	0.58	0.83	1.54	1.95	3.29
Average	-0.17	0.49	1.16	2.05	1.90	2.99
SMR81-8	-0.23	1.87	0.56	3.90	1.15	4.77
	0.01	1.51	0.17	1.91	2.46	3.80
Average	-0.11	1.69	0.37	2.91	1.81	4.29
40SA40	-0.11	1.16	1.04	3.62	3.98	5.56
	0.21	1.55	1.26	3.51	3.72	5.32
Average	0.05	1.35	1.15	3.56	3.85	5.44
V50	0.04	1.56	1.41	2.04	3.79	4.29
	-0.08	1.29	1.87	2.46	2.59	3.17
Average	-0.02	1.43	1.64	2.25	3.19	3.73
V51	0.52	1.00	1.35	2.48	2.29	3.41
	0.43	1.48	1.00	2.22	3.10	3.87
Average	0.47	1.24	1.17	2.35	2.69	3.64
V61	0.08	1.50	2.39	3.79	2.79	3.67
	0.62	2.33	1.83	3.50	3.04	4.29
Average	0.35	1.91	2.11	3.65	2.91	3.98
MX-4737	0.11	0.96	0.15	2.11	1.03	3.40
	0.11	0.99	0.13	1.83	1.04	3.96
Average	0.11	0.98	0.14	1.97	1.04	3.68
40SA2	-0.25	1.10	1.30	2.50	4.42	5.31
	-0.21	1.30	1.17	2.38	4.30	6.63
Average	-0.23	1.20	1.23	2.44	4.36	5.97

(1)Average ablation and regression rates during 8 heating cycles (15 sec on, 15 sec off) at heat flux levels of 50, 100, and 225 Btu/ft^2-sec.

(2)Synonymous with erosion rate.

(3)Negative regression rate is due to expansion in the char or ablation zone during testing.

Figure 22. Plasma Arc Tests[1]

Material	50 Btu/ft^2-sec Regression Rate mils/sec	50 Btu/ft^2-sec Ablation Rate mils/sec	100 Btu/ft^2-sec Regression Rate mils/sec	100 Btu/ft^2-sec Ablation Rate mils/sec	225 Btu/ft^2-sec Regression Rate mils/sec	225 Btu/ft^2-sec Ablation Rate mils/sec
[illegible]-15	-1.15	2.71	[illegible].25	3.83	0.77	4.51
					0.91	4.13
Average					0.84	4.32
[illegible]	-0.76	1.10	0.97	1.90	1.00	3.07
	-1.16	1.09	-	-	0.58	3.08
Average	-0.96	1.10	0.97	1.90	0.79	3.08
[illegible]	-0.27	0.85	-	1.41	1.58	3.50
	-0.29	1.21	0.3	2.96	-	-
Average	-0.28	1.03	0.3	2.19	1.58	3.50
[illegible]	-1.87	0.63	-1.00	1.59	0.46	2.96
	-1.71	0.79	-1.16	1.58	0.58	3.08
Average	-1.79	0.71	-1.08	1.59	0.52	3.02
[illegible]-15C	0	1.25	0.90	2.61	2.06	3.69
	-0.16	1.33	0.94	2.59	1.90	3.61
Average	-0.08	1.29	0.92	2.60	1.98	3.65

(1) Average ablation and regression rates during 8 heating cycles (15 sec on, 15 sec off) at heat flux levels of 50, 100, and 225 Btu/ft^2-sec.

Figure 22. Plasma Arc Tests(1)

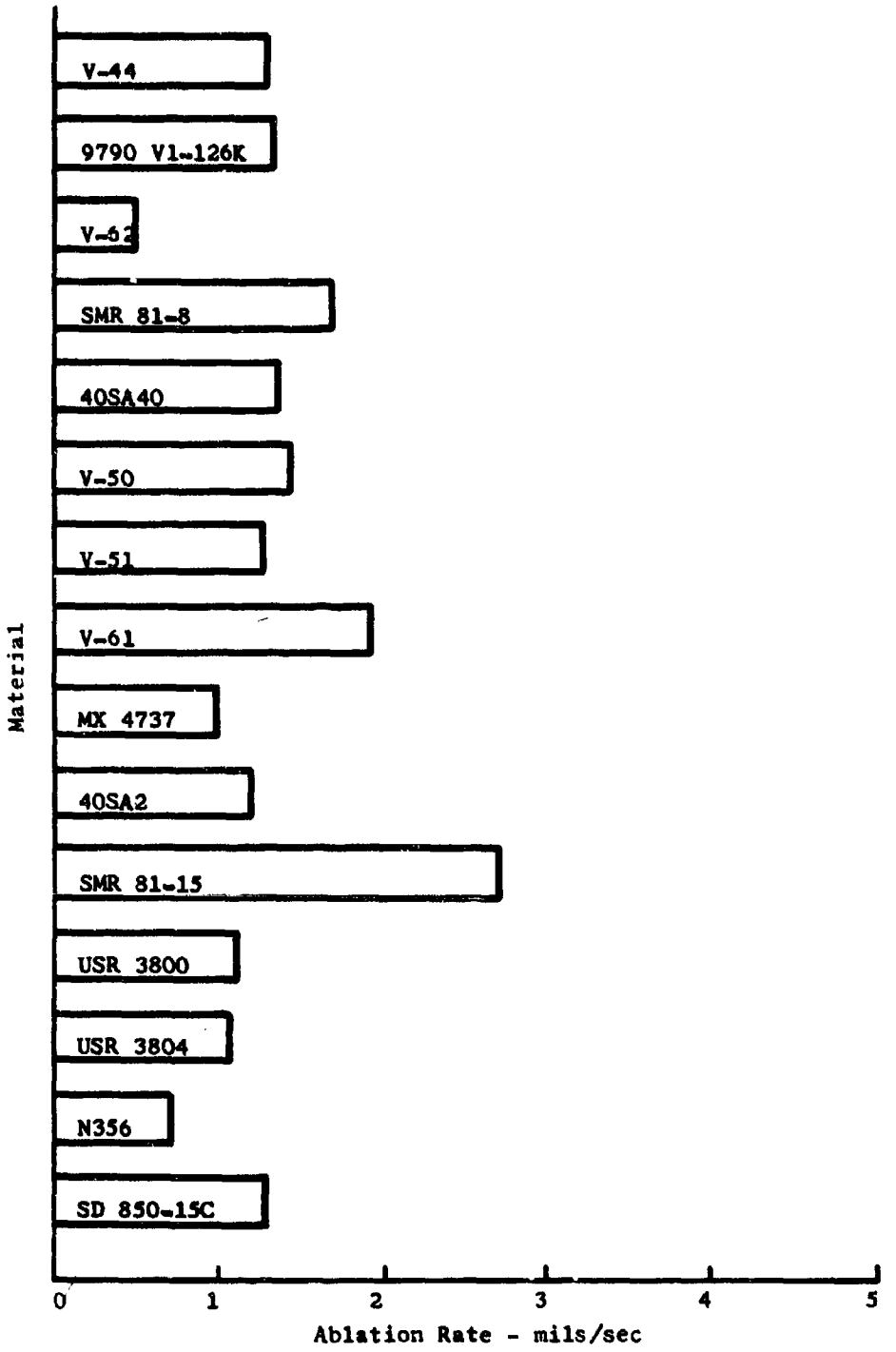

Figure 23. Plasma Arc Ablation Rates at 50 Btu/ft^2-sec

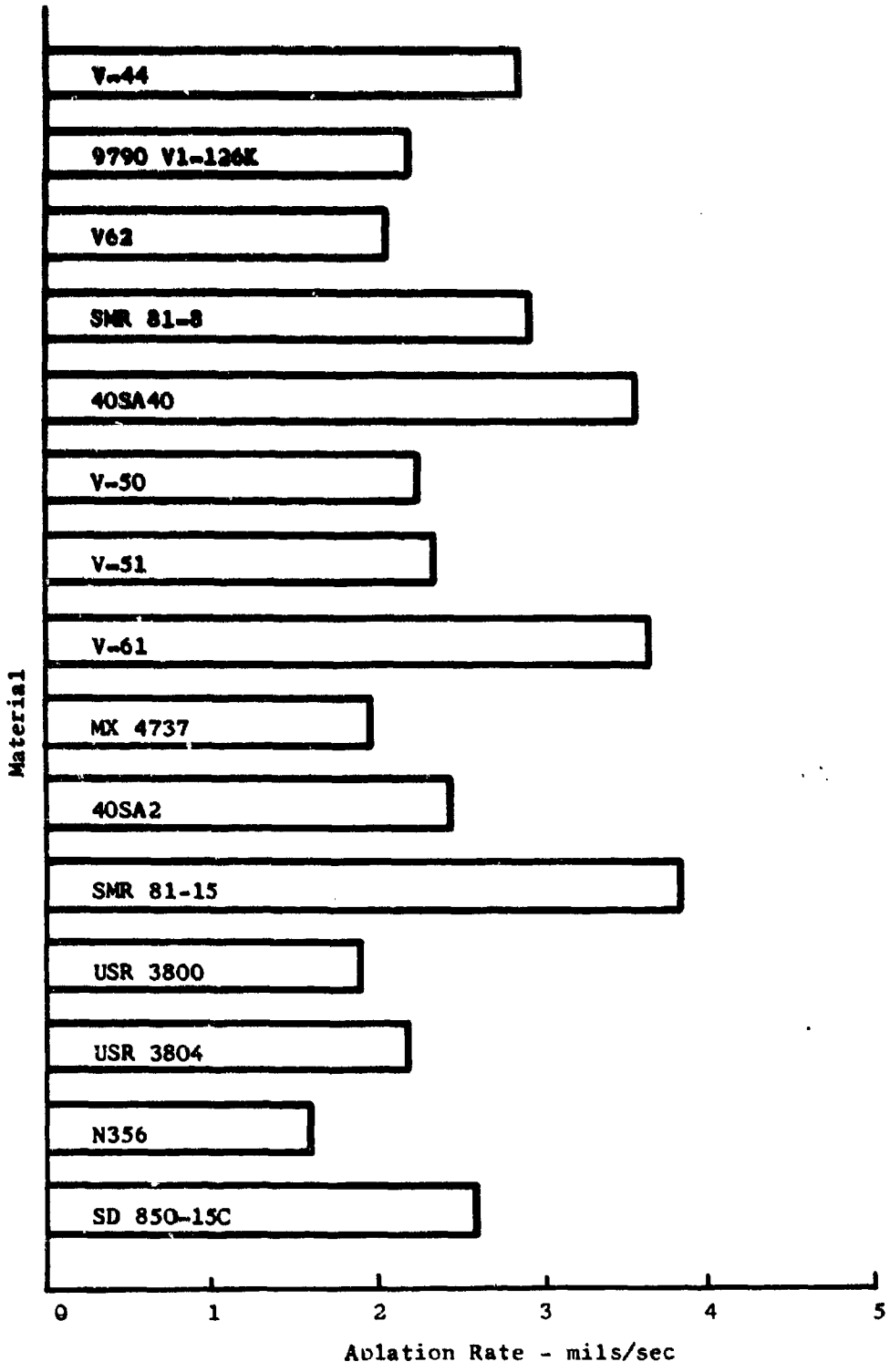

Figure 24. Plasma Arc Ablation Rates at 100 Btu/ft^2-sec

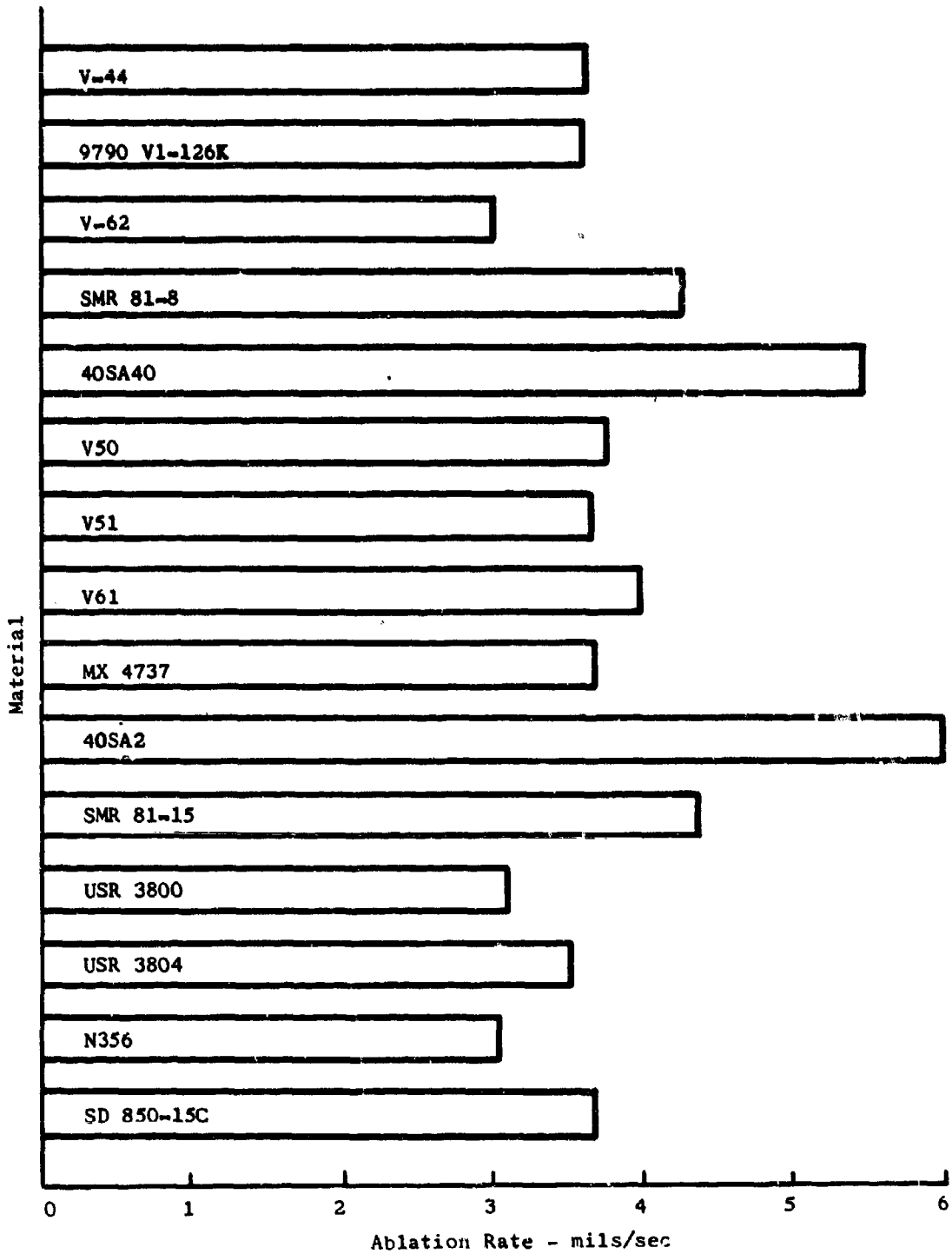

Figure 25. Plasma Arc Ablation Rates at 225 Btu/ft^2-sec

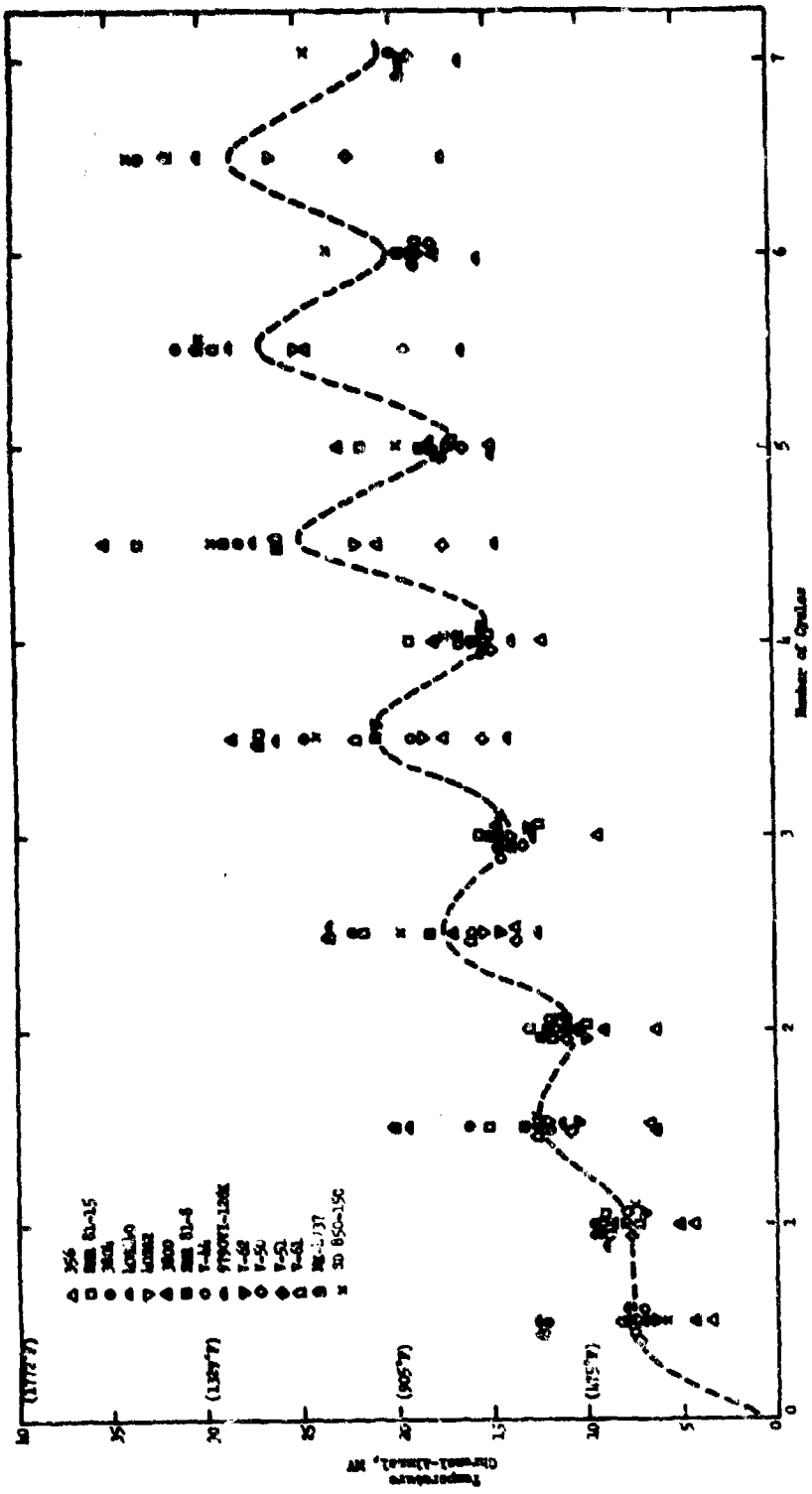

Figure 26. Temperature-Time Data* on 15 Materials Subjected to a 50 Btu/ft^2-sec Heat Flux Level

* Obtained from plasma-arc tests standardized for T/C Depth of 0.070". Plasma are cycled 8 times— 15 sec on, 15 sec off.

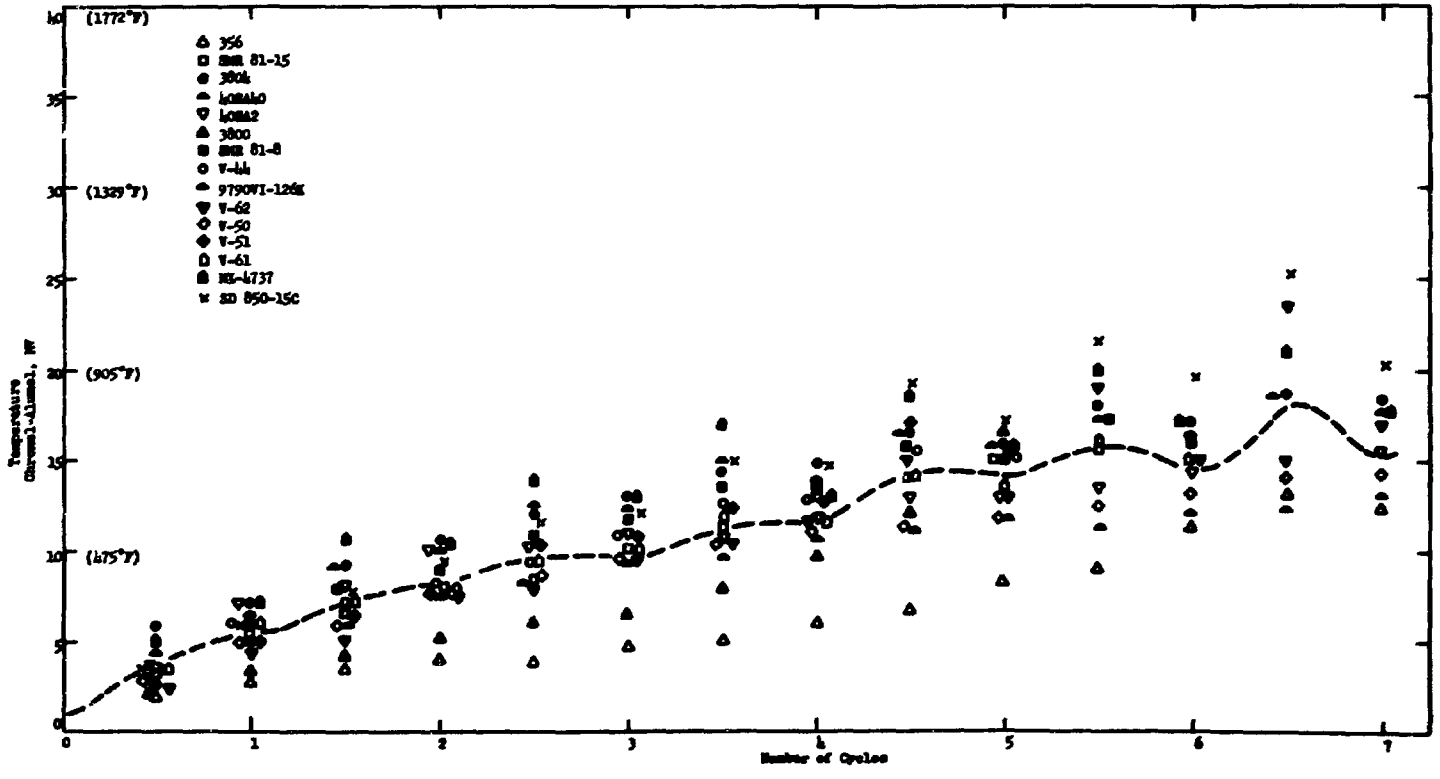

* Obtained from plasma-arc tests standardized for T/C Depth of 0.125". Plasma arc cycled 8 times— 15 sec on, 15 sec off.

Figure 27. Temperature-Time Data* on 15 Materials Subjected to a 50 Btu/ft^2-sec Heat Flux Level

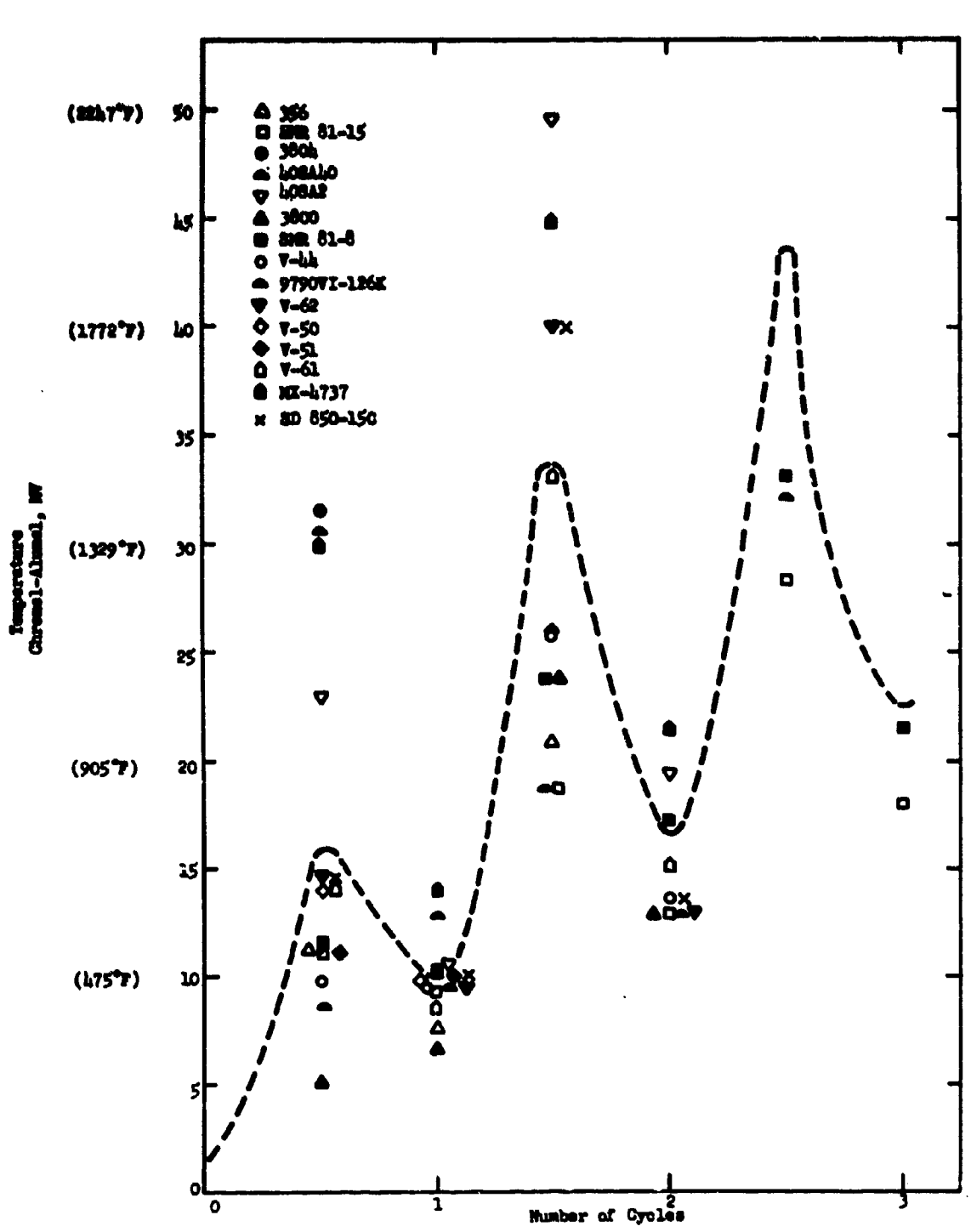

Figure 28. Temperature-Time Data* on 15 Materials Subjected to a 100 Btu/ft^2-sec Heat Flux Level

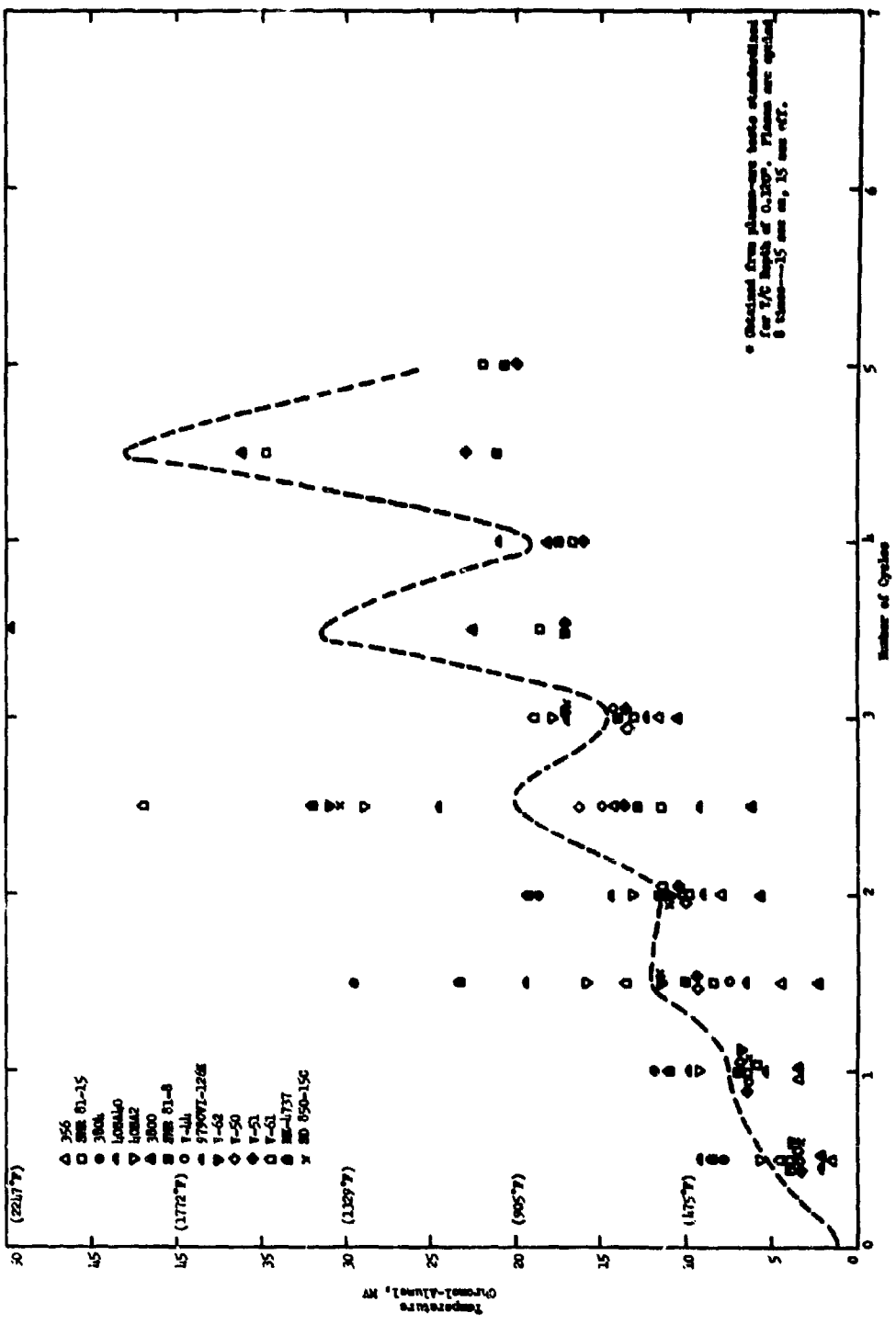

Figure 29. Temperature-Time Data* on 15 Materials Subjected to a 100 Btu/ft^2-sec Heat Flux Level

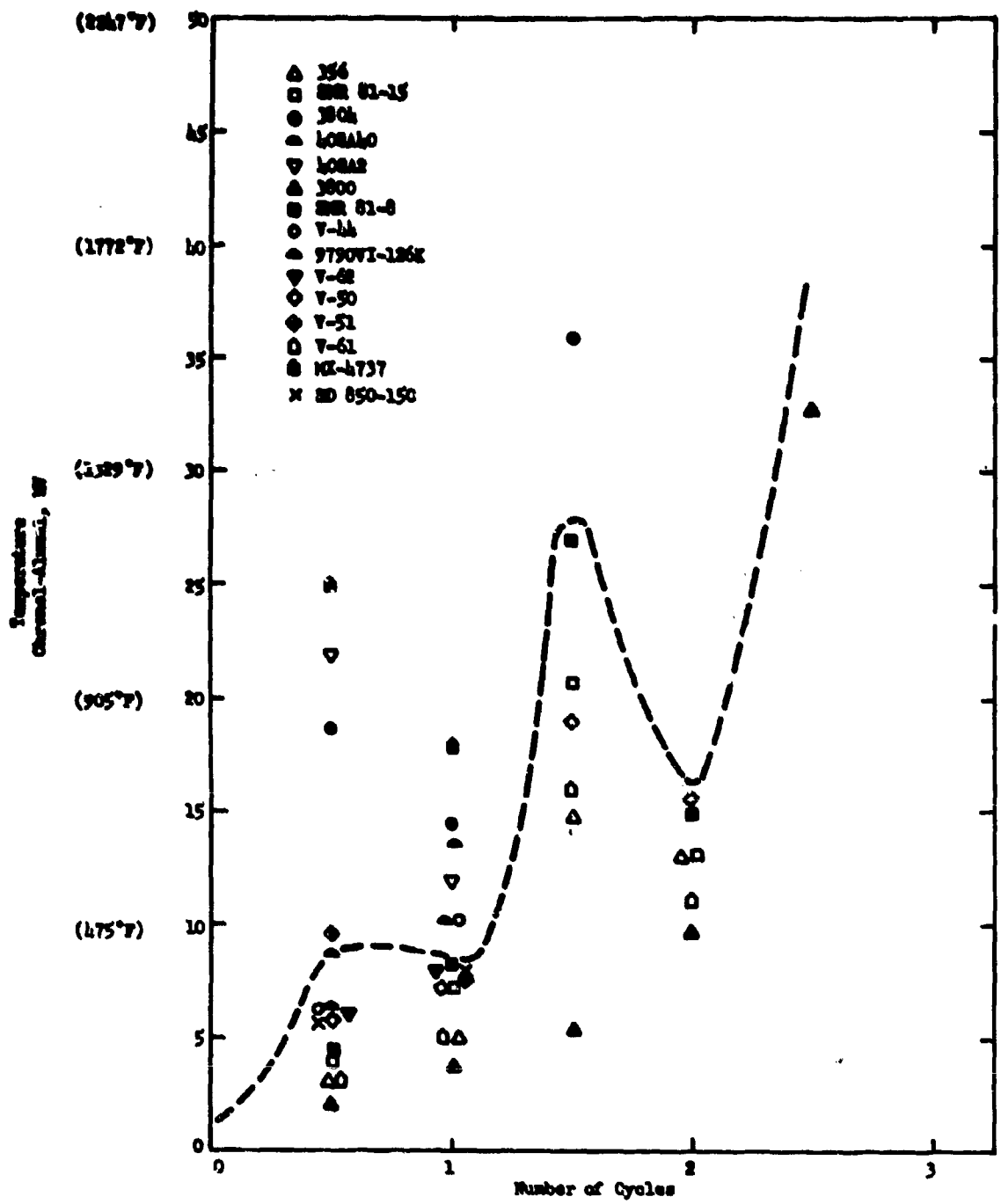

Figure 30. Temperature-Time Data* on 15 Materials Subjected to a 225 Btu/ft^2-sec Heat Flux Level

Material	Separation at Char-Virgin Interface	Soft Decomposition Zone	Char Cracks	Char Strength
N-356	No	No	No	Excellent
MX-4737	No	No	No	Excellent
850-15C	No	No	No	Excellent
V-61	No	No	Yes	Good(1)
USR 3800	No	Yes	No	Good(1)
40SA2	No	Yes	No	Good(1)
USR 3804	Yes & No	Yes	No	Good(1)
40SA40	Yes & No	Yes	No	Good(1)
SMR 81-8	Yes	Yes	Yes	Fair
SMR 81-15	Yes	Yes	Yes	Fair
9790V1-126K	Yes	Yes	Yes	Fair
V-44	Yes	Yes	Yes	Fair
V-50	Yes	Yes	Yes	Fair
V-51	Yes	Yes	Yes	Fair
V-62	Yes	Yes	Yes	Fair

(1) Char strength decreases from outer layer towards decomposition zone.

Figure 31. Observations on Char Properties after Plasma-Arc Exposures at 50, 100, and 225 Btu ft^2-sec

Constituent	V-44	V-62	40SA40	SMR 81-8	9790V1-126K
Toluene	0.3	1.0	---	0.4	0.4
Benzene	0.4	0.3	---	---	0.5
Tetrahydrofuran	---	---	7.7	---	---
1,3 Cyclohexadiene	0.4	0.6	---	---	---
2 Pentene	2.3	2.2	---	---	3.9
1,3 Pentadiene	1.6	2.3	---	---	2.1
Butane	1.4	3.4	6.2	---	3.9
1 Butane	4.3	9.6	3.2	---	10.3
1,3 Butadiene	0.8	1.1	---	---	---
CO_2	6.9	3.5	6.1	3.6	3.9
CO	11.9	7.2	33.2	2.8	5.7
H_2O	2.9	8.2	0.9	1.2	1.6
Methylacetylene	0.9	1.3	---	---	0.7
Propylene	4.7	2.0	5.6	5.7	7.8
Ethane	7.6	7.6	4.4	2.3	11.1
Ethylene	6.2	8.8	11.2	3.7	8.0
Acetaldehyde	---	---	---	---	---
Propane	---	---	---	---	5.6
HCN	0.2	0.2	---	---	---
Methane	18.6	18.1	6.9	14.4	21.1
Isobutane	---	---	---	9.2	---
Propyne	---	---	---	1.2	---
H_z	28.6	22.6	6.8	8.1	13.4
Isobutene	---	---	---	47.4	---

*Obtained from pyrolysis of virgin material at 550°C and 350 psi, in mole percent.

Figure 32. Quantitative Analysis* of Gaseous Products of Virgin Materials

Sample	Pressure, psig	Toluene*	Isobutane	Isobutene	CO_2	Propylene	Propyne	Ethane	Ethylene	CO	Methane	Hydrogen	H_2O
Virgin	349.3	0.4	8.3	39.4	3.6	4.7	1.3	2.7	3.3	12.8	14.3	8.0	1.2
Virgin	349.3	0.4	9.2	47.4	3.6	5.7	1.2	2.3	3.7	2.8	14.4	8.1	1.2
5 min	349.3	0.2	6.4	44.1	3.6	2.4	2.3	1.2	2.5	23.0	7.9	5.3	1.1
30 min	349.3	0.7	7.9	34.9	3.3	4.0	1.7	2.4	2.2	12.0	15.6	13.9	1.4
30 min	349.3	0.6	9.5	45.5	3.9	4.6	1.3	2.1	3.4	11.6	11.9	3.9	1.8

*Mole percent at 550°C

Figure 33. Comparison of Quantitative Analysis of Gaseous Products for Virgin and Heat-Soared Virgin SMR 81-8

III, A, Properties of Five Materials (Task A, Phase I) cont.,

The molecular types of gases obtained from the mass spectrographic analysis were as expected at this temperature and pressure level. The major constituents were generally the low molecular weight gases consisting of hydrogen, methane, ethane, ethylene, propylene, carbon monoxide, carbon dioxide, and water vapor. The higher molecular weight compounds, such as, the cyclic, heterocyclic, and straight-chained molecules were found to be present only in trace amounts. These data were compared to data obtained by Madorsky, et al., who investigated pyrolysis products obtained from similar types of materials, and it was found that, in general, similar gas species were generated.

The resulting residues obtained from the pyrolysis of the virgin materials were also analyzed for their chemical constituents. Standard techniques of X-ray diffraction, emission spectroscopy, and elemental analyses were employed in this determination. The results of this analysis are shown in Figure 34. The major solid constituents in this case were magnesium oxide, silicone oxide, carbon, zinc oxide, and in the case of 40SA40, titanium dioxide.

From the above identification of the gaseous pyrolysis products, heats of combustion data are being obtained for each of the pyrolysis gases from published literature. When this data has been obtained, the thermochemical properties of a one-mole mixture of gases will be calculated. These properties include heat of combustion and the transport properties, i.e., viscosity, heat capacity, and thermal conductivity. The heat of combustion of the charred gases will also be used, along with the heat of combustion of the charred materials shown in Figure 34 to calculate the heat of formation of the virgin composite materials. All of these data will be used in the analytical model equations in a later phase.

It is realized that the heating environment in a rocket motor is much more severe than in a laboratory type heating furnace. Consequently, different fragments or even increased or decreased amounts of the reported compositions may result because of thermal cracking of the polymers. Further refinement in this area is suggested to evaluate the effect of heat flux on polymer degradation.

d. Testing of Charred Materials

Work was first conducted on a procedure for obtaining charred materials in the quantities or sizes required for property tests. A high-pressure, high-temperature heating apparatus (see Appendix I) operating at 700 psi at a heat flux of 100 Btu/ft^2-sec was used in preparation of the samples. Various sample sizes and ways of exposing them to the simulated heat and pressure of actual firings were used. Samples of the five basic materials were first prepared by exposing the entire outer surface to the heat source (graphite susceptor) as shown in Figure 35 until steady-state temperatures were reached.

Constituent	V-44	V-62	40SA40	SMR 81-8	9790V1-126K
MgO	15.0*	10.0	---	15.0	13.0
SiO_2	40.0	23.0	45.0	65.0	40.0
TiO_2	---	---	35.0	---	---
Fe_2O_3	0.4	---	0.05	0.5	0.4
ZnO	5.0	4.5	---	3.5	5.0
Al_2O_3	---	---	0.4	0.05	---
C	24.4	55.1	10.1	3.87	27.2
H	2.16	3.39	1.17	1.26	3.02
N	1.60	0.29	0.33	0.15	0.12
O	5.37	2.83	1.44	5.80	5.20

*In weight percent

Heat of Combustion

	V-44	V-62	40SA40	SMR 81-8	9790V1-126K
	2973*	5122	1908	3183	3593
	2943	5212	1789	3202	3600
Average	2958	5167	1849	3193	3597

*Cal/gm

Figure 34. Quantitative Analysis and Heat of Combustion of Charred Materials

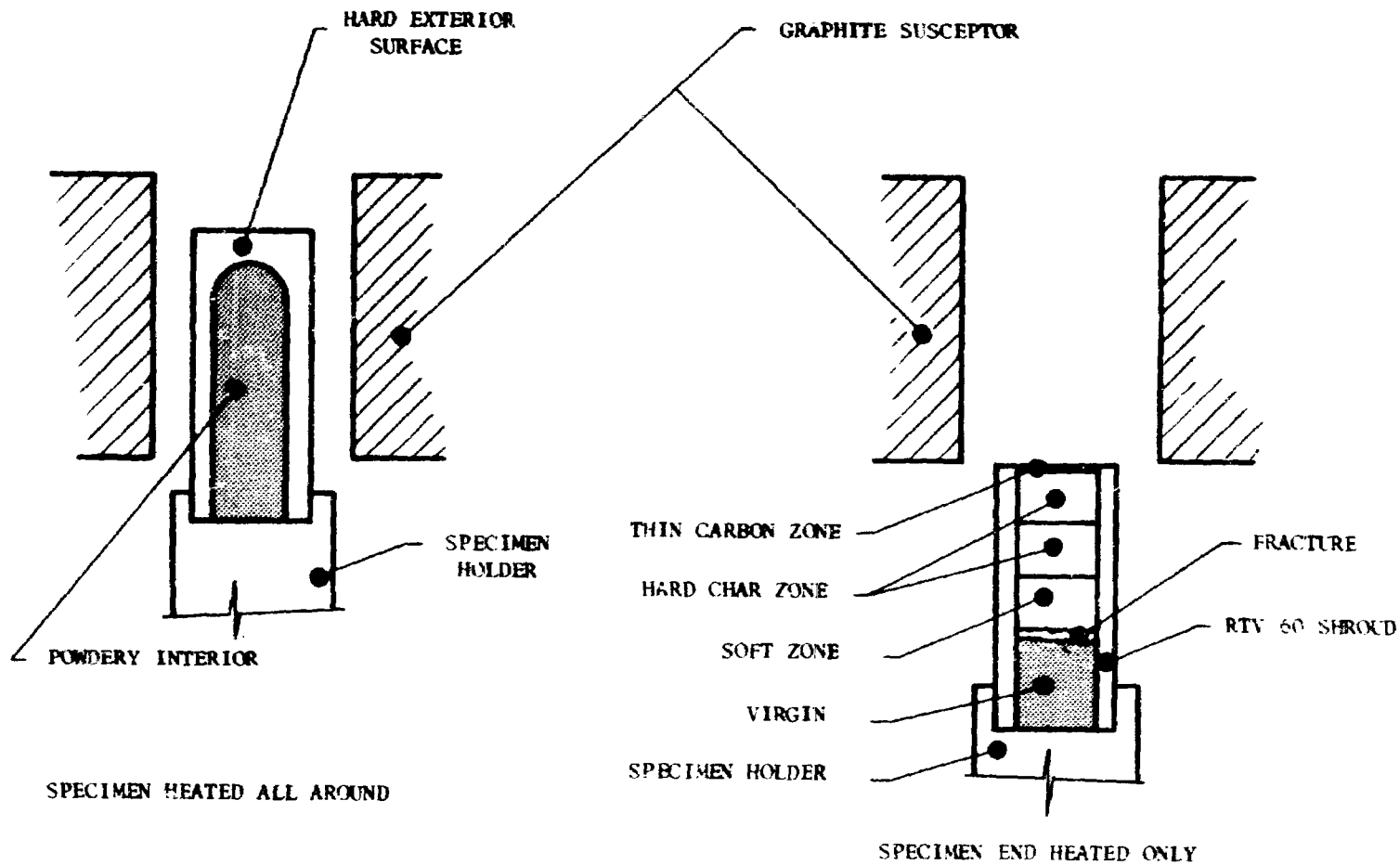

Figure 35. Charring of Elastomeric Materials

III, A, Properties of Five Materials (Task A, Phase I) (cont.)

In all cases, except for the 40SA40, which slumped without charring, (Figures 36 through 40) a hard surface containing carbon was formed by deposition of carbon in the pores of the material from the cracking of the gases emanating from the decomposition zone. Some delamination was noted running parallel to the direction that the materials were laid up in prior to vulcanization. When the samples were sectioned, a fine, powdery core was exposed. Because the samples were not uniform in structure, they were generally unsatisfactory for use in determining char properties.

Samples of the five basic materials were then prepared by exposing only the tops of the samples to the hot zone of the susceptor, as shown in Figure 35. The remaining surfaces of each sample were protected by a shroud of RTV-60. This creates an effect on the materials similar to that of an actual firing. The specimens were made long enough (2 in.) so that some virgin material would remain after charring. After steady-state temperatures were achieved on the top surfaces, the pressure was released and the samples dropped away from the heating source. Visual observations made during the runs, and comments on the condition of each sample, are presented in Figure 41. Photographs of each sample are shown in Figures 42 to 45 and indicate the extent of delamination and virgin material swelling that occurred after shutdown. All chars were loose from the virgin decomposition zone.

Charred specimens of V-44 material, 1/2 x 1/2 x 1 in. long, were then prepared by the end heating technique except that the specimens were heated to steady-state temperatures on both the top (1520°C) and bottom (470°C) surfaces. Steady-state temperatures were attained in approximately 25 min. A backside temperature of 470°C was selected because this should be approximately the ablation temperature of the materials involved and completely charred materials should then be obtained. Density and X-ray diffraction tests were conducted on these specimens to determine uniformity of composition. The results show that the specific gravity was the lowest at the flame surface (0.506), increased through the hard char areas (0.646-0.708-0.770), and decreased near the final decomposition or ablation zone (0.608). The specific gravity of the virgin material is 1.269, indicating that an average weight loss of approximately 50% occurred during charring. The density pattern is generally similar to that being considered in the analytical model studies being conducted in Phase II. The X-ray diffraction scans were quite similar along the length of the specimens, indicating that no essential changes in composition existed.

Because the end heating technique appeared to give satisfactory char for use in determining char properties, all test specimens for the program were thus prepared in this manner. All specimens were fabricated with the laminations running parallel with the end surface to simulate actual layup in motor applications. Figure 46 shows examples of various specimens as

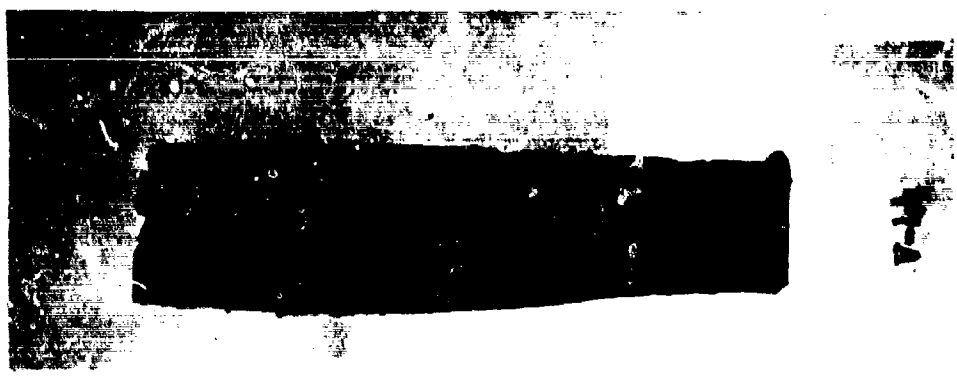

As Removed from Charring Apparatus

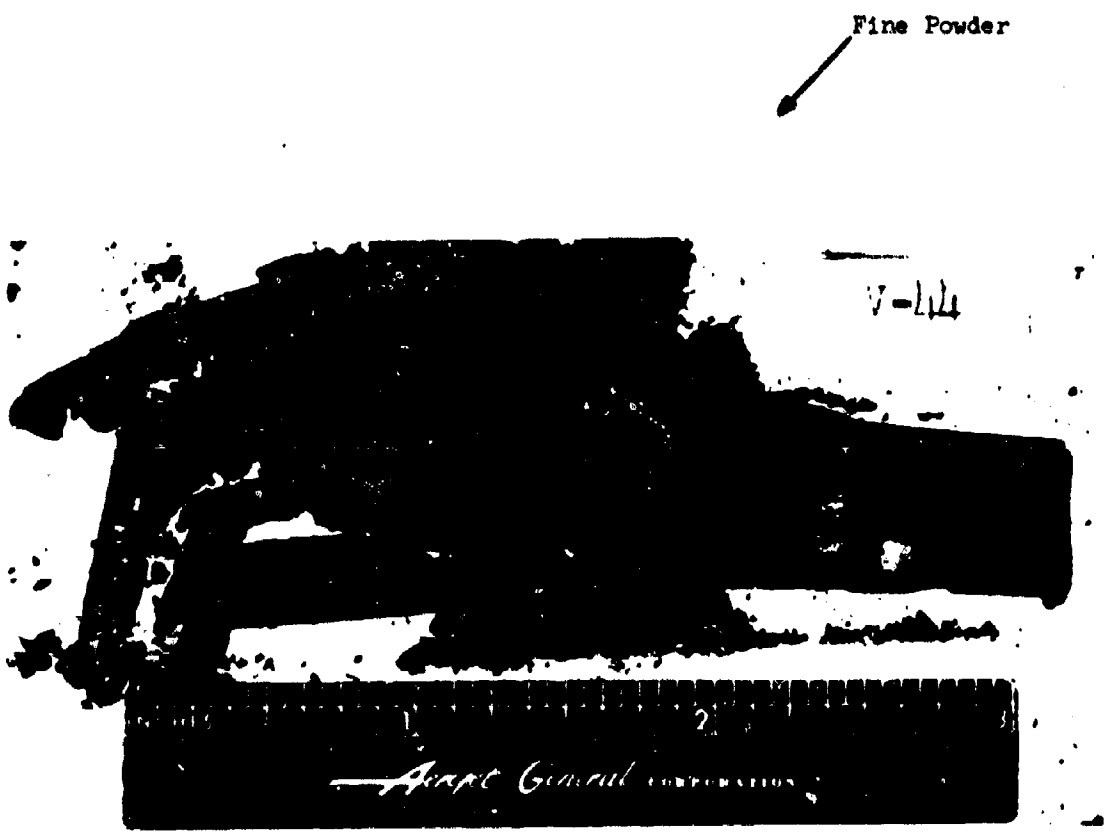

After Further Handling

Figure 36. V-44 Charred by Exposing Entire Surface to Heat Source

As Removed from Charring Apparatus

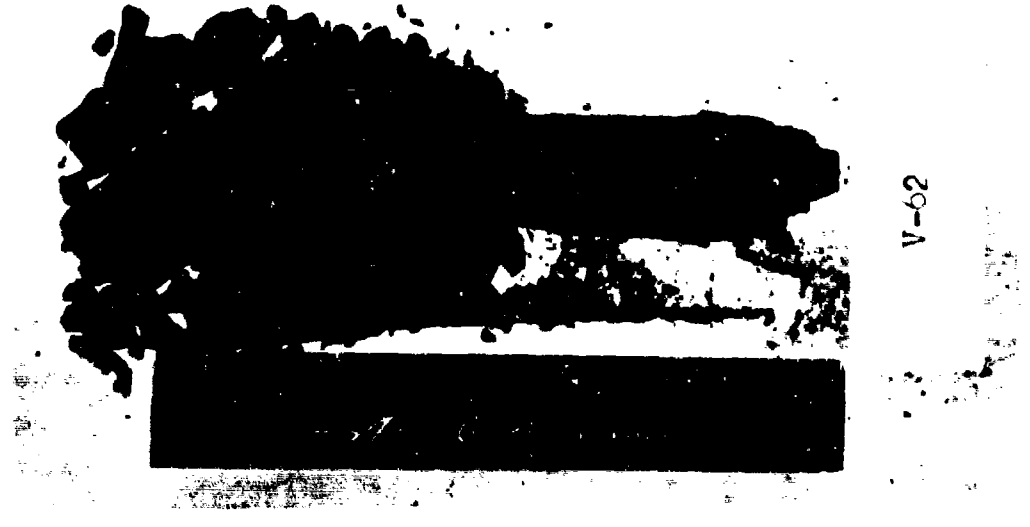

After Further Handling

Figure 37. V-62 Charred by Exposing Entire Surface to Heat Source

As Removed from Charring Apparatus

Figure 38. 40SA40 Charred by Exposing Entire Surface to Heat Source

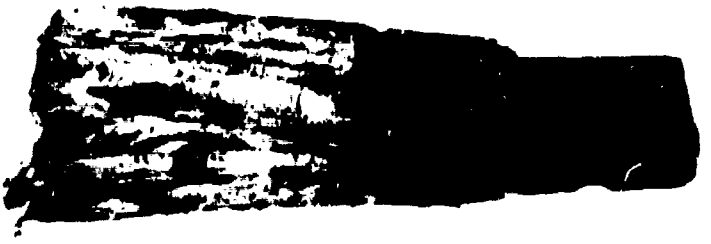

As Removed from Charring Apparatus

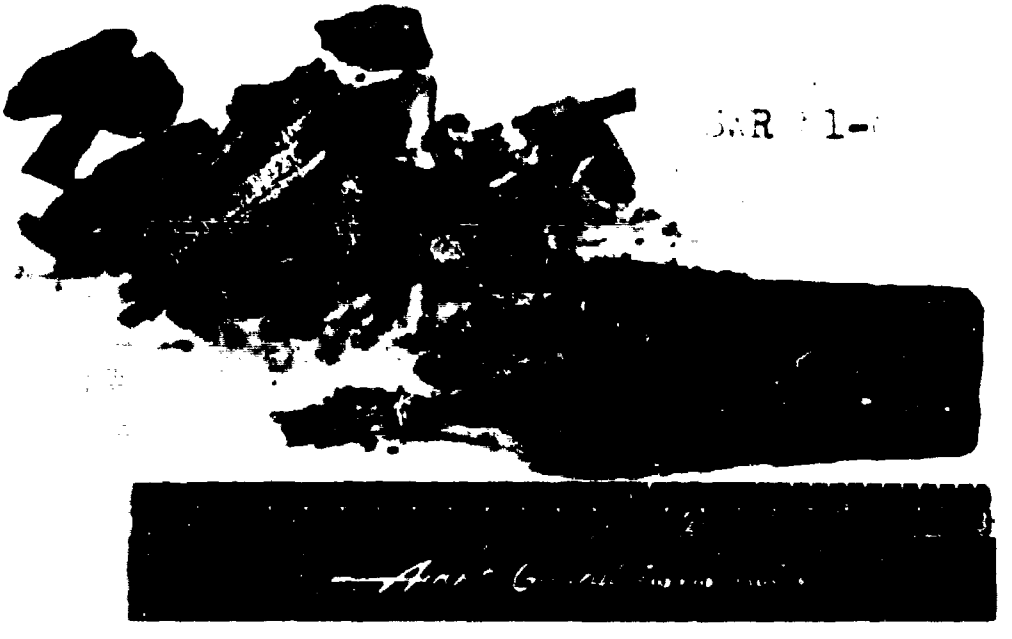

After Further Handling

Figure 39. SMR-81-8 Charred by Exposing Entire Surface to Heat Source

As Removed from Charring Apparatus

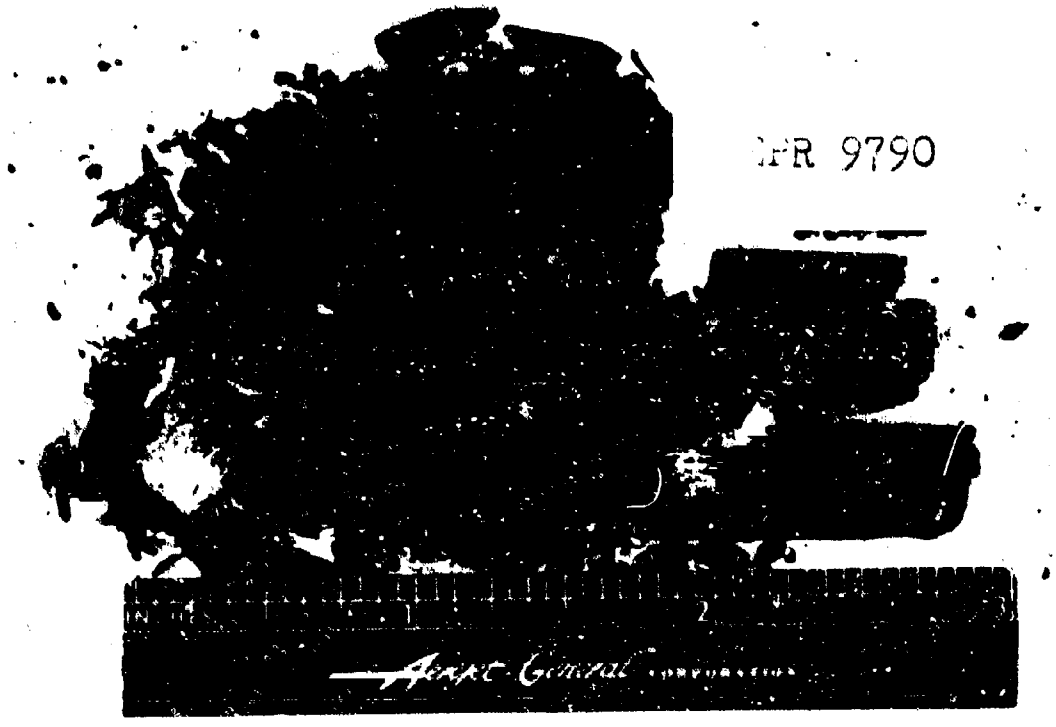

After Further Handling

Figure 40. 9790VI-126K Charred by Exposing Entire Surface to Heat Source

Material Designation	Surface Temp.,	Observations During Run	Comments (Based on observations of internal surface)
Con-Cast V-44	1550°C	Heavy smoking from spec. during run. Steady-state temp. was reached in 10 min. Spec. temp. was difficult to read because of smoke.	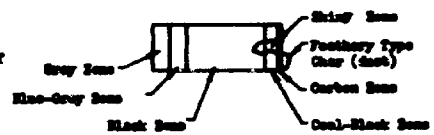	1) Feathery type char was formed on flame surface. 2) No loose powder evident. 3) Considerable swelling of virgin material. 4) Spec. showed no signs of delamination. 5) Gray zone softer than other zones.
Con-Cast V-46	1405°C	Heavy smoking from spec. during run. Spec. showed signs of delamination on heated surface after first 5 min. of run. Steady-state temp. reached in 10 min.	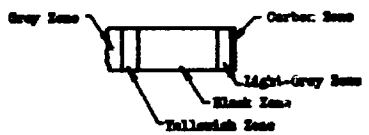	1) Slight delamination was noticeable on heated surface. 2) Very little swelling in virgin material. 3) Small amounts of powder evident. 4) Gray zone softer than other zones.
AGMAD	1530°C	Heavy smoking during run. Steady-state temp. reached after 10 min. Smoking continued through entire run.	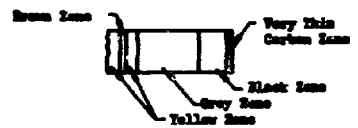	1) Very thin carbon zone. 2) No evidence of powder. 3) Spec. quite soft and flaky in gray and black zones. 4) Yellow zones are soft and mushy. 5) Virgin material melted. 6) Spec. was quite hard to split.
[illegible] SL-6	1430°C	Heavy smoking during run. Steady-state temp. reached in 10 min.	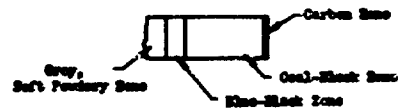	1) Flame face thin carbon zone. 2) Spec. shows no signs of delamination. 3) Gray feathery zone consists of a [illegible] powder. 4) Considerable swelling of virgin material.
[illegible]-12SE	1470°C	Very little smoking during run. Steady-state temp. reached after 10 min.	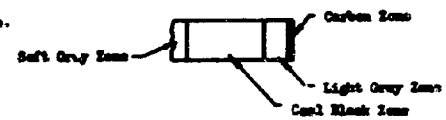	1) Flame face thin carbon zone. 2) Spec. shows no signs of delamination. 3) Considerable swelling of virgin mat'l. 4) Gray zone consists of a soft, mushy powder.

Figure 41. Observations Made on Charring Tests (End Heated)

After Removal of Shrouding

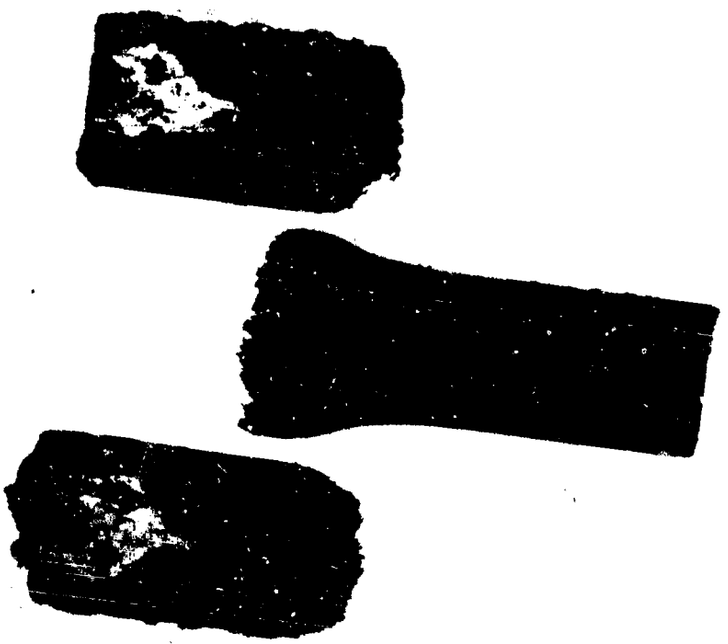

After Sectioning of Char

Figure 42. V-44 Charred by End Heating Only

SMR-81-8

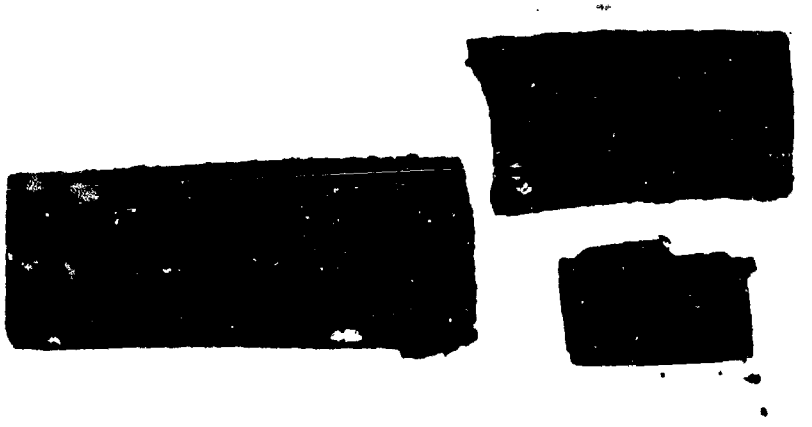

V-62

Figure 43. SMR-81-8 and V-62 Charred by End Heating Only

After Partial Removal of Shrouding

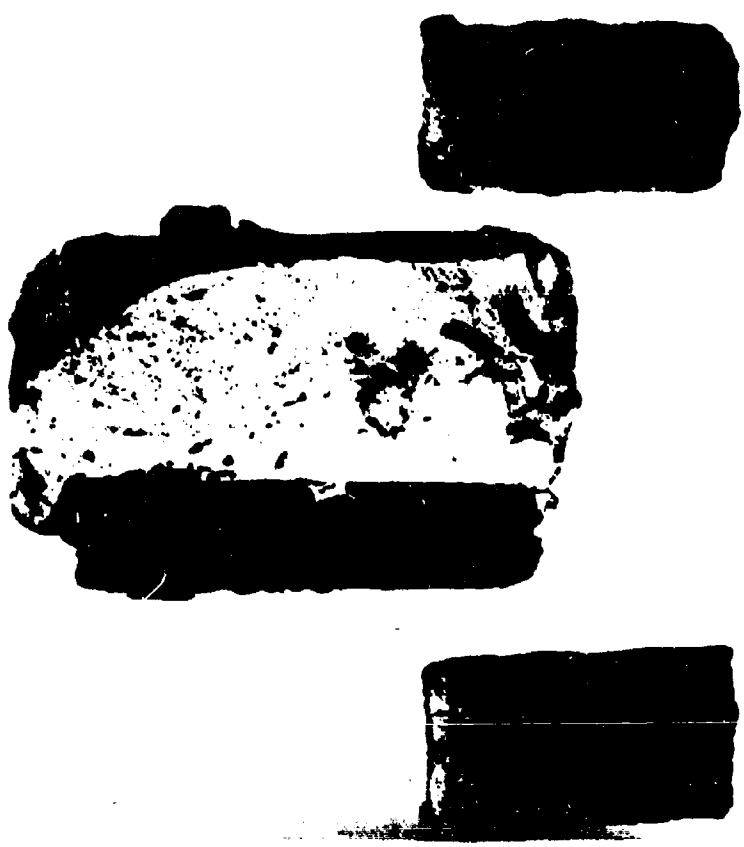

After Sectioning of Char

Figure 44. 40SA40 Charred by End Heating Only

After Removal of Shrouding

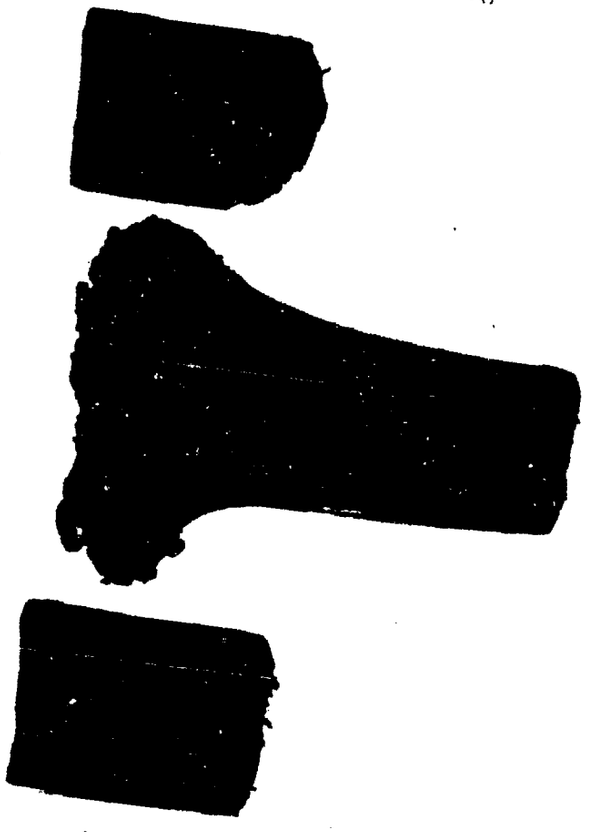

After Sectioning of Char

Figure 45. 9790/I-126K Charred by End Heating Only

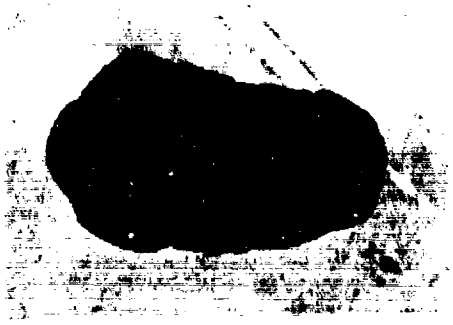

40SA40
½ in. OD x 1 in. long

V-44
½ x ½ x 1

V-62
7/8 in. OD x 1 in. long

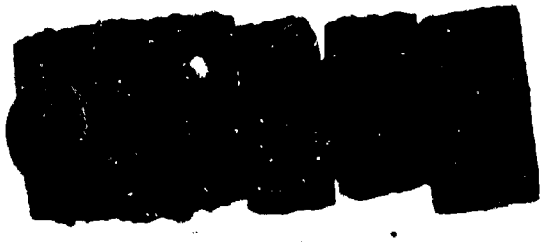

SMR-81-8
½ x ½ x 1

9790 VI-126K
½ in. OD x 1 in. long

Figure 46. Examples of Charred Specimens Used for Property Testing

III, A, Properties of Five Materials (Task A, Phase I) (cont.)

charred. Note how some of the specimens delaminated, apparently at the interfaces where the materials were laid up prior to vulcanization. See Appendix I for a discussion of the test procedures used in determining the following properties:

(1) Bulk Density

The bulk densities of the charred materials were obtained both from Correlation Motor specimens and from laboratory specimens. See Paragraph B below for discussion on Correlation Motors. As shown in Figure 47, the densities of each material exhibited some variation, not only between the motor specimens and the laboratory specimens, but within the motor specimens. The average densities of the Correlation Motor specimens and the average densities of the laboratory specimens were both approximately 40% of the density of the virgin materials, indicating a 60% weight loss during charring.

Weights were also taken prior to and after the charring on all other specimens used throughout the program. Although no correction was made for any possible specimen expansion that might have occurred during charring, the average weight retentions were essentially the same as those reported in Figure 47 (V-44 - 49.6%, V-62 - 33.5%, 40SA40 - 42.3%, SMR 81-8 - 53.5%, and 9790VI-126K - 39.5%).

(2) Permeability

The permeability of the charred specimens has not been determined for each particular material, as further analysis of the data shown in Figure 48 is required in order to mathematically describe the relationship between the mass flux of gas through the charred materials and the associated pressure-loss function. The data shown in the figure above is not completely described by the classical Darcy equation for compressible flow through small conduits. The initial portion of the data, where the upstream pressure is of the order of 0.200 psig with a corresponding and relatively low mass flow, appears however, to verify Darcy's equation. It is believed that a second-order term involving the mass flow rate is needed in addition to the first-order term in Darcy's equation to adequately describe the entire regime. Therefore, the data shown in this figure will be further analyzed prior to conducting the statistical analysis which will correlate properties with motor performance.

(3) Pore Spectra

The pore spectra results are shown in Figure 49 for both laboratory specimens and specimens taken from the single-pulse correlation motors. These data show that V-44 and SMR 81-8 had the lowest pore volume.

Material	Density* Virgin Material	Correlation Motors					Laboratory Char			
		Single-Pulse	Two-Pulse	Three-Pulse	Average	% of Virgin	Method 1**	Method 2	Average	% of Virgin
V-44	1.269	L - 0.549 C - 0.495 N - 0.414	L - 0.435 C - 0.623 N - 0.426	L - 0.465 C - 0.436 N_1 - 0.447 N_2 - 0.414			0.506 0.646 0.708 0.788 0.608	0.536 0.587		
		0.486	0.495	0.440	0.474	37.5	0.651	0.562	0.591	46.5
V-62	1.062	0.430 0.522 0.450	L - 0.347 C_1 - 0.839 C_2 - 0.646 N - 0.570	L - 0.210 C - 0.196 N - 0.327			0.358 0.449 0.424 0.417	0.344 0.289		
		0.467	0.605	0.244	0.438	41.2	0.412	0.316	0.364	34.2
40SA40	1.338	0.549 0.580 0.480	L - 0.500 C_1 - 0.512 C_2 - 0.766 N - 0.768	L - 0.586 C - 0.520 N - 0.505			0.580 0.628 0.549	0.522 0.553		
		0.536	0.634	0.537	0.566	42.4	0.586	0.537	0.562	42.2
SMR 81-8	1.351	0.390 0.456 0.435 0.519 0.435	L - 0.899 C - 0.716 N - 0.524	L - 0.428 C - 0.496			0.390 0.435 0.455	0.856 0.886		
		0.447	0.713	0.462	0.544	40.4	0.426	0.871	0.648	47.8
9790V1 0126K	1.092	0.471 0.493 0.428 0.485	L - 0.447 C - 0.649 N - 0.492	L - 0.273 C_1 - 0.322 C_2 - 0.381 N - 0.391			0.381 0.410 0.497 0.471	0.385 0.350		
		0.469	0.529	0.342	0.443	40.4 40.4	0.440	0.367	0.403	37.0 41.5

Figure 47. Bulk Density* of Char

*Specific Gravity, gm/cc

**Method 1 - Sample heated only until temperature of flame surface stabilized. One sample per material tested. Individual readings reflect density along length of sample. V-44 sample, however, was heated as per Method 2.

Method 2 - Sample heated until temperature of both flame surface and backside surface stabilized. Two samples per material.

L - Sample located near large end of aft closure.

C - Sample located near center of aft closure.

N - Sample located near nozzle end of aft closure.

Figure 47. Bulk Density* of Char

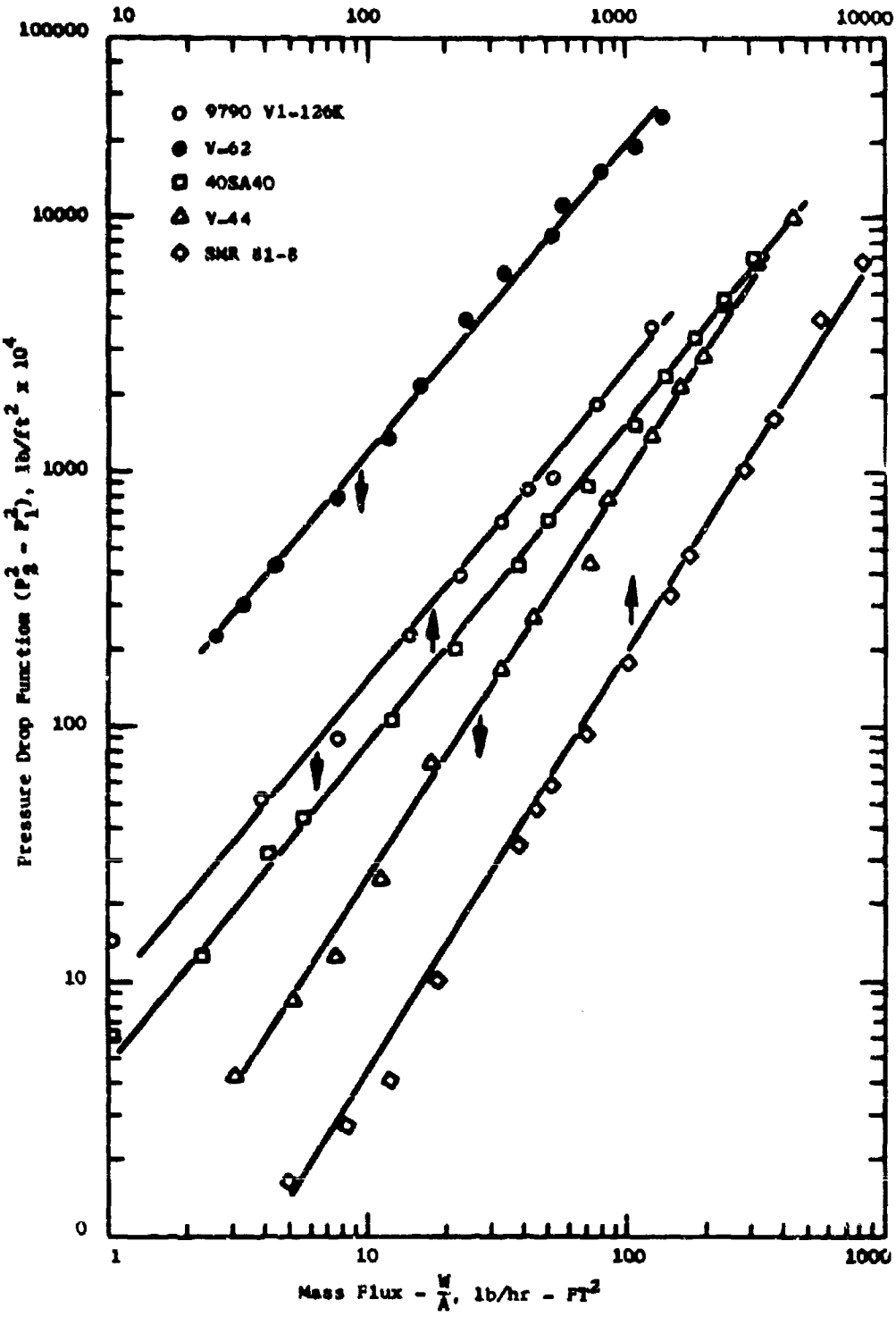

Figure 48. Pressure Drop in Charred Material

Property	V-44	V-62	40SA40	SMR 81-8	9790VI-126K
Pore Spectra, % @ 5000 psi Lab	54.6	66.7	59.1	34.4	52.6
Motor, Single Pulse	46.7	59.3	58.8	48.1	59.0
Shear Strength, psi	28.2	103.7	17.2	104.4	80.2
	53.7	55.1	11.6	44.5	42.8
	36.8	91.0	67.7	-	-
Average	39.6	83.2	32.1	74.4	61.5
Compressive Strength, psi	444	323	185	170	333
	417	524	428	143	240
	369	381	246	-	-
Average	410	409	286	156	286
Tensile Strength/Modulus, psi	20.86/235	26.02/929	15.81/487	1.65/.5	N/A

Figure 49. Physical and Mechanical Properties of Charred Materials

III, A, Properties of Five Materials (Task A, Phase I) (cont.)

The 34.4% obtained in the lab specimens for SMR 61-8 is questionable because at a total pressure of 5000 psi, the amount of mercury being intruded into the open pore structure was still increasing with volume. Normally, at these elevated pressures, a maximum pore volume is reached whereby an increase in pressure does not force additional mercury into the specimen.

(4) Shear, Compressive, and Tensile Strength

The shear, compressive, and tensile strength properties shown in Figure 49 indicate that V-62 char has the best overall properties. These properties are quite difficult to measure because of the frangible nature of the chars, so the results should be considered more qualitative than quantitative.

(5) Emissivity and Reflectivity

The emittances of the charred specimens were calculated according to the following equation:

$$E = \frac{(T_s)^4}{(T_B)^4}$$

where
E = normal total emissivity
T_s = surface temperature, °R
T_B = block-body temperature, °R

At thermal equilibrium, the energy emitted must equal that absorbed, since no energy is transferred; consequently, the emissivity must be equal to the fraction absorbed. Since all radiant energy reaching an opaque body must be either absorbed or reflected, the fraction absorbed (equal to the emissivity) is related to fraction reflected by 1.0 minus the amount absorbed.

The emissivity and reflectivity test results are given in Figure 50. These data indicate that the emittances of the specimens increased with temperature from their point of incandescence to approximately 3100°F. These values were compared to literature values for graphite and phenolic-nylon chars, and it was found that the latter values were generally consistent with the calculated values. Of the five charred materials tested, V-62 had the lowest observed emissivity.

No attempt was made to study the emittance characteristics of the materials as a function of surface condition or surface roughness. That is, the emittance characteristics of the char may be directly dependent

Property	V-44	V-62	40SA40	SMR 81-8	9790VI-126K
Emissivity					
T_1, °C*	1325 - 0.899	1375 - 0.815	1315 - 0.955	1340 - 0.963	1285 - 0.880
T_2, °C	1555 - 0.978	1625 - 0.801	1620 - 0.989	1580 - 1.000	1520 - 0.982
T_3, °C	1715 - 0.994	1750 - 0.807	Specimen disintegrated	1710 - 0.942	1705 - 0.986
Reflectivity					
T_1, °C*	1325 - 0.101	1375 - 0.185	1315 - 0.045	1340 - 0.037	1285 - 0.120
T_2, °C	1555 - 0.022	1625 - 0.199	1620 - 0.011	1580 - 0	1520 - 0.018
T_3, °C	1715 - 0.006	1750 - 0.193	-	1710 - 0.058	1705 - 0.014

*Black body temperature

Figure 50. Emissivity and Reflectivity of Chared Materials

III, A, Properties of Five Materials (Task A, Phase I) (cont.)

upon the method of formation of the char, whether it be by an aerodynamic heating method or by a static (oven) heating method. It has been found, for example, that the emittance of carbon changes rather abruptly from a polished surface to an oxidized surface. In the case of carbon, the emittance changes from about 0.70 for a polished surface to about 0.90 upon initial oxidation, and then to 0.97 with further oxidation. Further investigation in this field is warranted.

(6) Thermal Conductivity

The thermal conductivity test results are shown in Figure 51 and graphically presented in Figure 52. In all cases, the thermal conductivity of the charred materials increased with temperature. At approximately 750°F, electronic noise level in the apparatus was of such a magnitude that interpretation of further data was not possible. The exact nature and cause of the noise response at this temperature level is not known. Preliminary observations indicate that the charred material continued to lose its structural integrity beyond its original fragile and flaky nature. This introduced thermal contact problems between the charred specimen and the measuring backface thermocouple probe. For adequate time-temperature response curves obtained according to the flash technique for determining thermal diffusivity, it is necessary and very important that good thermal contact be made between sample and sensing thermocouple. Generally, a small external force is placed upon the thermocouple to insure contact. However, in this case, no external force could be used; but, instead, the thermocouple was carefully allowed to just rest against the samples.

It is believed, at this point, that some progress can be made in eliminating the problems associated with thermocouple contact, electronic noise level, and very fragile specimens. Recent advances in the field of infrared detectors indicate that it may be possible to replace the thermocouple sensing technique with a much more reliable system based upon optical techniques. In addition, using this latter system, it would also be possible to determine thermal diffusivity at much higher temperatures.

Another problem encountered with some of the charred specimens was that the pyrolyzed sample was nonconductive electrically. With the use of the thermocouple sensor, the sample material is used as part of the hot-junction of the thermocouple to definitely insure that contact is made with the sample; and, consequently, for nonconductors, this method fails. To alleviate this problem somewhat, an atomic layer of aluminum was deposited on one face of the sample by vapor deposition. Although this provided for good thermal contact and good electrical conduction, the deposited aluminum did not adhere very well to the flaky specimens. The use of aluminum with its relatively low melting point also limits the operating temperature range. Further investigation in this field should be pursued.

V-44		V-62		40SA40		SMR 81-8		9790VI-126K	
Temp.*	K**	Temp.	K	Temp.	K	Temp.	K	Temp.	K
RT	0.466	RT	1.134	RT	2.155	RT	0.600	RT	0.269
RT	0.400	150	1.555	156	2.255	RT	0.579	144	0.291
144	0.456	250	2.038	250	2.655	165	0.671	200	0.287
230	0.494	500	2.475	440	3.019	200	0.631	302	0.528
450	0.466	760	2.478	510	3.283	222	0.599	515	0.518
514	0.500			650	3.313	400	0.754	670	0.562
630	0.858			938	2.835	550	1.195	785	0.570
630	0.869					585	1.582		
715	0.886					735	1.463		

* °F

** Btu/in/ft^2-hr.°F

Figure 51. Thermal Conductivity of Charred Materials

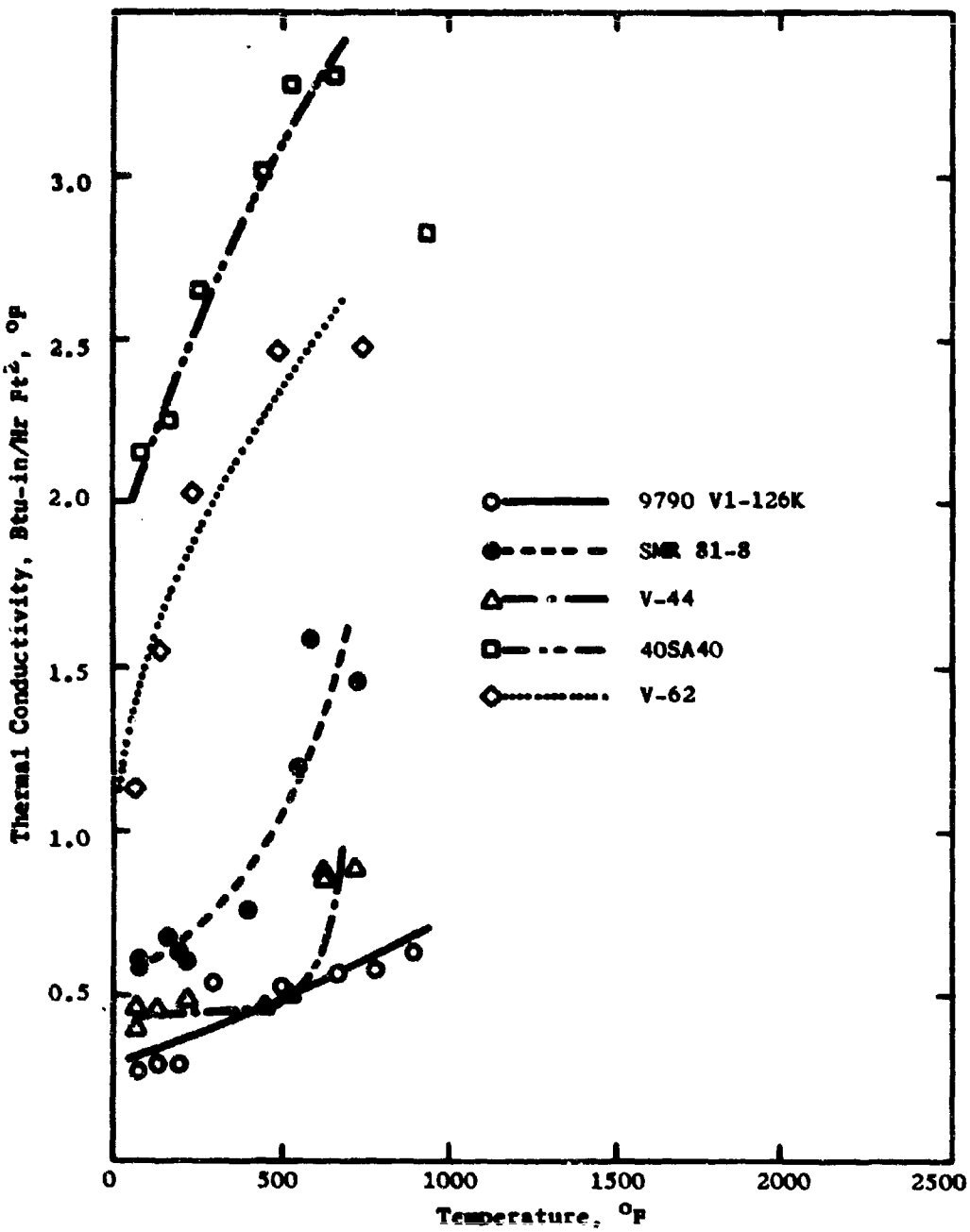

Figure 52. Thermal Conductivity of Charred Materials

III, A, Properties of Five Materials (Task A, Phase I) (cont.)

(7) Heat Capacity

The heat capacity test data are presented in Figure 53 and graphically presented in Figure 54. The data show that the V-62 and 9790VI-126K chars have the highest heat capacity.

(8) Thermal Expansion

The thermal expansion data are shown in Figure 55 in in./in.°F, and graphically presented in Figure 56 as in./in. These data show that the V-62 char would expand the least over a range of temperatures.

All data will now be used in Task C where the significant properties are to be selected by correlating these data with motor performance results from Task B.

e. General Comments

One of the significant factors that influence the performance of elastomeric insulation materials in multiple restart applications is the strength and integrity of the char layer-virgin material interface after shutdown. In the correlation motors discussion in Section B, it was shown that the chars from the five representative materials were separated from the virgin materials at the end of each firing and thus were undoubtedly lost immediately after ignition of the next pulse. This led to higher ablation rates than would have resulted if the chars had remained in place. The existence of this weak zone was shown in both the plasma-arc and charring apparatus specimens. In only a few instances was the interface intact and, in addition, the virgin decomposition zone was generally a weak, soft structure. This type of structure existed in only one location in the cycled plasma specimens, indicating that, because the char was maintained in position by the shrouding, gases from each successive heat cycle had "coked" out the previous decomposition zone.

Another factor that can influence the performance of the materials is the effect of prolonged heat soak on the virgin materials at temperature just below the char forming temperature during shutdown. Even at temperatures as low as 400°F, it was shown that some of the properties were significantly affected and that certain of the materials exhibited considerable swelling at ambient pressure, such as would be encountered during shutdown. Swelling was also evident on certain of the plasma-arc specimens and on the virgin material portion of the charring apparatus specimens. This occurred on the charring apparatus specimens after the pressure had been released and the specimens dropped away from the heating source. No swelling was noted on the portion of the specimens charred under pressure. This was evident not only from a visual examination, but also from a comparison of weight loss on machined and

Temperature, °F		V-44	V-62	40SA40	SMR81-8	9709V1-126K
500		0.2397*	0.2214	0.2561	0.2286	0.2503
		0.2384	0.2238	0.2454	0.2253	0.2587
	Average	0.2390	0.2226	0.2508	0.2269	0.2545
932		0.2741	0.2870	0.2678	0.2820	0.2852
		0.2752	0.2813	0.2652	0.2892	0.2859
	Average	0.2747	0.2855	0.2665	0.2856	0.2856
1652		0.2967	0.3077	0.2535 0.2544	0.2957	0.3342
		0.2915	0.3210	0.2593	0.3047	0.3291
	Average	0.2941	0.3144	0.2557	0.3002	0.3316

*Btu/[illegible]/°F

Figure 53. Heat Capacity of Charred Materials

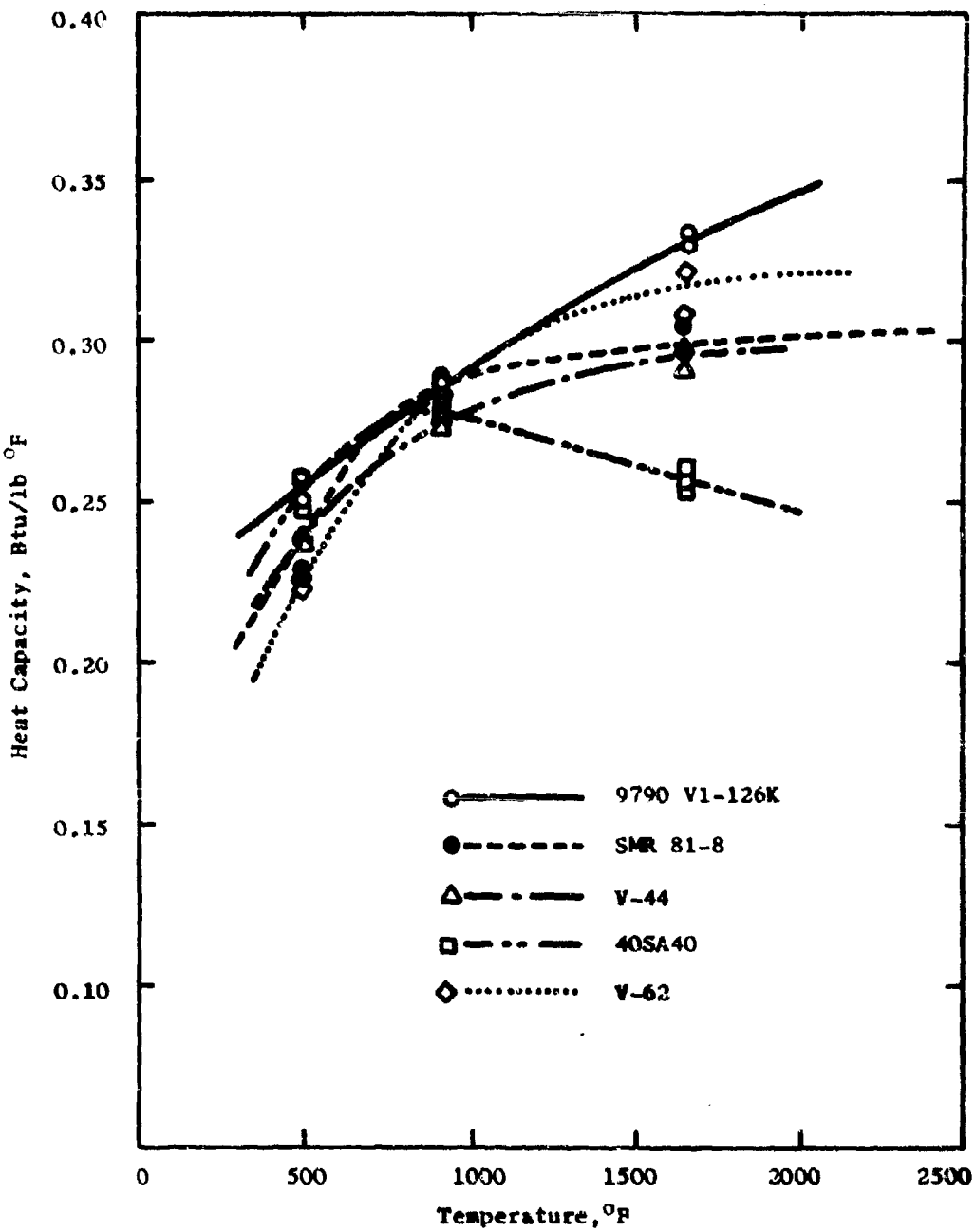

Figure 54. Heat Capacity of Charred Materials

Temperature, °F	40SA40	V-44	V-62	SMR81-8	9790V1-126K
212	3.45	0.81	0.0	5.31	0.0
572	7.75	2.34	1.11	17.8	-1.7
932	5.31	1.70	1.17	12.5	-2.33
1292	3.91	1.20	0.59	9.30	-2.42
1652	0.86	-1.12	-0.45	5.86	-4.20
Room Temperature Change	0.0012	0.0010	-0.0007	-0.0005	-0.0010

* $\frac{\text{in.}}{\text{in.-°F}} \times 10^{-6}$

Figure 55. Thermal Expansion* of Charred Material

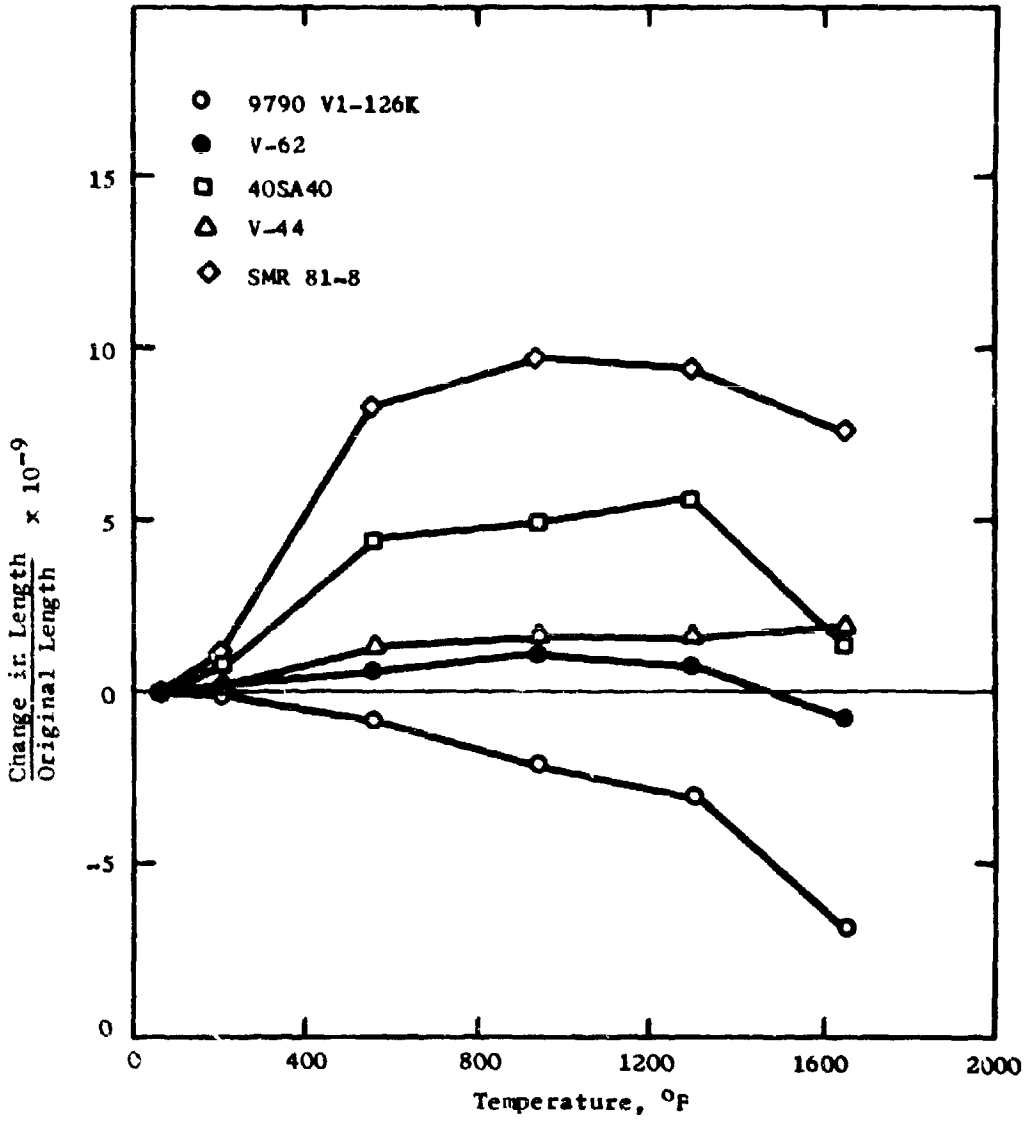

Figure 56. Thermal Expansion of Charred Materials

III, A, Properties of Five Materials (Task A, Phase I) (cont.)

measured samples versus those that were just weighed before and after charring with no correction for possible changes in dimensions.

A preliminary comparison of the five materials by their properties is shown in Figure 57. These data show that V-62, 9790VI-126K, and V-44 should perform the best in motor firings. This is the same general order obtained during the firing of the three-pulse motors.

B. CORRELATION MOTOR FIRINGS (TASK B, PHASE I)

The performances of the five basic insulation materials were obtained by using standard DM-14 (Genie) motors modified to pulse motors. The insulation specimens were located in the aft end of the motor and instrumented with thermocouples so that heat-transfer data could be obtained along with regression and ablation rates. In addition to being used in the selection of significant material properties in Task C of Phase I, these data will also be compared with computer-calculated values in Phase II. Any discrepancy observed between the experimental and calculated values will be studied to refine the model equations. Three motor-firing tests were conducted under ambient temperature conditions: a single-pulse, a two-pulse, and a three-pulse motor. End burning, cartridge-loaded grains of ANB-3066 propellant were used, operating at a nominal chamber pressure of 700 psi.

1. Design

Figure 58 shows the overall configuration of the motors, details of which are covered in Drawing 1127224. Motor design calculations (Appendix III), using the latest available property data on Minuteman propellant ANB-3066-2, indicate that a 0.958- to 0.962-in.-dia nozzle is needed to attain the desired nominal operating pressure of 700 psi. Segments of all five of the insulation materials were installed in each aft closure. Silver-infiltrated-tungsten throats and silica-phenolic nozzle approaches and insulators were used.

The heat-flux pattern expected in the aft closures was calculated with the heat-transfer coefficient given by the Colburn equation. Figure 59 shows that the cold-wall heat flux varied from approximately 40 to 565 Btu/ft^2-sec. Thermocouples were installed as shown in Figure 60. These thermocouples were located along lines passing through positions B and D (see Figure 59), corresponding to expected heat-flux levels of 225 and 100 Btu/ft^2-sec.

2. Firing of Single-Pulse Motor

The single-pulse correlation motor was successfully fired on 30 September 1966. An evaluation of the ballistic data indicates a nominal

	V-44	V-62	40SA40	SMR 81-8	9790-V1-126K
Virgin					
Heat Soak	2	1	5	4	3
Density	3	1	4	5	2
Heat Capacity	3	2	5	4	1
Thermal Conductivity	4	1	5	3	2
Heat of Combustion	3	1	4	5	2
Plasma Arc	3	1	3	4	2
Char					
Density	4	1	3	5	2
Pore Spectra	2	4	3	-	1
Shear Strength	4	1	5	2	3
Compressive Strength	1	2	3	5	3
Tensile Strength	2	1	3	4	-
Emissivity	3	5	2	1	4
Thermal Conductivity	2	4	5	3	1
Heat Capacity	4	2	5	3	1
Thermal Expansion	2	1	4	5	3

Figure 57. Property Ratings for Five Materials

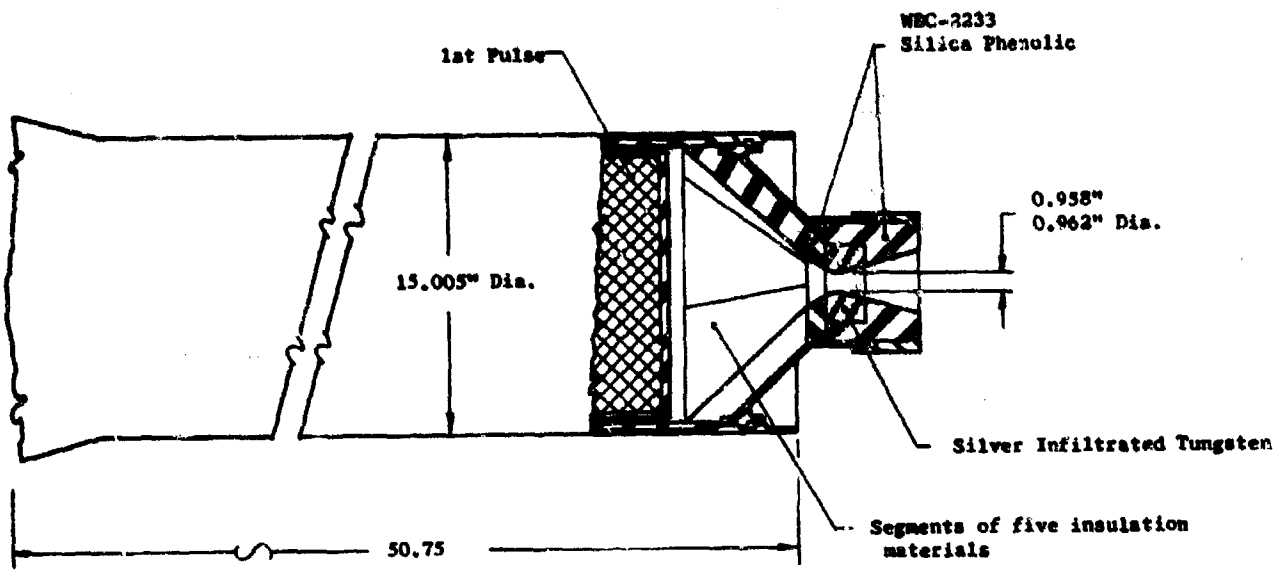

Figure 58. Correlation Pulse Motor Configuration

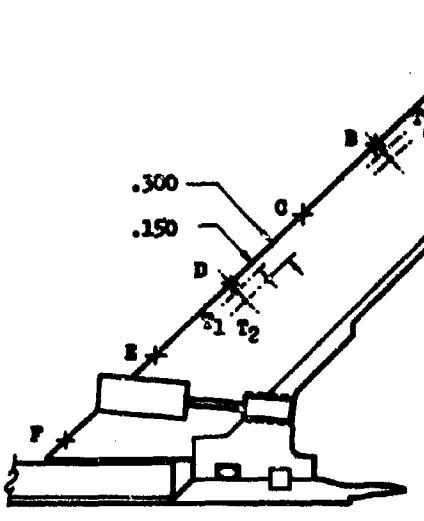

Position	Dia.	Area in.	Area Ratio	Heat Flux Btu/ft²-sec
A	3	7.069	9.791	565
B	5	19.635	27.195	225
C	7	38.485	53.303	120
D	9	63.617	88.112	78
E	11	95.033	131.625	56
F	13	132.732	183.839	41

Figure 59. Aft Closure Heat Flux Pattern, Correlation Pulse Motors

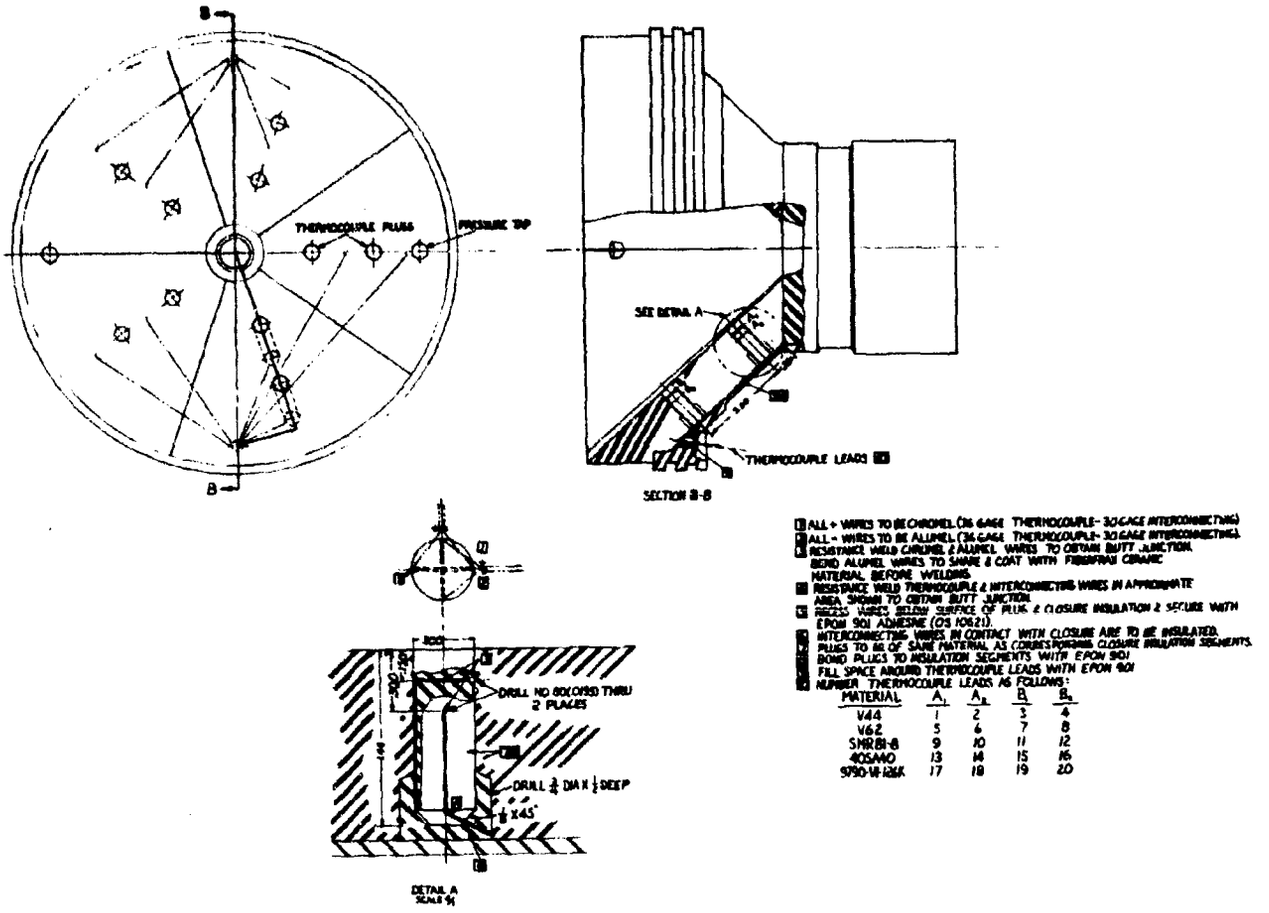

Figure 60. Thermocouples for Correlation Motors

III, B, Correlation Motor Firings (Task B, Phase I) (cont.)

operating chamber pressure of 615 psi, a burn time of 34.71 sec, and a burning rate of 0.321 in./sec. The pressure-time trace for the motor is presented in Figure 61. Prefiring and postfiring photographs of the motor and insulated aft closure are shown in Figures 62 to 67.

3. Firing of Two-Pulse Motor

The first pulse of the two-pulse correlation motor was successfully fired on 10 October 1966, but a hang-fire occurred on second-pulse ignition. The hang-fire was traced to an open circuit in the ignition system within the motor, which presumably occurred during first pulse firing, since the circuitry had been checked for continuity just before countdown. The hang-fire necessitated disconnecting all instrumentation and removing of the motor from the test stand. New ignition leads were installed, and the second pulse was fired successfully on 18 October 1966. The ballistic data indicate nominal operating chamber pressures of 657 and 640 psi, burn times of 17.74 and 17.06 sec, and burning rates of 0.319 and 0.322 in./sec, respectively. Figure 68 presents the pressure-time trace for the motor. Postfiring photographs of the motor are shown in Figures 69 and 70. Postfiring views of the insulated aft closure are shown in Figure 71 for the first pulse and in Figure 72 for the second pulse. In both the two- and three-pulse motors, the V-62 samples were 2-in.-wide bars rather than 1/5 segments. 40SA40 was used on both sides of the bars.

4. Firing of the Three-Pulse Motor

The three-pulse correlation motor was successfully fired on 7 November 1967. Evaluation of the ballistic data indicates nominal operating chamber pressures of 678, 715, and 718 psi; burn times of 10.75, 10.92, and 10.55 sec; and burning rates of 0.345, 0.340, and 0.351 in./sec, respectively. The pressure-time trace for the three-pulse motor is presented in Figure 73. Postfiring photographs of the motor and insulated aft closure are shown in Figures 74 to 75.

The firing data for all three correlation motors are summarized in Figure 76. The variability in the nominal operating pressures between the three correlation motors can be partially explained by slight differences in propellant burning rates, but the basic explanation is revealed in the shape of the pressure curves in relation to burn time. All curves had the same general shape, exhibiting higher pressures during the initial phases of the firing and gradually dropping off as the firings progressed. However, in the three-pulse motor in particular, and to some degree in the two-pulse motor, the firings terminated while the pressures were at higher levels than in the single-pulse motor. This led to higher nominal operating pressures.

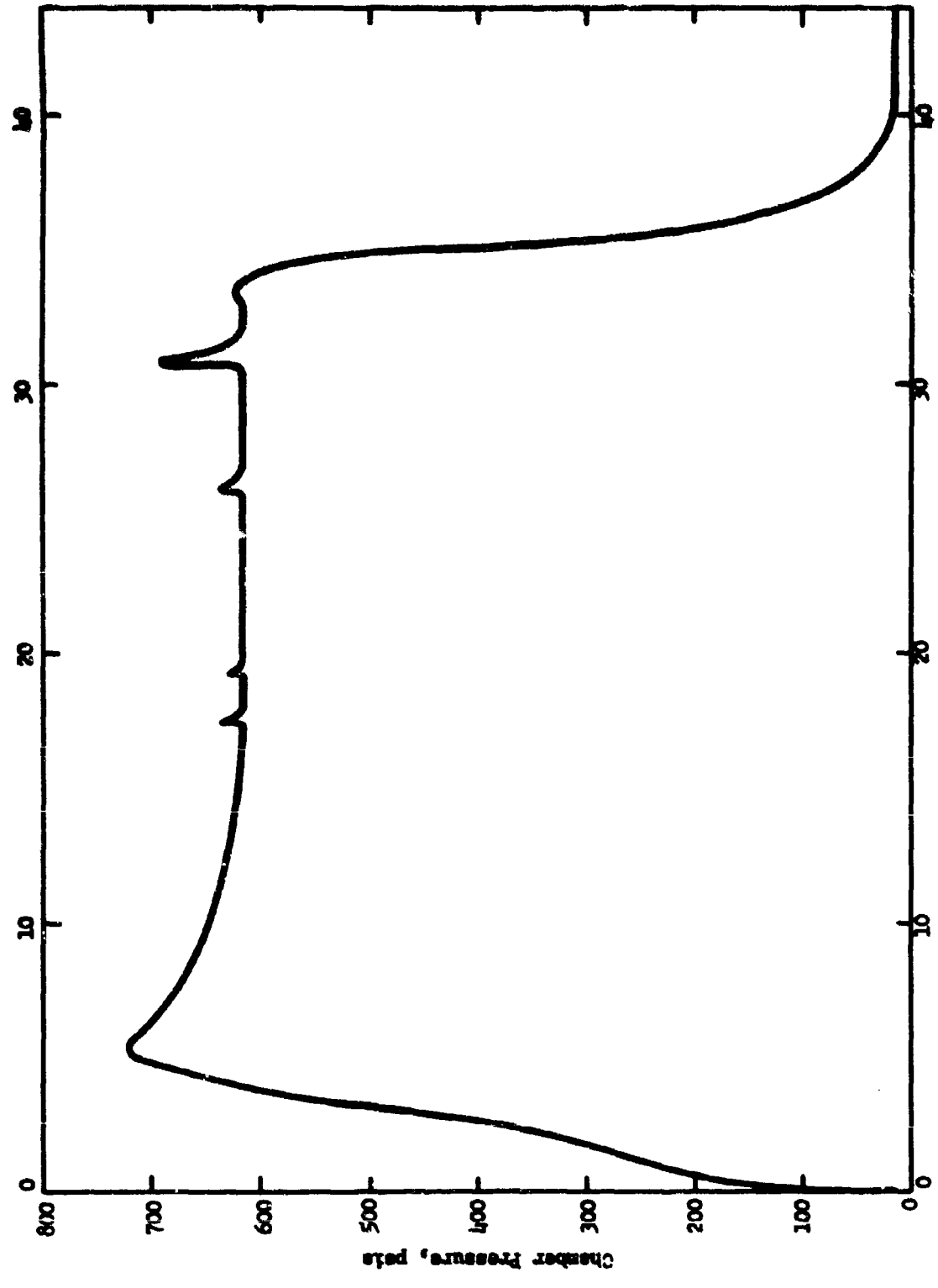

Figure 61. Chamber Pressure, Correlation Motor 1--Single Pulse

Figure 62. Prefire Close-up of Nozzle on Single-Pulse Motor

Figure 63. Prefire View of Single-Pulse Motor

Figure 64. Postfire Close-up of Nozzle on Single-Pulse Motor

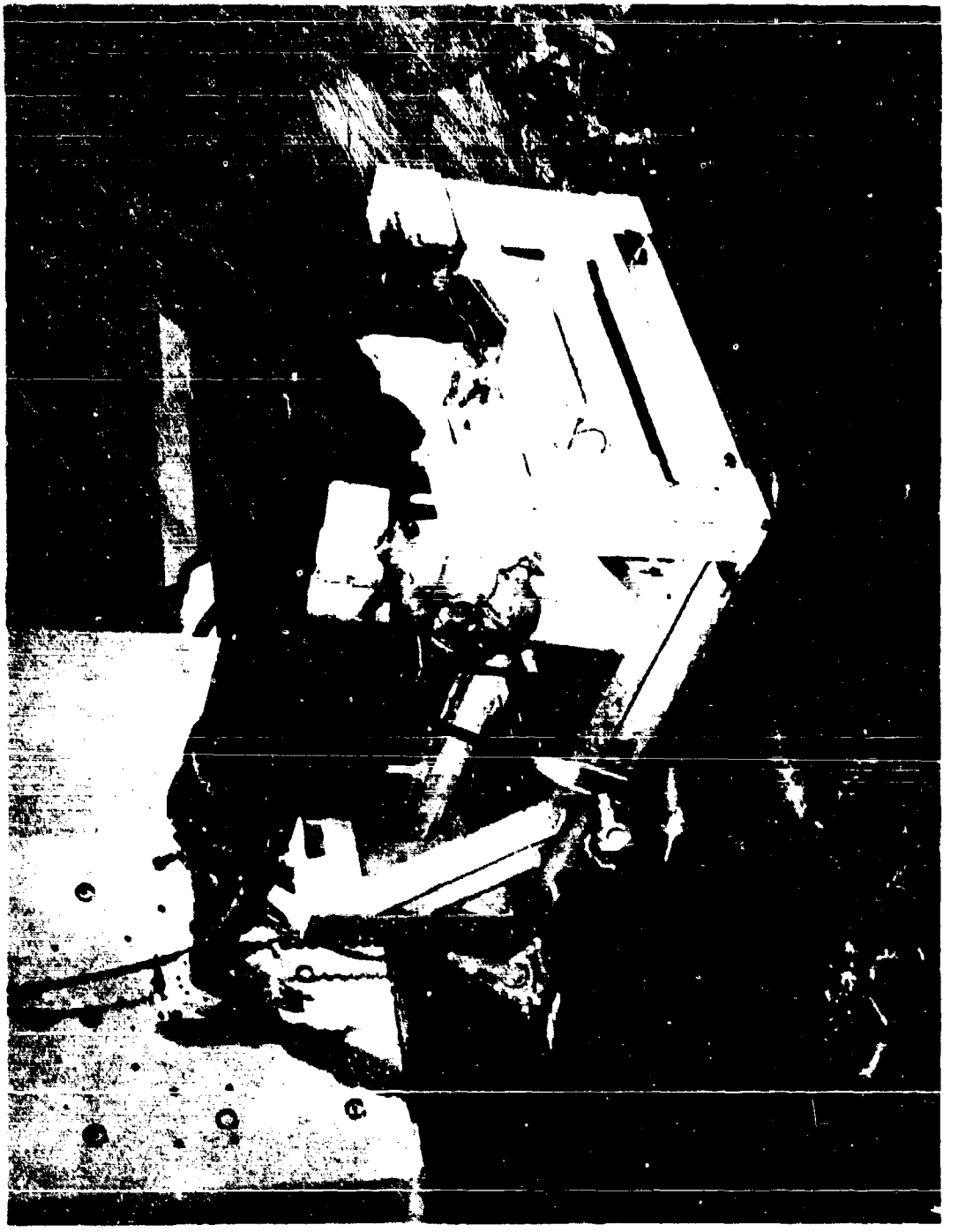

Figure 65. Postfire View of Single-Pulse Motor

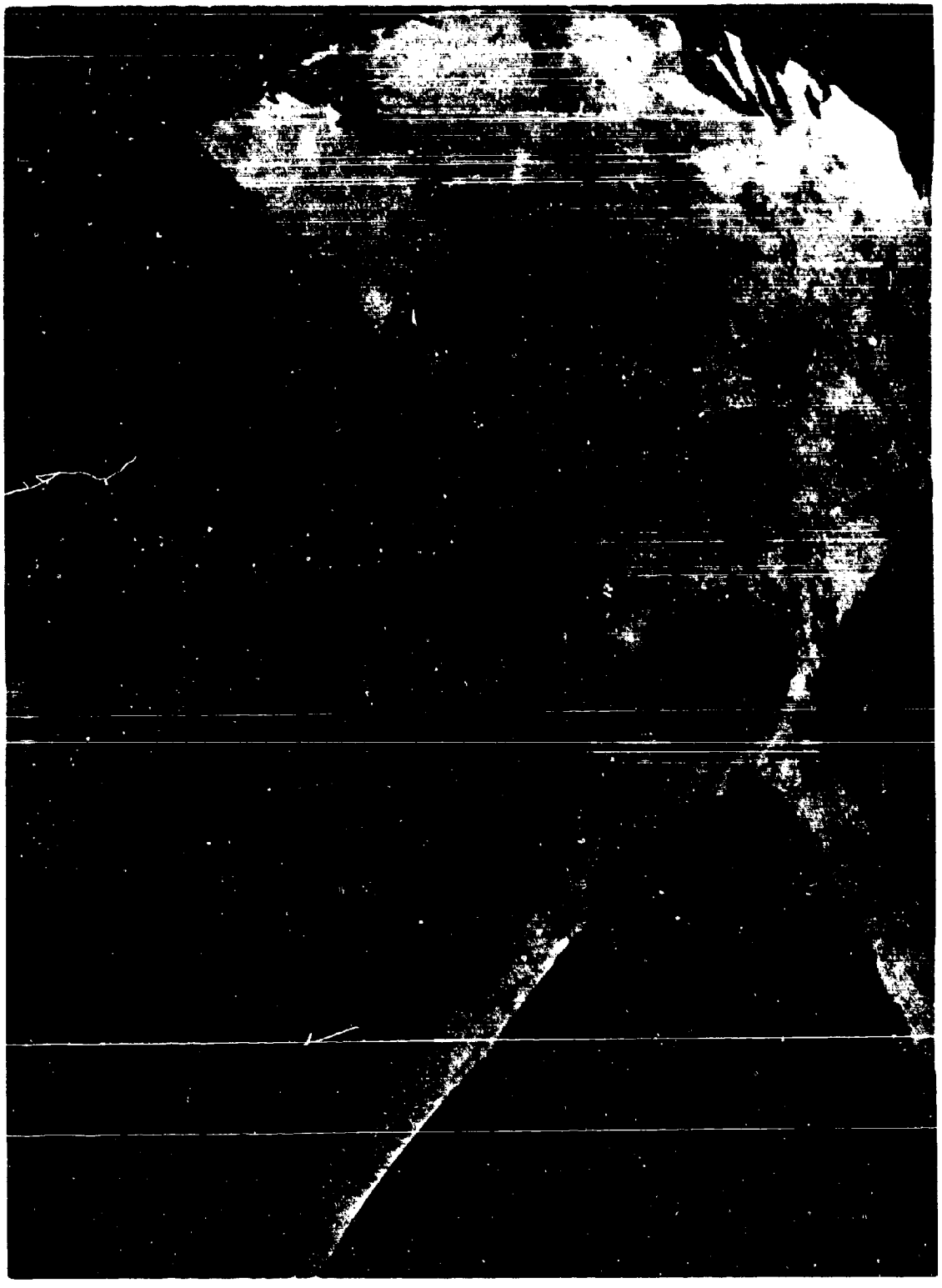

Figure 66. Prefire View of Insulated Aft Closure on Single-Pulse Motor

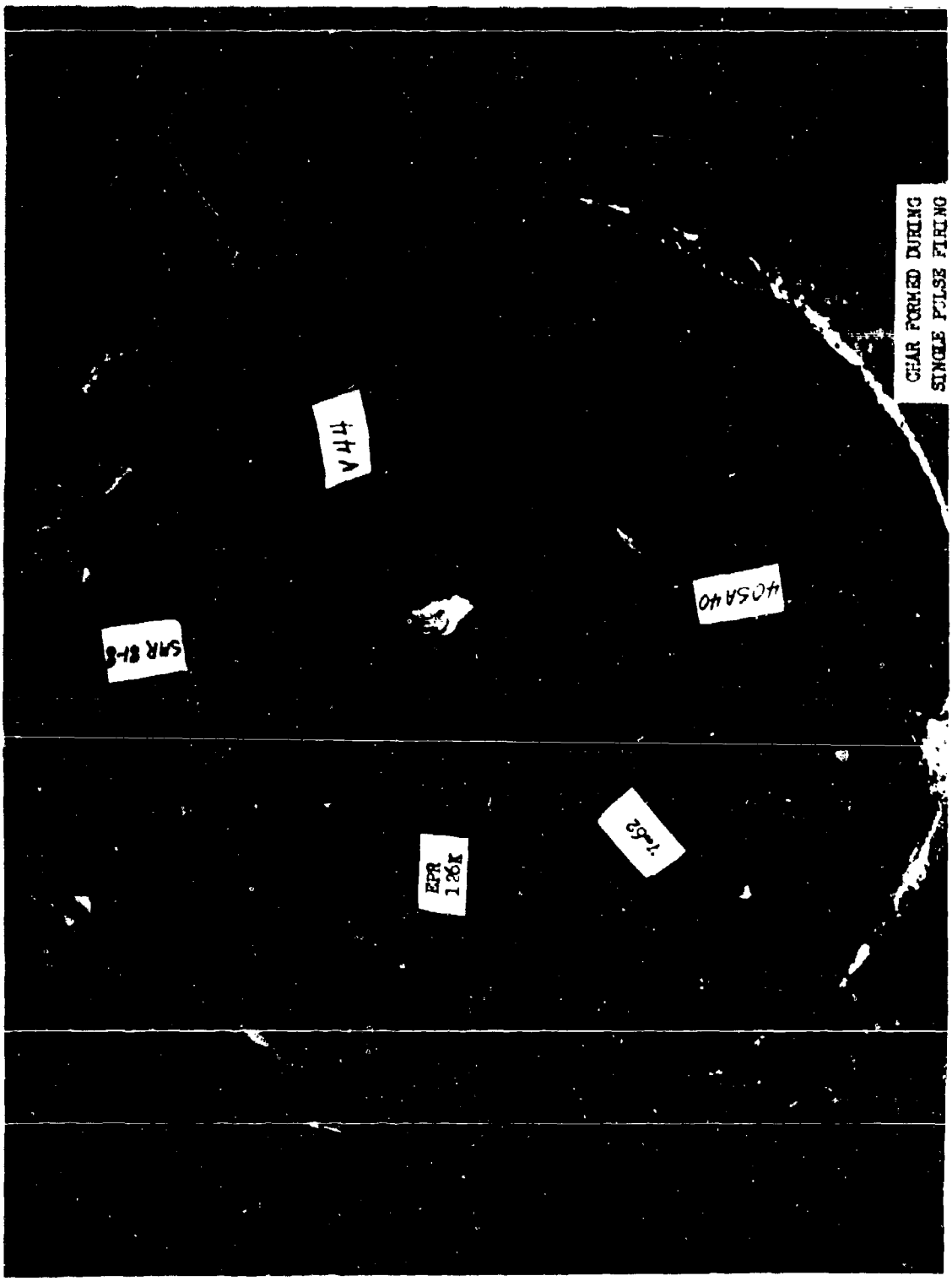

Figure 67. Postfire View of Insulated Aft Closure on Single-Pulse Motor

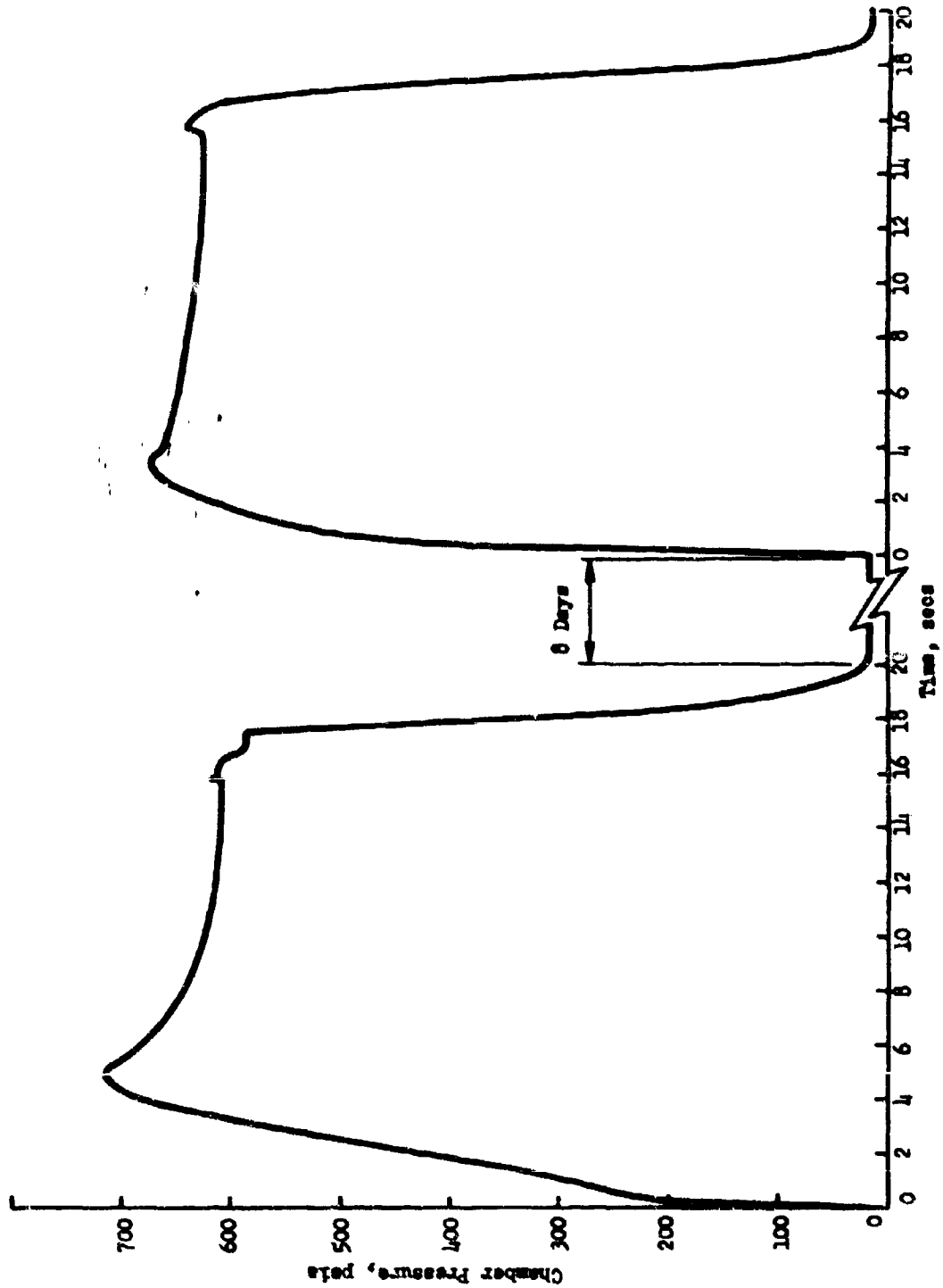

Figure 68. Chamber Pressure, Correlation Motor 2, Two-Pulse Motor

Figure 69. Postfire Close-up of Nozzle on Two-Pulse Motor

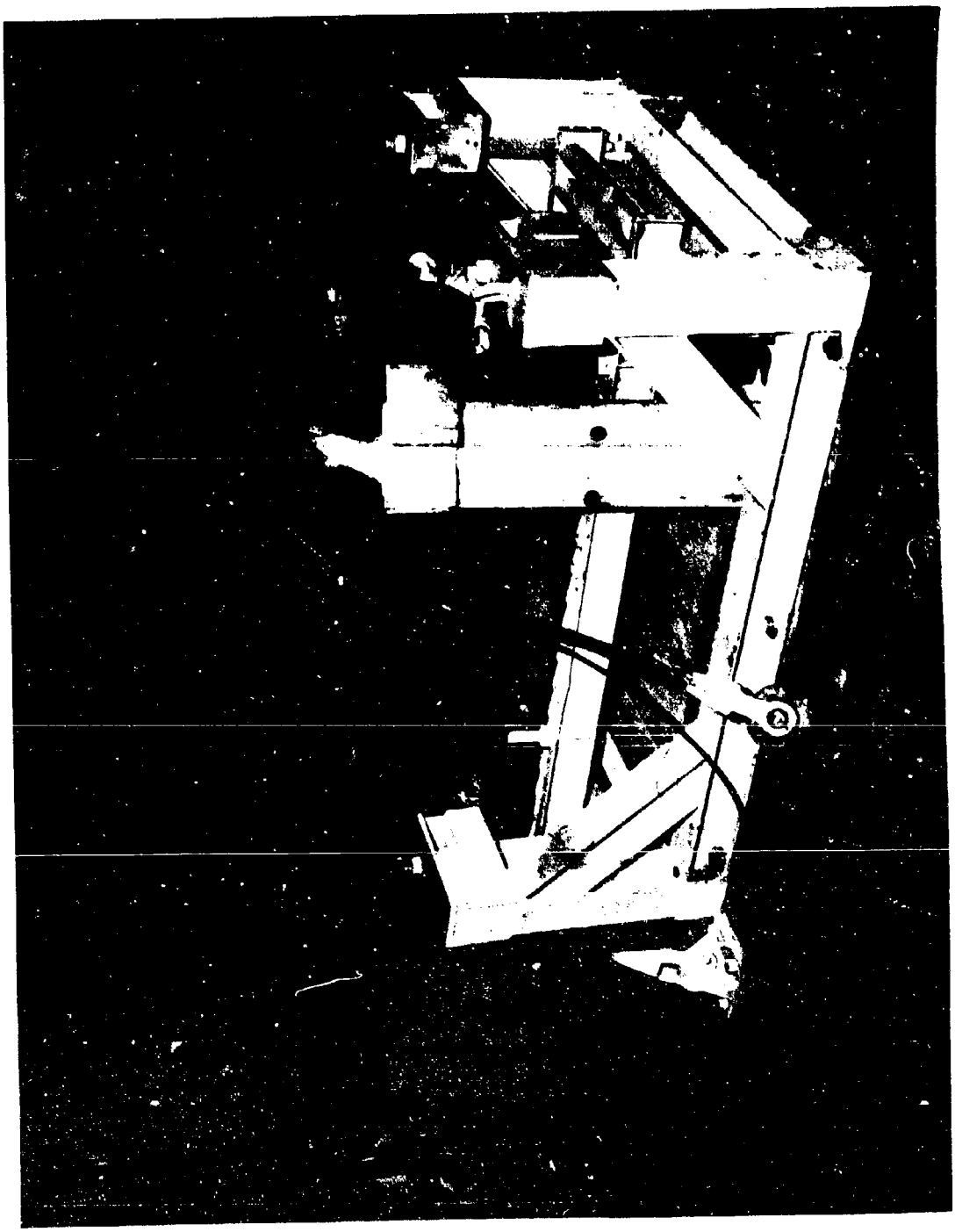

Figure 70. Postfire View of Two-Pulse Motor

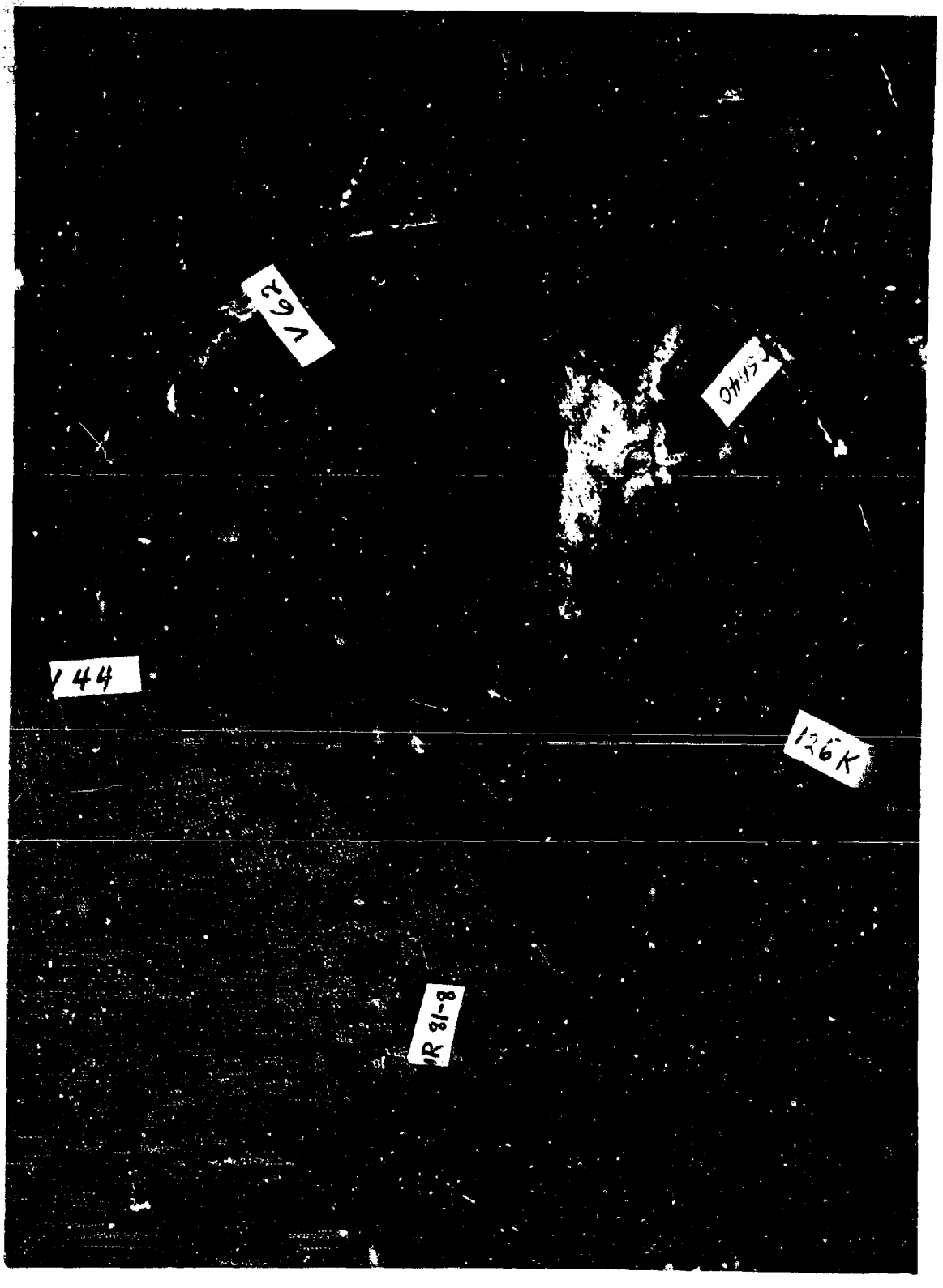

Figure 71. Postfire View of Insulated Aft Closure after First Pulse on Two-Pulse Motor

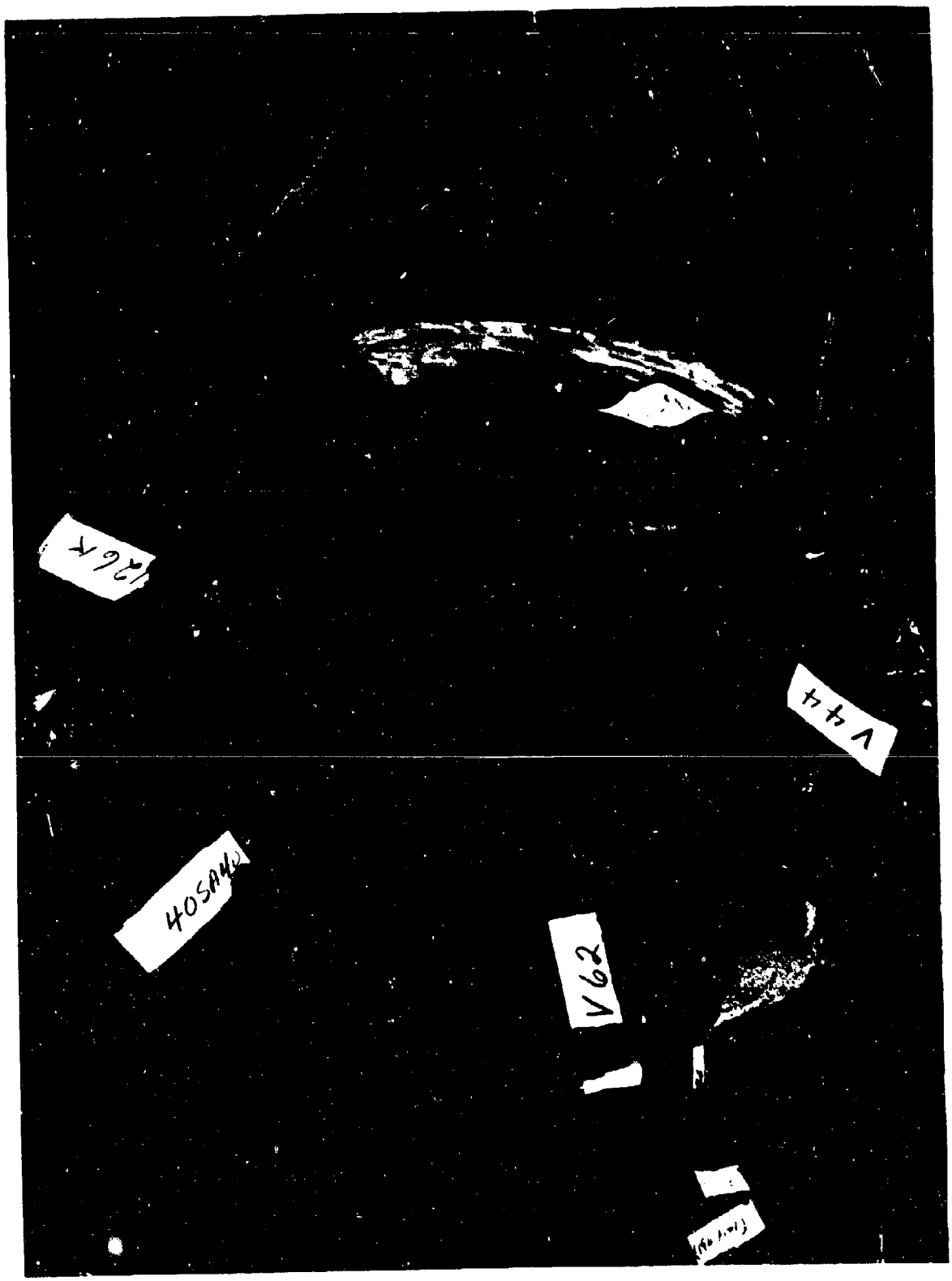

Figure 72. Postfire View of Insulated Aft Closure after First Pulse on Two-Pulse Motor

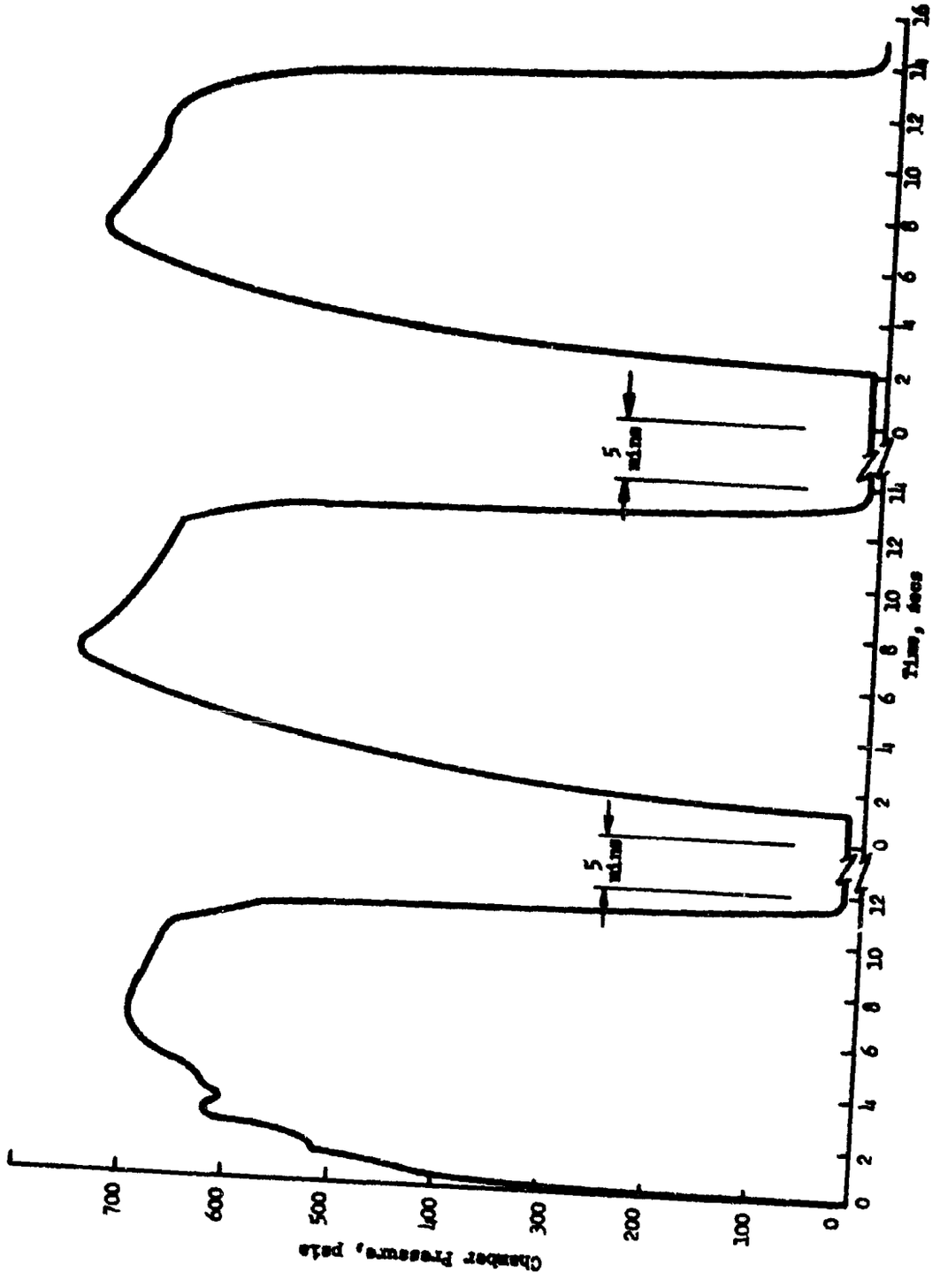

Figure 73. Chamber Pressure, Correlation Motor 3, Three-Pulse Motor

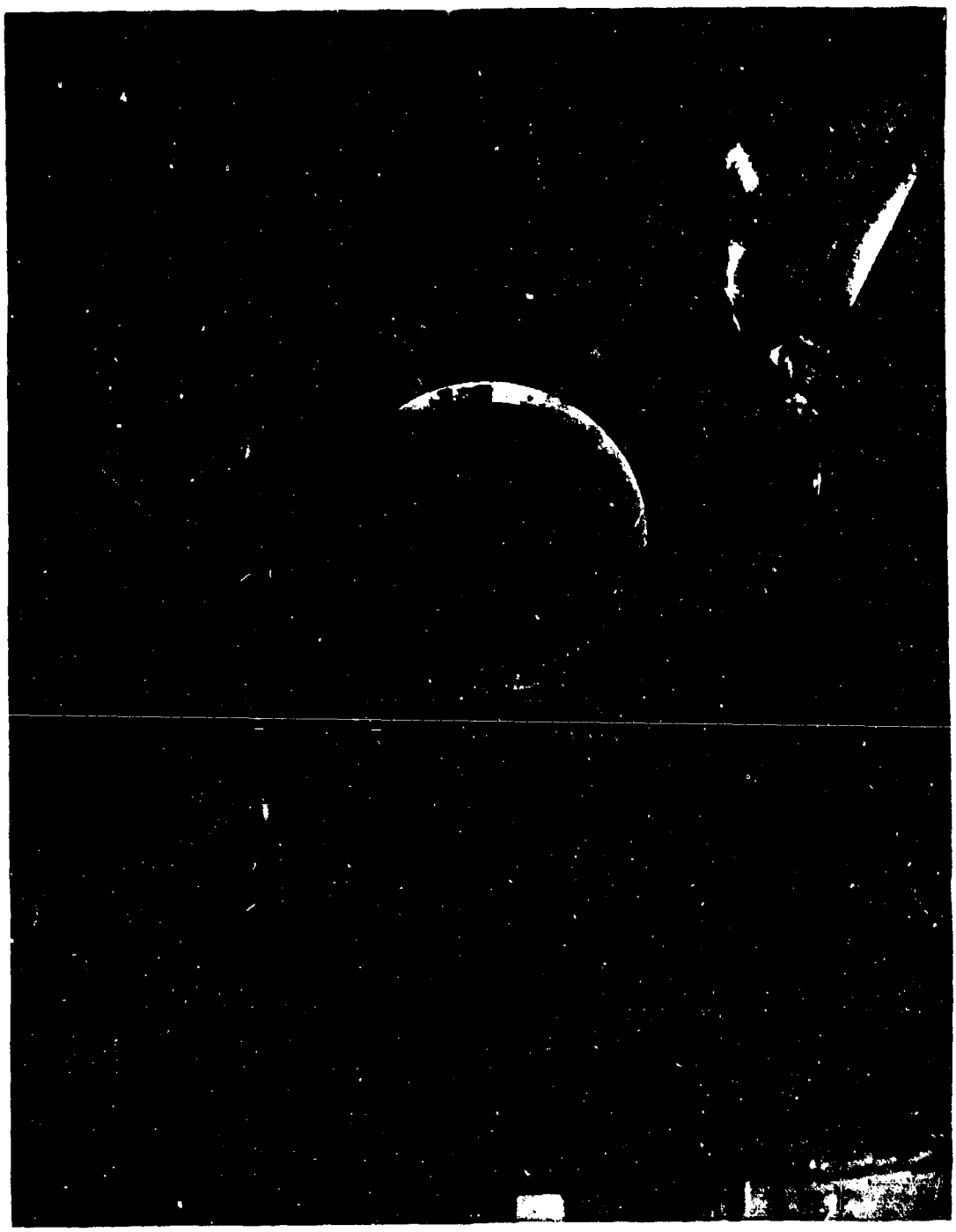

Figure 74. Postfire Close-up of Nozzle on Three-Pulse Motor

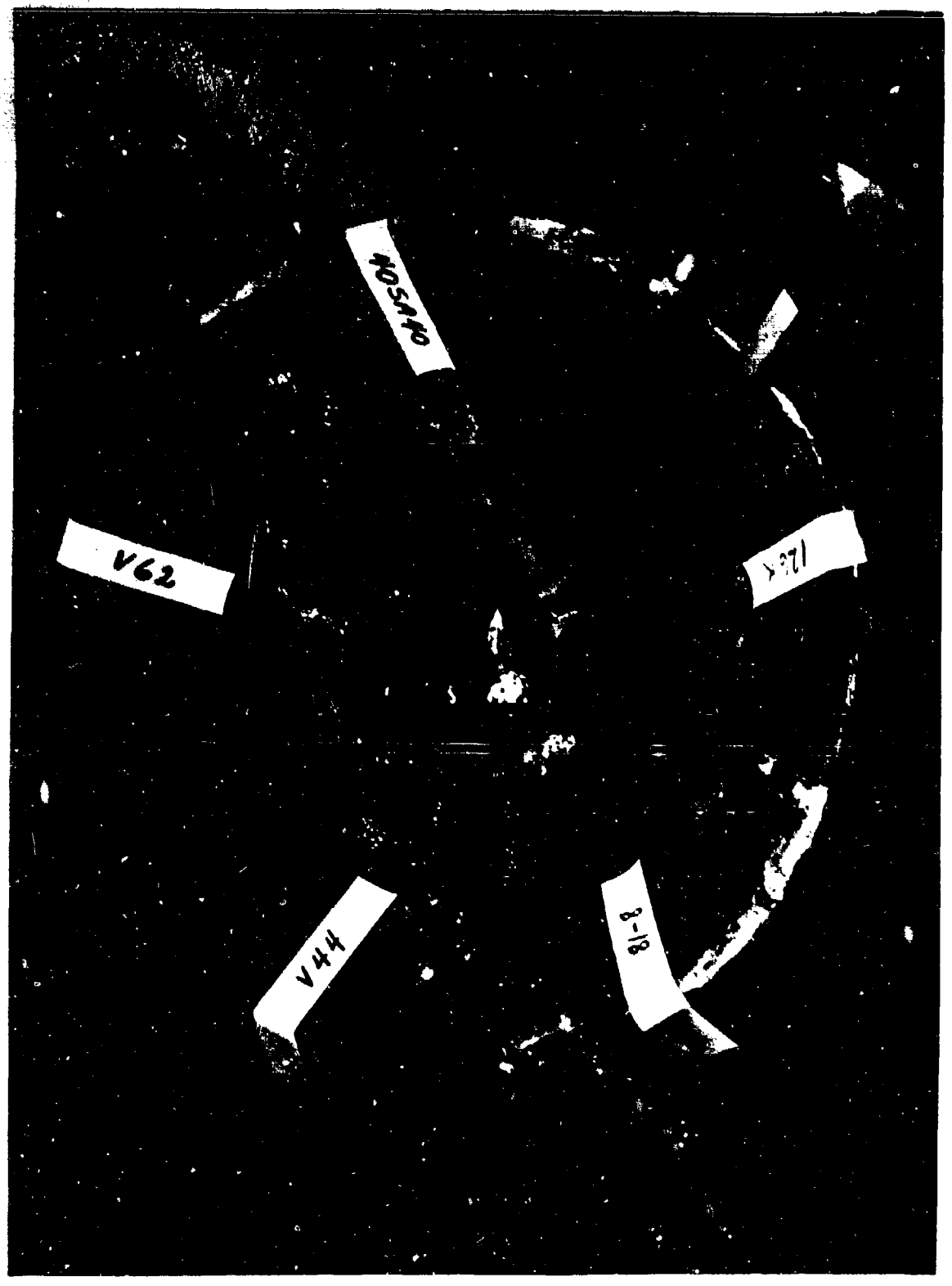

Figure 75. Postfire View of Insulated Aft Closure on Three-Pulse Motor

	Motor Number					
	1	2		3		
Pulse	1	1	2	1	2	3
Nominal Operating Pressure, psig	615	657	640	678	715	718
Burn Time, sec	34.71	17.74	17.06	10.74	10.92	10.55
Time Between Pulses	-	8 days		5 mins	5 mins	
Average Thrust, lbs	564	550	579	631	612	619
Total Impulse, lb-sec	21,949	10,895	10,839	7,304	7,280	7,309
I_s, sec	228.9	228.9	230.6	229.6	231.1	232.0
Propellant Weight, lb	95.9	47.6	47.0	31.8	31.5	31.5
Propellant Dims., in						
Length	11.15	5.558	5.500	3.71	3.71	3.70
Diameter	13.125	13.120	13.122	13.120	13.125	13.125
Burning Rate, in/sec	0.321	0.319	0.322	0.345	0.340	0.351
Insulation Materials						
Chamber Side Wall	SD829	SD829		40SA40		
Nozzle Entrance	WBC-2233	WBC-2253		WBC-2230		
Nozzle Exit	WBC-2233	WBC-2253		WBC-2230		
Aft Closure	← V-44, V-62, 81-8, 9790VI-126K, 40SA40 →					

Figure 76. Summary of Correlation Motor Firing Data

III, B, Correlation Motor Firings (Task B, Phase I) (cont.)

5. Postfiring Analysis

At the conclusion of each firing, the remaining char thicknesses were measured first, and then the aft closures were sectioned into five pieces and measured for lost virgin material. Average char thicknesses and observations on the condition of the char are presented in Figure 77. All char had separated from the virgin material at the end of the firings, except in a few areas of the 408A40 material. Section drawings covering the regression and ablation profiles for all materials are shown in Figures 78 through 80. The resulting regression and ablation rates for all three motors are tabulated in Figure 81 and graphically presented in Figures 82 and 83 as a function of mass flux. These data indicate that of the five materials tested, the V-62 and 9790VI-126K materials performed the best in the single-pulse motor. In the multipulse motors, the V-62 exhibited the best performance at the lower mass-flux levels, while V-44 had the best performance at the higher mass-flux levels. These results correlate quite well qualitatively with plasma-arc data on the same materials (see Figure 84).

The three motor firings, conducted under the same firing conditions and for the same total durations, have also demonstrated (see Figure 85) that all five materials had higher ablation and regression rates in the two- and three-pulse firings than in the single-pulse firings, undoubtedly because much of the protective char formed during each pulse was lost immediately after ignition of the next pulse. That the char is lost is indicated by the progressive reduction in remaining char thicknesses in the two- and three-pulse motors and, as mentioned above, by separation of all char from the virgin material at the end of each firing.

As also noted in Figure 85, the ablation rates of some of the materials were higher in the two-pulse than in the three-pulse motor. If the char is lost between pulses, as surmised above, each subsequent firing is essentially a new firing. The ablation rates should, therefore, have been the highest in the three-pulse motor because of its shorter burn time per pulse: 34.7, 17.4, and 10.74 sec for the single-, two-, and three-pulse motors, respectively. It is not yet known whether the hang-fire in the two-pulse motor, with its long delay between pulses (8 days versus 5 min in the three-pulse motor) could have contributed to the increased rates. The exact significance of this delay will be verified in Phase III of the program, when the 5- and 12-pulse verification motors are fired. Along this same line, total ablation has been plotted against burn time per pulse in Figure 86 for heat-flux levels of 50, 100, 225, and 400 Btu/ft^2-sec. These curves, presumably, can be used to estimate total ablation for any combination of pulses. For example, if V-62 is selected as one of the materials to be tested in the 5- and 12-pulse motors, it should have, at the heat-flux level of 100 Btu/ft^2-sec, a total ablation

Motor	Material				
	V-44	V-62	408A40	SMR 81-8	9790V1-126K
Single-Pulse					
Thickness:	0.139	0.173	0.142	0.100	0.041
Comments:	Tough char; some erosion pattern; soft flakey spots; broken into good-size pieces when handled.	Fragile char; somewhat tougher than SMR 81-8.	Held together very well; some local erosion.	Very fragile; delaminated easily; broke into small pieces when handled.	Tough char; quite uniform in thickness; no erosion pattern; broke into large pieces when handled.
Two-Pulse					
Thickness:	0.095	0.075	0.096	0.071	0.057
Comments:	Broke into medium-size pieces when handled; pieces quite tough.	Char mostly disappeared; very fragile; delaminated.	Held together very well; good tough char; broke into large pieces when handled; portion of char integral with virgin material near nozzle.	Very fragile; broke into very small pieces when handled.	More erosion than single pulse; char more fragile; broke into smaller pieces when handled.
Three-Pulse					
Thickness:	0.058	0.042	0.083	0.035	0.043
Comments:	Broke into medium-size pieces when handled; fairly tough char.	Very fragile and flakey char; number of small pieces delaminated.	Number of large pieces; good tough char.	Very fragile; number of small pieces.	More fragile than single-pulse; broke into small pieces when handled.

Figure 77. Average Char Thicknesses in Correlation Motors

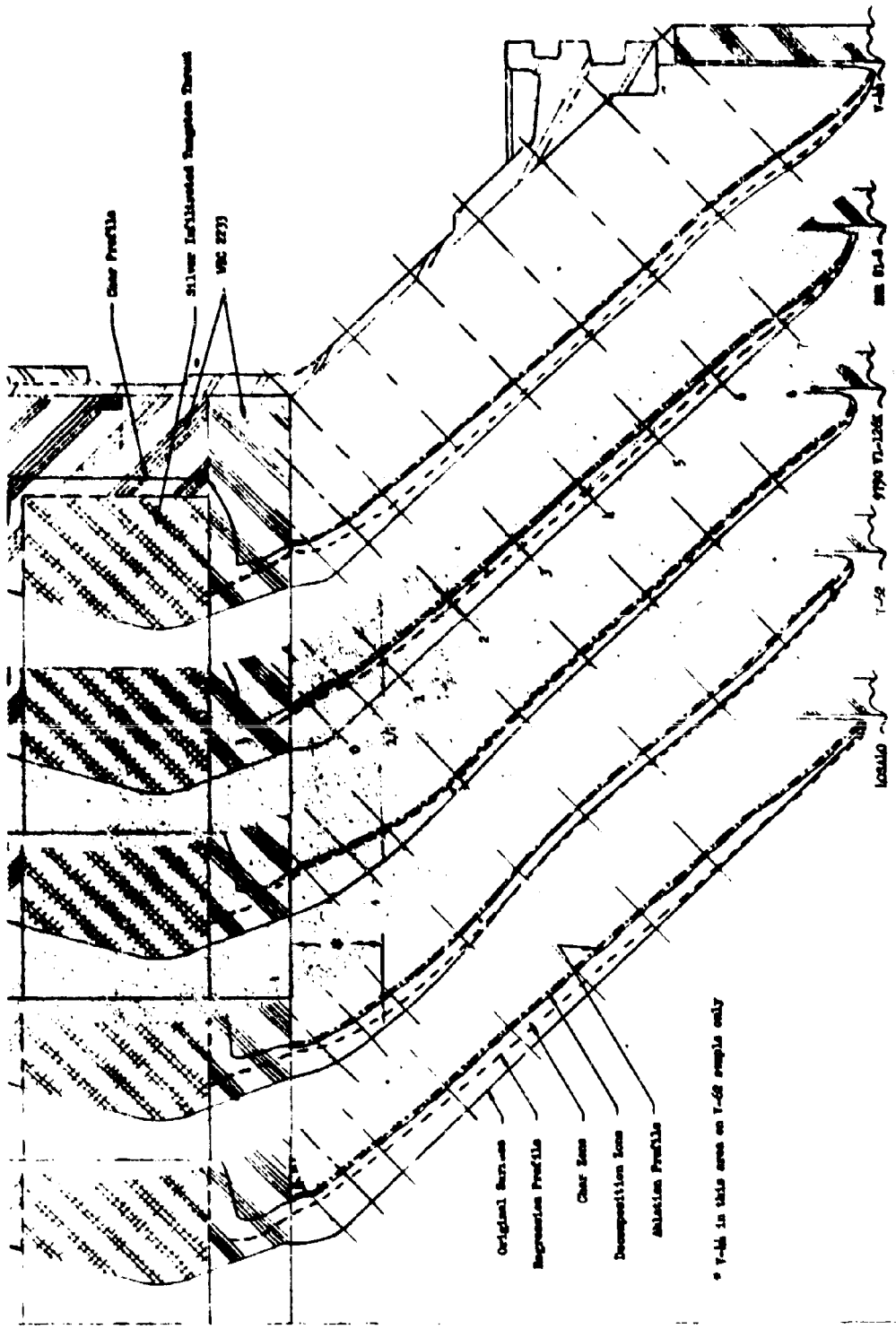

Figure 78. Section through Aft Closure of Single-Pulse Motor Showing Regression and Ablation Profiles

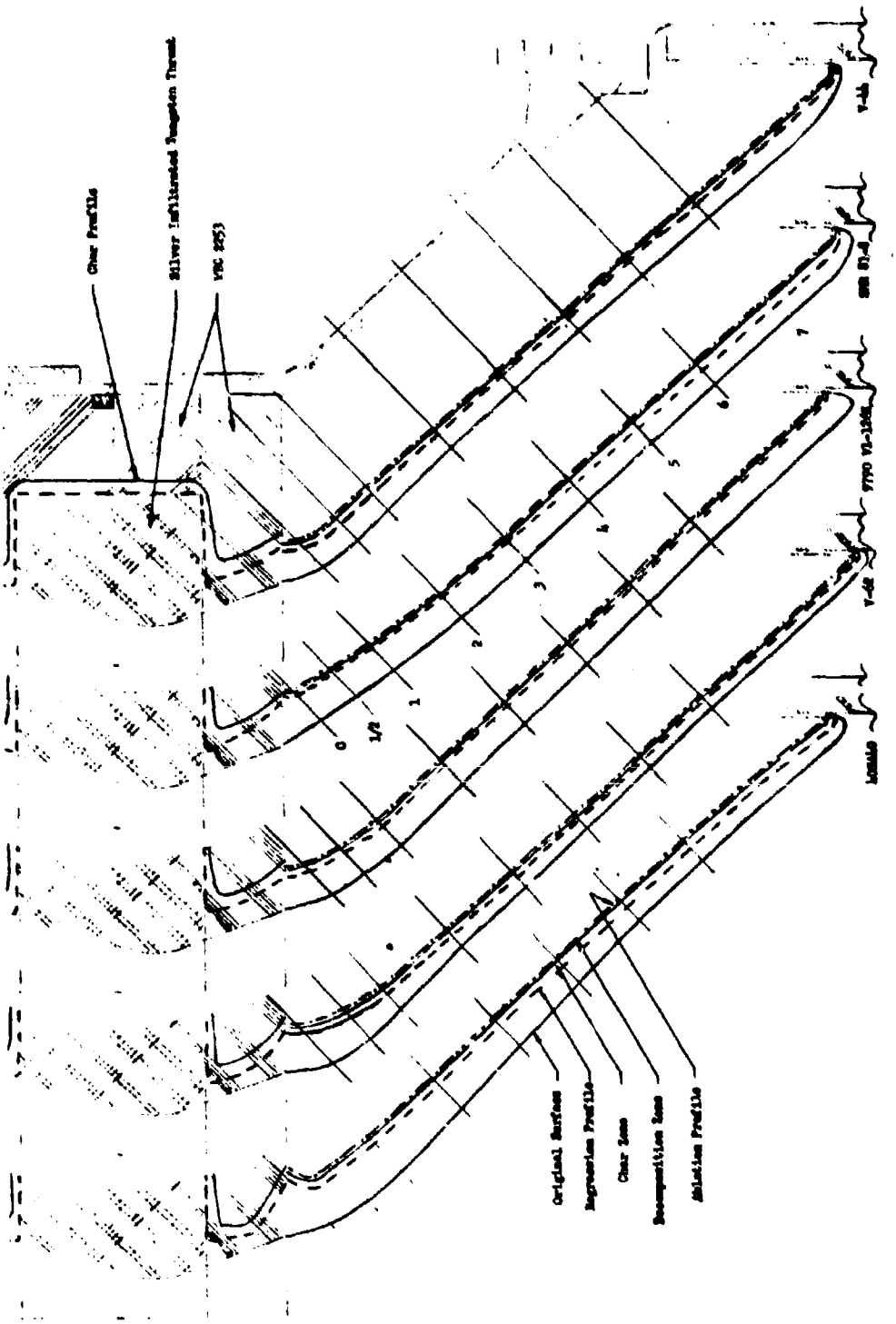

Figure 79. Section through Aft Closure of Two-Pulse Motor Showing Regression and Ablation Profiles

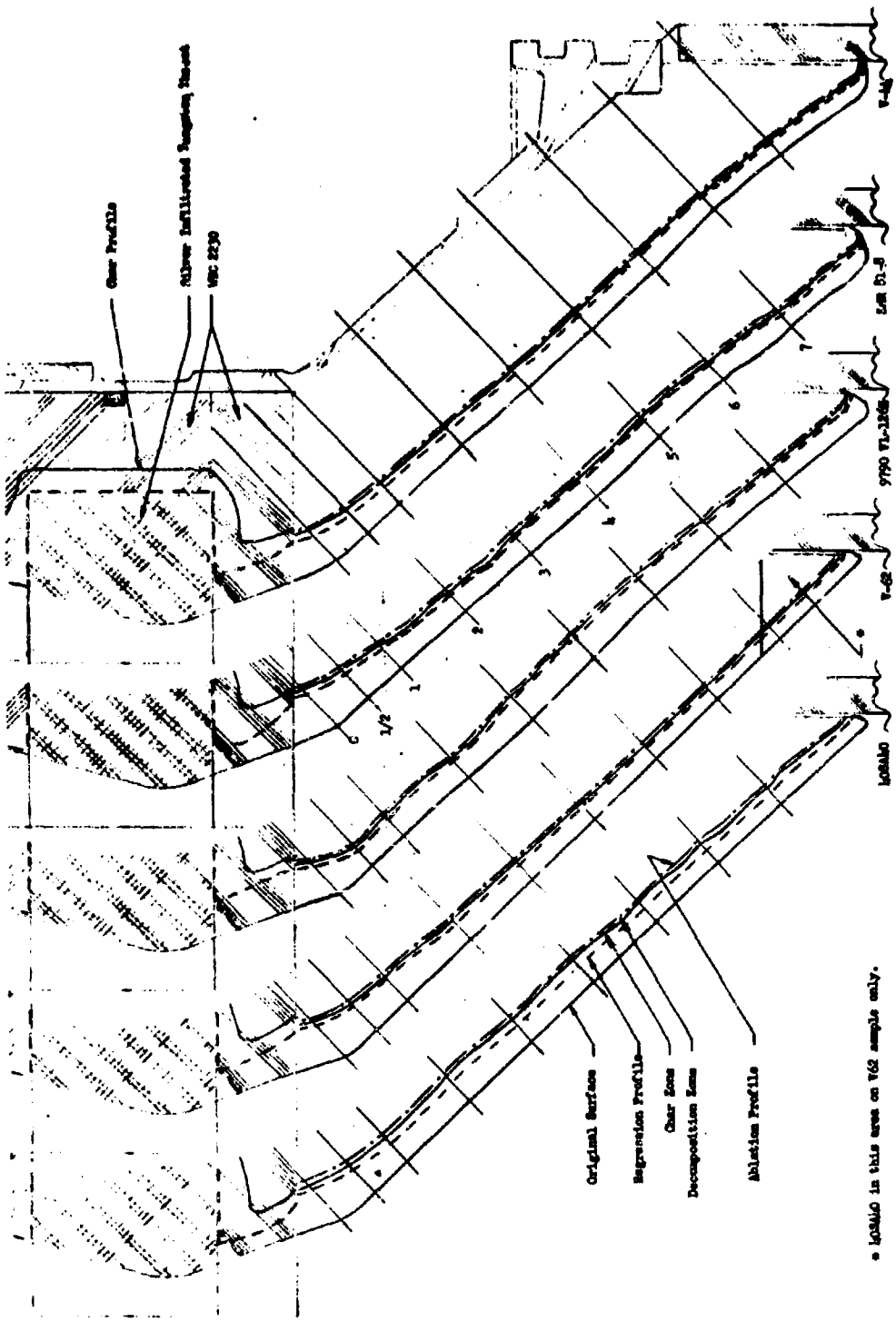

Figure 80. Section through Aft Closure of Three-Pulse Motor Showing Regression and Ablation Profiles

Station No.(1)	0	1/2	1	2	3	4	5	6	7
	5.78	9.05	13.55	26.4	44.1	65.6	90.7	120.5	154.1
Ablation Rates, mils/sec									
Single-Pulse									
9790V1-126K	14.7	11.9	8.4	4.9	4.3	4.3	4.2	3.7	3.9
V-62	-	-	8.6	5.9	4.5	4.4	4.4	4.8	4.4
V-44	15.1	10.9	9.9	8.2	7.1	6.6	6.3	6.3	6.6
SMR 81-8	16.4	12.9	10.8	9.7	8.8	8.4	7.7	7.2	5.6
40SA40	17.3	14.8	13.5	11.5	10.4	9.3	7.9	6.9	4.6
Two-Pulse									
9790V1-126K	12.6	11.6	11.3	10.9	10.6	10.5	10.0	9.9	-
V-62	17.6	13.4	10.9	8.8	7.5	6.7	6.6	6.2	-
V-44	11.2	10.5	10.4	9.8	9.6	9.5	9.3	9.1	-
SMR 81-8	14.2	12.6	11.8	11.6	11.2	10.9	10.8	10.6	-
40SA40	17.2	16.5	16.1	14.6	13.0	11.7	9.8	9.5	-
Three-Pulse									
9790V1-126K	17.8	12.5	12.0	10.5	10.9	10.4	9.2	8.9	8.8
V-62	18.8	13.2	12.4	9.8	8.4	7.9	6.8	5.8	-
V-44	15.1	11.1	10.5	9.9	10.1	9.8	9.3	7.5	6.5
SMR 81-8	19.9	15.5	13.5	11.3	11.2	11.0	10.8	10.6	8.9
40SA40	22.5	16.0	14.5	13.1	11.0	11.1	9.7	9.3	8.7
Regression Rates, mils/sec									
Single-Pulse									
9790V1-126K	13.0	10.2	6.7	3.1	2.7	2.4	2.4	2.0	2.0
V-62	-	4.3	2.6	1.2	-0.1	-0.7	-0.9	-1.2	-1.2
V-44	10.4	6.1	4.9	3.5	2.3	2.3	2.	2.5	2.3
SMR 81-8	13.1	9.9	7.3	5.9	4.3	3.0	2.3	2.4	2.0
40SA40	12.7	10.7	9.3	6.9	4.9	3.7	2.1	0.9	-0.1
Two-Pulse									
9790V1-126K	10.5	9.7	9.3	8.7	8.5	8.2	7.9	7.7	-
V-62	14.2	9.7	6.8	5.2	4.3	4.1	4.3	3.9	-
V-44	7.6	7.9	6.6	6.1	6.0	6.3	6.0	5.7	-
SMR 81-8	11.6	10.0	9.3	8.9	8.4	7.3	6.8	6.0	-
40SA40	12.7	12.1	11.7	10.4	8.9	7.7	6.2	6.3	-
Three-Pulse									
9790V1-126K	15.1	11.2	9.3	8.5	8.7	8.4	7.6	7.3	7.3
V-62	13.7	11.4	10.5	7.6	6.1	6.3	5.1	4.2	-
V-44	11.2	8.4	8.0	7.5	7.4	7.0	6.7	5.7	5.0
SMR 81-8	17.1	12.9	10.9	9.0	9.2	9.0	8.2	8.2	7.2
40SA40	19.3	12.4	11.0	8.3	7.0	7.4	5.8	5.4	5.2

(1) Located axially along insulation surface, 1" spacing starting 1/2" from nozzle end.

Figure 81 Ablation and Regression Rates for Correlation Motors

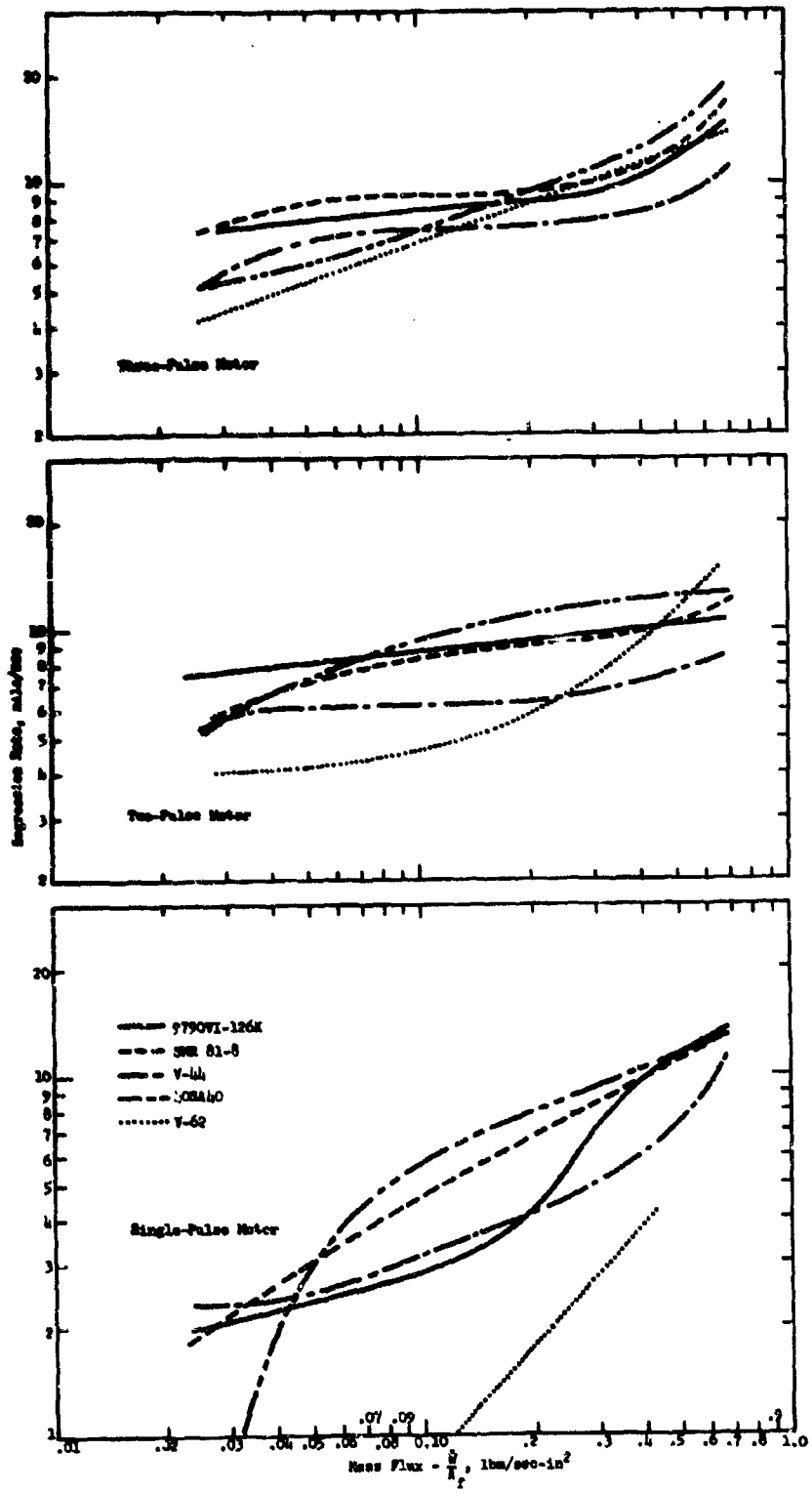

Figure 82. Regression Rate of Correlation Motors vs Mass Flux

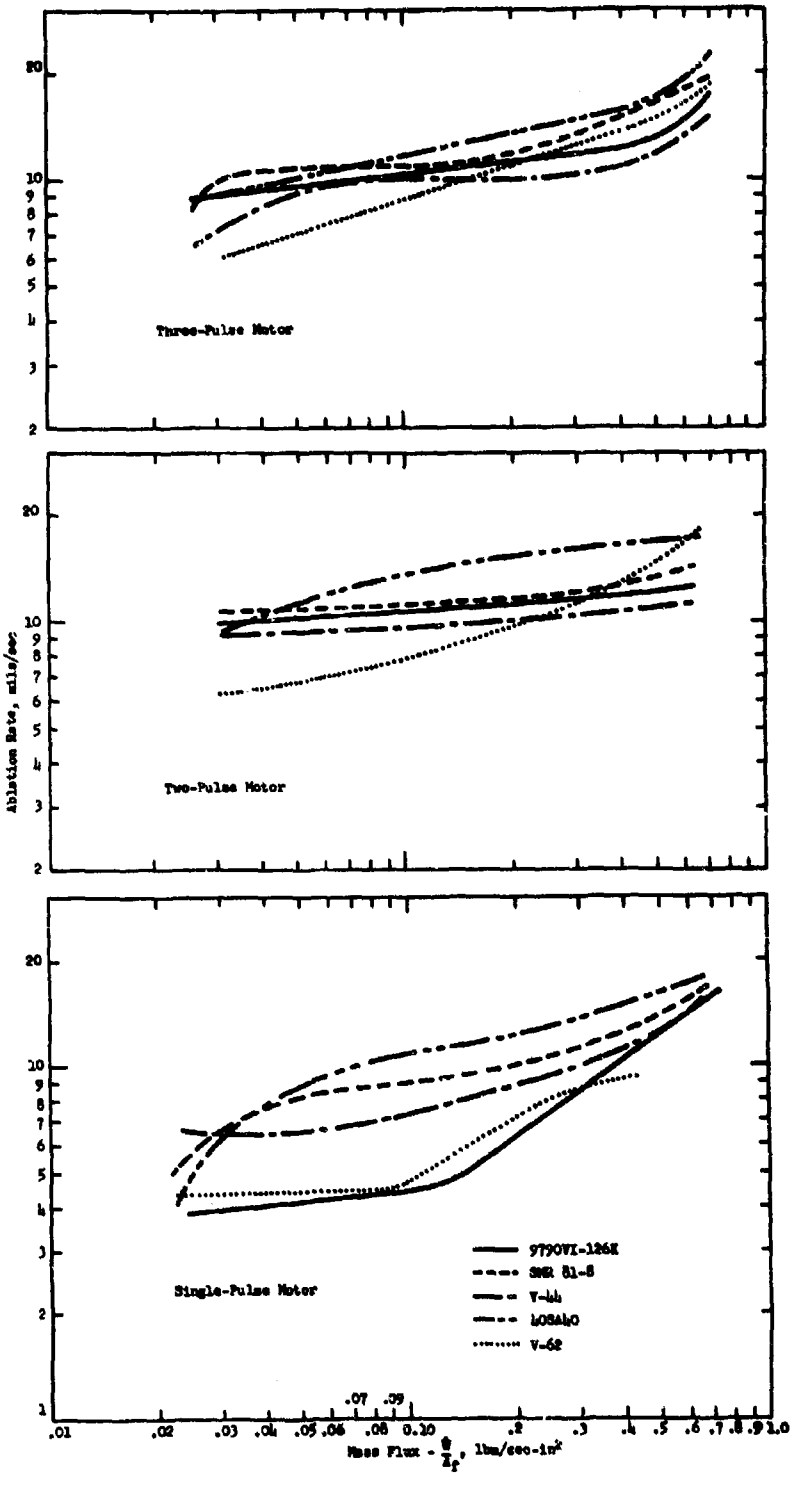

Figure 83. Ablation Rate of Correlation Motors vs Mass Flux

Heat Flux, Btu/ft^2-sec	50				100				225			
Source	Plasma Arc	Single Pulse	Two Pulse	Three Pulse	Plasma Arc	Single Pulse	Two Pulse	Three Pulse	Plasma Arc	Single Pulse	Two Pulse	Three Pulse
V-44	2*	3	2	2	3	3	2	2	3	3	2	2
V-62	1	2	1	1	1	2	1	1	1	2	1	1
40SA40	4	5	3	4	5	5	5	5	5	5	5	5
SMR 81-8	5	4	5	5	4	4	4	4	4	4	4	4
9790 V1-126K	3	1	4	3	2	1	3	3	2	1	3	3

*Rating based on ablation performance; No. 1 base.

Figure 84. Correlation of Plasma Arc Data and Motor Firing Data

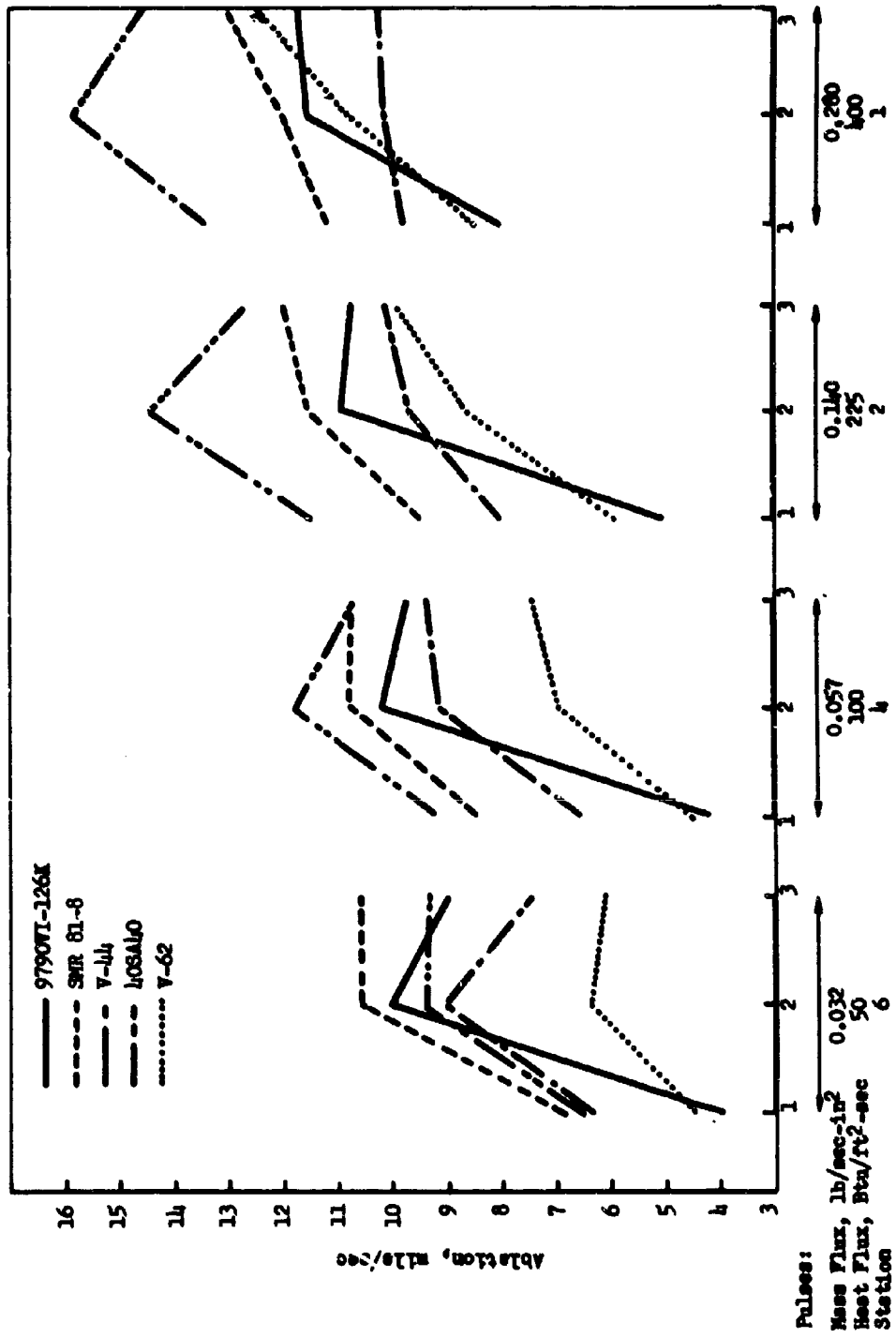

Figure 85. Ablation Rates vs Number of Pulses

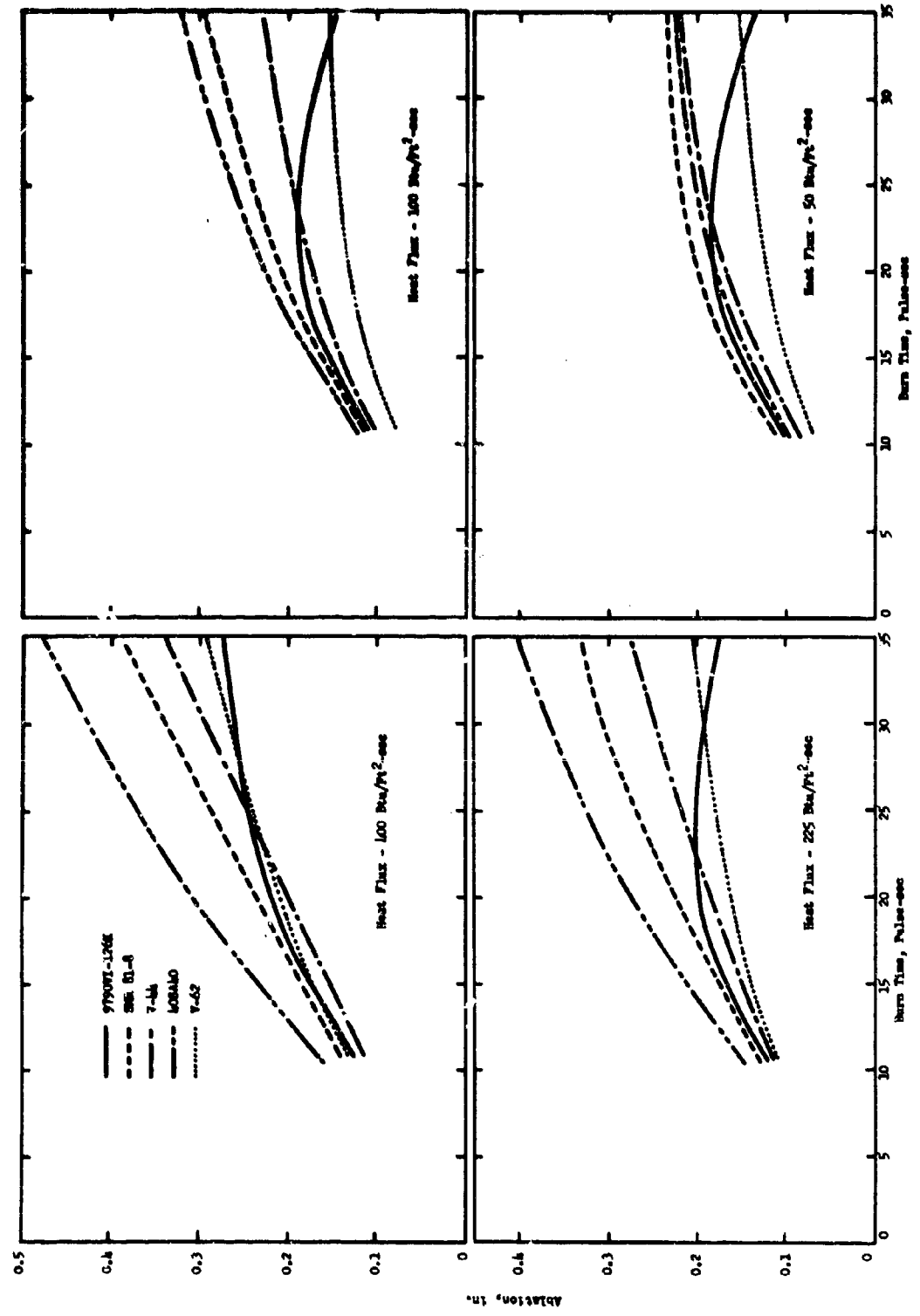

Figure 86. Ablation vs Burn Time per Pulse

III, B, Correlation Motor Firings (Task B, Phase I) (cont.)

of approximately 0.650 in. in the 5-pulse motor (20 sec per pulse, 100-sec total duration) and 0.420-in. in the 12-pulse motor (5 sec per pulse, 60-sec total duration).

If the selection of insulation for a solid rocket is not configuration (thickness) limited, then a factor consisting of the density times the ablation rate can be useful in identifying the more desirable materials. Figure 87 shows this product for the materials used in the correlation motors. The lower the number, the better the material. On this basis, V-62 and 9790 V1-126K are the best candidates.

Thermocouple data were obtained for each pulse during the three motor firings. These data provide temperature-time histories from two predetermined depths (0.150 and 0.300 in.) within each material and at two heat-flux positions (100 and 225 Btu/ft^2-sec), as shown in Figures 59 and 60. They will be used in the analytical model studies in Phase II of the program, where they will be compared to computer-calculated values.

C. EFFECT OF HEAT SOAKING AND THERMAL CYCLING ON INSULATION-CASE BONDS (TASK G, PHASE I)

Lap shear strength was used as the criterion to evaluate the integrity of the insulation-case bond under heat-soaking and thermal-cycling environments. The specimens were prepared with the following vulcanized insulation materials and adhesive systems on 4130 steel substrates.

Insulation	Adhesive	Supplier
V-44	Thixon P4/1209	Dayton Chemical Products Laboratory
V-62	Thixon XD9777/XD8394	Dayton Chemical Products Laboratory
40SA40	Multron R12/Mondur CB-75	Mobay Co.
SMR 81-8	Chemlock 203/231	Hughson Chemical
9790V1-126K	Epon 921 A/B	Shell Chemical

The adhesive systems are briefly described below:

Thixon P4/1209 is a nitrile-type, thermosetting system with good flexibility and high strength. P4 is the primer, and 1209 is the adhesive.

Thixon XD 9777/XD 8394 is a styrene-butadiene-type thermosetting system, again with good flexibility and high strength. XD 9777 is the primer, and 8394 the adhesive.

Station No.	0	1/2	1	2	3	4	5	6	7
Area Ratio:	5.78	9.05	13.55	26.4	44.1	65.6	90.7	120.5	154.1
Single Pulse									
9790 V1-126K	16.1	13.0	9.2	5.3	4.7	4.7	4.6	4.1	4.3
V62	-	9.7	9.1	6.3	4.8	4.7	4.7	5.1	4.7
V44	19.2	13.9	12.5	10.4	9.1	8.4	8.1	8.1	8.4
SMR 81-8	22.2	17.4	14.6	13.1	11.9	11.3	10.4	9.7	7.6
40SA40	23.2	19.8	18.0	15.4	13.9	12.4	10.5	9.2	6.2
Two Pulse									
9790 V1-126K	13.8	12.7	12.3	11.9	11.6	11.5	10.9	10.8	-
V62	18.7	14.3	11.6	9.4	8.0	7.1	7.0	6.6	-
V44	14.2	13.3	13.2	12.5	12.2	12.1	11.8	11.6	-
SMR 81-8	19.2	17.0	16.0	15.7	15.2	14.8	14.6	14.4	-
40SA40	22.9	22.0	21.5	19.5	17.4	15.6	13.1	12.7	-
Three Pulse									
9790 V1-126K	19.5	13.7	13.1	11.5	11.9	11.4	10.1	9.7	9.6
V62	19.9	14.0	13.2	10.4	8.9	8.4	7.2	6.2	-
V44	19.2	14.1	13.3	12.6	12.8	12.5	11.8	9.5	8.3
SMR 81-8	26.9	21.0	18.2	15.3	15.2	15.0	14.6	14.4	12.0
40SA40	30.0	21.5	19.4	17.5	14.7	14.8	12.9	12.4	11.6

Figure 87. Density--Ablation Rate Product for Correlation Motors

III, C, Effect of Heat Soaking and Thermal Cycling on Insulation-Case Bonds (Task G, Phase I) (cont.)

Multron R12/Mondur CB-75 is a two-component polyurethane system used for bonding metals to themselves or to polyurethanes. When the two components are mixed (100 parts Multron R12 to 200 parts Mondur CB-75), the system can be cured at room or elevated temperature to give excellent bonds.

Chemlock 203/231 is a versatile elastomeric bonding agent. It bonds to virtually all elastomers. The 203 is the primer, and the 231 the adhesive.

Epon 921 A/B is a two-component, aluminum-powder-filled epoxy adhesive having 15% elongation and good structural properties. Part A is the adhesive and Part B the hardener. They were used in a ratio of 100 gm A to 25 gm B. The system can be cured at room temperature for one week or at slightly elevated temperatures such as 1 hr at 180°F.

The lowest temperature limit to which the insulation-case bond in motor applications may be exposed is expected to be -65°F. The upper limit is expected to be in the range of 200 to 250°F, since this is the maximum allowable temperature without loss in strength for case materials such as glass-filament structures or titanium, and insulation thicknesses are designed accordingly. The heat-soaked specimens were, therefore, subjected to 5- and 30-min soak periods at 250°F and tested at room temperature. The thermal-cycling specimens were subjected to single- and ten-cycle thermal conditions of -65 to +250 to -65°F and tested at +250°F. Test procedures are discussed in Appendix I.

The test results are shown in Figures 88 through 90. These data indicate the following:

1. V-44

Strength did not significantly change as a result of heat soak. Strength at -65°F also showed no change as a result of the single- or ten-cycle thermal environment. Strengths retained at 250°F after both one and ten cycles were approximately 18% of the strengths at -65°F.

2. V-62

Strength did not significantly change as a result of heat soak. In thermal cycling, strength at -65°F was 280% greater after ten cycles than after a single cycle, for some unknown reason. Strengths retained at 250°F, after thermal cycling, were approximately 39% of the strengths at -65°F.

Insulation Material	Control Specimens		5-Min Heat Soak*		30-Min Heat Soak*	
	Lap Shear Strength, psi	Failure Mode	Lap Shear Strength, psi	Failure Mode	Lap Shear Strength, psi	Failure Mode
V-44	875.7	Cohesive-rubber	864.5	Cohesive-rubber	807.5	Cohesive-rubber
	825.7		599.0		762.9	
	732.2		811.8		782.6	
	911.7		547.3		590.4	
Average	836.8		705.7		735.9	
V-62	141.4	Cohesive-rubber	160.7	Cohesive-rubber	139.0	Adhesive
	136.1		170.4		154.2	Cohesive-rubber
	168.1		157.4		162.3	
	148.6		153.9		169.3	
Average	148.6		160.6		156.2	
40SA40	452.9	Cohesive-rubber	218.5	Cohesive-rubber	163.5	Cohesive-rubber
	542.5	Cohesive-adhesive	113.4	Adhesive	168.9	
	487.3	Cohesive-rubber	176.1	Cohesive-rubber	235.4	
	499.7		223.4		149.9	
Average	496.0		183.0		179.0	
SMR 81-8	105.0	Adhesive	120.4	Adhesive	131.0	Adhesive
	118.3		131.1		125.9	
	113.1		98.8		110.8	
	117.3		110.3		107.9	
Average	113.4		115.2		118.9	
9790V1-126K	530	Adhesive	384	Adhesive	511	Adhesive
	416		282		450	
	400		388		435	
Average	449		351		465	

*Soaked at 250°F; - tested at room temperature.

Insulation Material	Control		Single Cycle*		Ten Cycles*	
	Lap Shear Strength, psi	Failure Mode	Lap Shear Strength, psi	Failure Mode	Lap Shear Strength, psi	Failure Mode
V-44	593	Adhesive	514	Adhesive	469	Adhesive
	407		492		405	
			640			
	465		564		561	
Average	488		528		478	
V-62	145	Adhesive	213	Cohesive-rubber	717	Adhesive
	280		225		638	
	150		209		710	
			246			
Average	192		223		722	
40SA40	1903	Cohesive-rubber	1508	Cohesive-rubber	1567	Cohesive-rubber
	1779		1724		1209	
	1524		1713		1670	
			1696			
Average	1735		1660		1482	
SMR 81-8	149	Adhesive	185	Adhesive	292	Adhesive
	163		142		222	
			148			
Average	156		160		257	
9790V1-126K	1890	Cohesive-Adhesive	1690	Cohesive-Adhesive	1681	Cohesive-Adhesive
	2218		2005		1621	
	2329		2196		1408	
Average	2146		1964		1570	

* -65°F to 250°F to -65°F

Figure 89. Effect of Thermal Cycling on Lap Shear Strength of Insulation/Case Bonds When Tested at -65°F

Insulation Material	Single Cycle* Lap Shear Strength, psi	Single Cycle* Failure Mode	Ten Cycles* Lap Shear Strength, psi	Ten Cycles* Failure Mode
V-44	90.4	Adhesive	83.3	Adhesive
	96.1		95.0	
	84.8		87.3	
	95.0		92.2	
Average	91.6		89.5	
V-62	76.0	Adhesive	66.0	Adhesive
	68.0		77.0	
	80.0		79.0	
	76.0		77.0	
Average	75.0		74.8	
40SA40	4.15	Cohesive-rubber	3.63	Cohesive-rubber
	6.89		3.64	
	7.22		6.15	
	7.14		6.96	
Average	6.50		5.00	
SMR 81-8	40.0	Adhesive	41.0	Adhesive
	40.0		46.0	
	44.0		____	
Average	41.3		43.5	
9790V1-126K	46	Adhesive	54	Adhesive
	53		51	
	57		52	
Average	52		52	

* -65°F to 250°F to -65°F
** Control specimens were also run on 9790V1-126K, averaging 55 psi

Figure 90. Effect of Thermal Cycling on Lap Shear Strength on Insulation/Case Bonds when Tested at 250°F

III, C, Effect of Heat Soaking and Thermal Cycling on Insulation-Case Bonds (Task G, Phase I) (cont.)

3. 40SA40

A significant difference was noted in the strength as a result of heat soak for both the 5-min and 30-min periods. There was no significant difference in strength at -65°F after the cycling environment. Strengths at 250°F after thermal cycling dropped to approximately 0.3% of the strengths at -65°F, which was expected because of the heat characteristics of this material.

4. SMR 81-8

Strength did not significantly change as a result of heat soak. Strength at -65°F after ten cycles showed an improvement of 65% over the single-cycle strength--again, the reason is unknown. Strengths retained at 250°F after thermal cycling were approximately 25% of the strengths at -65°F.

5. 9790V1-126K

While there was some reduction in strength as a result of the 5-min heat soak, the 30-min specimens were equivalent in strength to the control specimens, possibly as a result of additional curing. The strength at -65°F after ten thermal cycles was 25% lower than in the control specimens. The strengths retained at 250°F after thermal cycling were approximately 2% of the strengths at -65°F.

The adhesive materials used in this program were standard off-the-shelf items. Higher strengths and more heat-resistant joints would undoubtedly have been obtained if unvulcanized elastomers had been used instead of vulcanized stock because of the superior bonding properties of the unvulcanized materials. Application of special, more heat-resistant adhesives, such as the polyimides and polyimidazoles, would produce joints that break in the elastomers. However, modifications might be necessary to produce satisfactory behavior at -65°F. These materials were not tested because using them would require development effort.

SECTION IV

WORK PLANNED FOR THE SECOND STAGE

A. LABORATORY INVESTIGATIONS

1. Task C, relating to the selection of the significant properties of elastomeric insulation, will be completed.

2. Task D, pertaining to the testing of the significant properties on the remaining ten materials, will be completed.

3. Task E work on the influence of ingredients on behavior and performance of elastomeric insulation will be completed.

4. Task F, relating to the selection of the best materials for later installation in three verification motors, will be completed.

APPENDIX I

TEST PROCEDURES FOR MATERIAL PROPERTIES

I. VIRGIN MATERIALS

A. KINETIC STUDIES

The apparatus used for these studies was the thermogravimetric (TGA) balance (Figure 1) consisting of an automatic recording balance and a heavy-duty furnace. Sample temperatures were obtained by monitoring identical samples within the apparatus. A linear heating rate of 20°C/min was used up to a maximum temperature of 800°C. Weight loss and temperature as a function of time were recorded on all samples. Testing was conducted in an argon atmosphere.

B. DIFFERENTIAL THERMAL ANALYSIS

The differential thermal analysis apparatus was used to obtain data on the exotherms and endotherms of the various materials. In this apparatus, changes in the sample temperature were referenced against graphite. A heating rate of 20°C/min was used up to a maximum temperature of 600°C. Testing was conducted in a nitrogen environment.

C. DENSITY

The density of the virgin materials was obtained at three temperatures using the liquid-displacement apparatus shown in Figure 2. Testing was conducted in air.

D. HEAT CAPACITY

To determine the heat capacity of virgin material, a calorimeter of the type shown in Figure 3 was used. This method is based upon the standard drop-method technique. The calorimeter consists of a Dewar flask equipped with a Beckman mercury thermometer and a fitted aluminum receiving cup immersed in a heat-transfer medium. The samples are heated to the desired temperatures with an electric multiple-tube furnace. The calorimeter is initially calibrated using a known weight of copper or zinc. The heat capacity of a material is finally calculated from the following equation:

$$W_s C_s (T_2 - T_f) = W_c C_c (T_f - T_i - W_w C_w (T_f - T_i)$$

where W_s = Weight of sample

W_c = Weight of calorimeter

W_w = Weight of distilled water

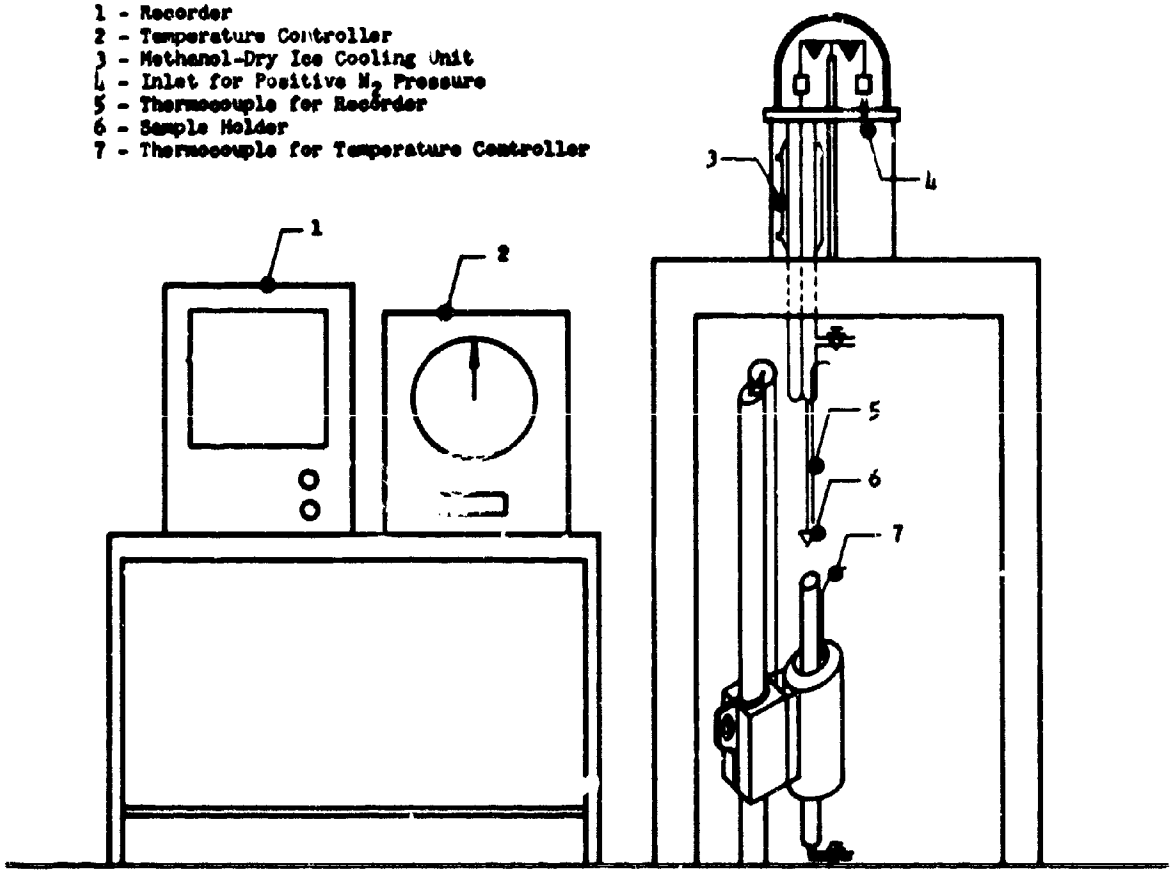

Figure 1. Thermal Decomposition Apparatus

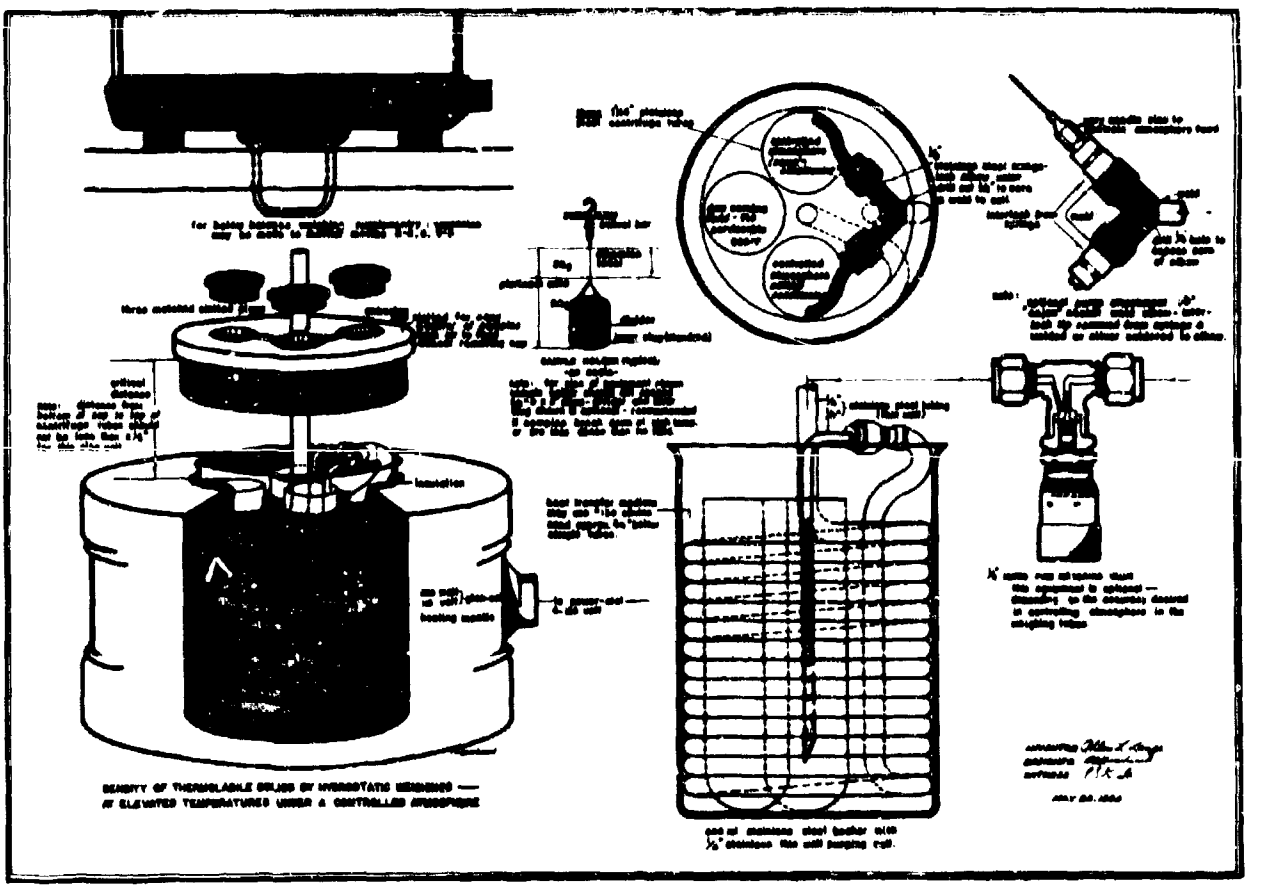

Figure 2. Liquid Displacement Apparatus

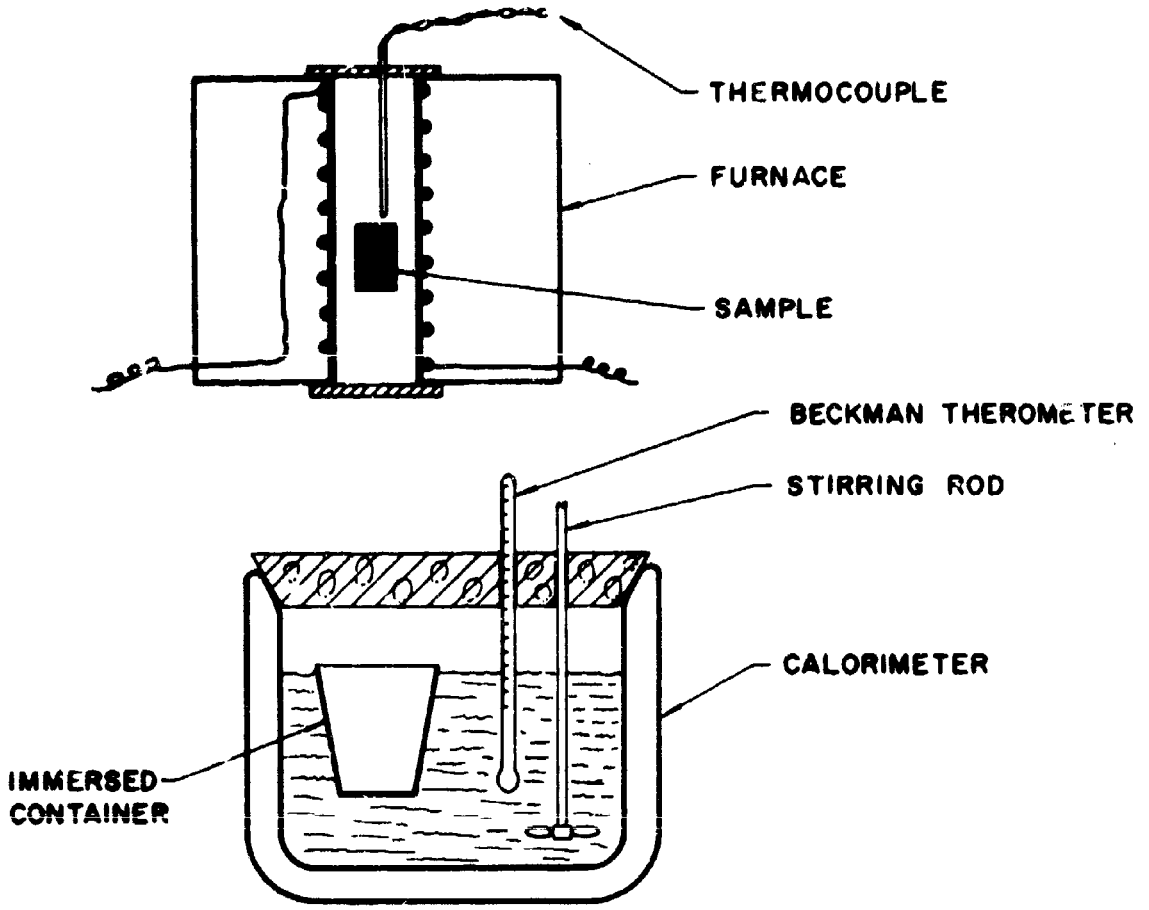

Figure 3. Heat Capacity Apparatus

I, D, Heat Capacity (cont.)

C_s = Heat capacity of sample

C_c = Heat capacity of calorimeter

C_w = Heat capacity of distilled water

T_2 = Temperature of sample

T_f = Final temperature of calorimeter

T_i = Initial temperature of calorimeter

E. HEAT OF COMBUSTION

Heat of combustion was determined by the bomb-calorimeter technique. A known weight of sample was electrically ignited in a "bomb," and the heat evolved from the combustion was determined by noting the temperature rise of the heat transfer medium.

F. TENSILE STRENGTH AND ELONGATION

Tensile strength and elongation were determined using 0.075-in.-thick standard dumbbell specimens. Testing was conducted at room temperature at 20 in./min in accordance with ASTM D 412 (Die C).

G. WEIGHT LOSS

The weight loss due to long heat soak was determined by weighing before and after heating. Specimens approximately 4 by 4 by 1/2 in. were heat-soaked for 5 and 30 min after reaching 400°F as indicated by thermocouples embedded in the materials. The approximate time required to bring the center of the specimens up to 400°F was 20 min. After heating, the specimens were removed and weighed immediately to avoid absorption of moisture from the atmosphere.

H. REGRESSION RATES

The regression characteristics of the virgin materials were determined by using a plasma-arc jet in conjunction with instrumented specimens 1/2 in. dia by 2 in. long. Three sets of thermocouples were installed at nominal depths of 0.70, 0.120, and 0.370 in. from the end. The cylindrical surfaces of the materials were shrouded with RTV 60 or EC 108. Heat flux levels of 50, 100, and 225 Btu/ft^2-sec were used to establish regression rates, ablation rates, and time-temperature profiles. Eight heating cycles were used on each specimen (15 sec on, 15 sec off) with argon as the plasma gas.

I, H, Regression Rates (cont.)

The plasma-arc system utilized for testing was the 80 KW installation shown in Figure 4. The power supply consists of two 40-KW, three-phase, direct-current transformer rectifiers connected in series. The plasma head is located in a chamber 30 in. dia by 5 ft long. The unit is water cooled. The test-specimen positioner has adjustable arms for forward and backward motion. A Kenney vacuum pump is used for chamber evacuation. The heat flux of the gas stream is measured with a cold-wall calorimeter.

I. THERMAL DIFFUSIVITY

The flash method of determining thermal diffusivity (thermal conductivity) consists essentially of the absorption of a very short pulse of radiant energy in the front of a specimen, and the recording of the resultant temperature history of the rear surface.

In the ideal case of a perfectly insulated specimen with a constant absorptivity across its surface, uniformly irradiated with a pulse of thermal energy short compared with the time required for heat to flow through the material, the back-surface temperature history is given by

$$\frac{T(L,t)}{T_m} = 1 + 2 \sum_{n=1}^{\infty} (-1)^n \exp(-n^2 \pi^2 \alpha t/L^2) \qquad \text{(Eq 1)}$$

where T(L,t) represents the instantaneous back surface temperature rise at time t, T_m is the maximum back surface temperature rise, α is the thermal diffusivity in $in.^2/sec$, L is the specimen thickness in cm, and n represents successive integers. At the time $t_{1/2}$, where $T(L,t) = 0.5\ T_m$, Eq 1 reduces to

$$\alpha = \frac{k}{\rho C_p} = \frac{1.37L^2}{\pi^2 t_{1/2}} = \frac{0.139L^2}{t_{1/2}} \qquad \text{(Eq 2)}$$

Hence, the thermal diffusivity of a material can be determined from the specimen thickness and the time in seconds required for the back-surface temperature to reach half its maximum value.

The success of the method depends upon adequately meeting the boundary conditions which lead to Eq 1. Figure 5 is a dimensionless plot of Eq 1 and represents the form that the back-surface temperature history of the sample will take if these boundary conditions are satisfactorily met. A departure of the data from this curve illustrates that these conditions have not been met and invalidates the data.

Figure 4. Plasma Arc Facility

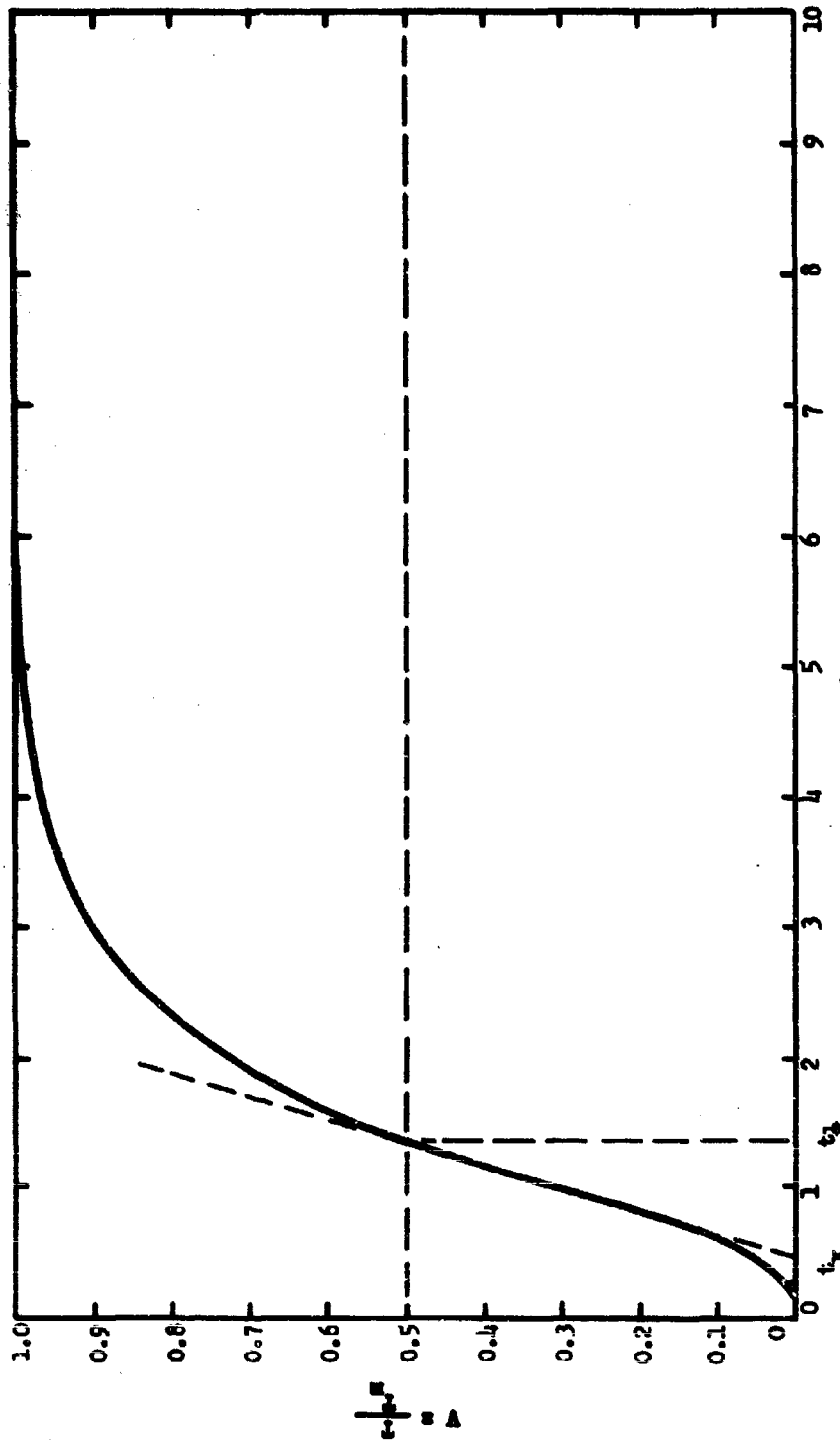

Figure 5. Dimensionless Plot of Rear Surface Temperature History

I, I, Thermal Diffusivity (cont.)

A condition vital in the use of Eq 1 is that the front surface of the sample be uniformly irradiated with a pulse of thermal energy in a time which is short compared to the rise time of the back-surface temperature. To accomplish this, a xenon flash lamp is used as the source of that thermal pulse. The lamp used is a General Electric Type 524 through which 600 joules are discharged. The pulse was essentially completed in 500 microsec, while the time to one-half of the maximum of the rear surface temperature was for the most part 50 to 300 microsec. It should be noted in Eq 2 that, for a given material, the rise time of the rear surface temperature is a function of the square of the sample thickness. A sample thickness sufficient to satisfy this condition of a short pulse duration should be used. However, for a given amount of input energy, the maximum temperature rise attained, T_m, is an inverse function of the thickness of the sample, and in order to maximize the temperature of the irradiance, the distribution of that irradiance on the front surface of the sample is important as noted earlier. It is a simple procedure to obtain uniform irradiation on a small flat surface from a flash lamp, but it is a boundary condition which must nevertheless be satisfied; otherwise, the shape shown in Figure 1 may be distorted. The 2-in.-dia helical lamp is placed without optics only a few centimeters from the sample.

The other boundary condition imposed on Eq 1 is that the specimen be perfectly insulated. The degree to which this is satisfied within the time limits of interest is indicated by the decay rate of the back-surface temperature after the maximum T_m is attained. Because of these factors, the sample holder should be designed so as to minimize all heat losses. Conductive heat losses are minimized by supporting the sample on a small area. If appropriate care is exercised by the experimenter, conduction heat losses, as well as convective heat losses, are negligible because of the short times involved in the flash technique. Radiative heat losses at high temperatures cannot be eliminated and, therefore, could constitute the greatest problem in the satisfaction of this boundary condition.

This method of diffusivity measurements has been successful at ambient temperature in air* and up to 1000°C in an argon atmosphere** using a resistance furnace and a thermocouple as the rear-surface temperature detector.

Radio-frequency induction heating is the most convenient means of heating small samples to high steady-state temperatures. In addition to satisfying the requirement of producing high temperatures, this form of heating is very fast and temperature equilibrium is reached quite rapidly. Induction heating has another advantage in that, by using ceramic supports, only the

*Thermal Diffusivity of Stainless Steel Over the Temperature Range 20°C-1000°C, R. J. Jenkins and R. W. Westover, USNRDL, TR-184, December 1960

**"Flash Method of Determining Thermal Diffusivity Heat Capacity and Thermal Conductivity," W. J. Parker, R. J. Jenkins, C. P. Butler, and G. L. Abbott, J. Appl. Phys. 32, 1679 (1961)

I, I, Thermal Conductivity (cont.)

sample itself attains the high temperature. The radiating surface area is therefore less, and consequently the walls of the vacuum chamber are easier to keep cool, and the use of rubber seals is facilitated.

The experimental apparatus used in these measurements is shown schematically in Figure 6. The induction-heater coil leads are fed into the vacuum chamber and form a coil with an ID of about 1 in. The sample is held in position in the coil by a mount machined from lava and baked to a ceramic. Shields of baked lava prevent heating of the chamber walls by radiation from the sample. Fused quartz is used for the top window because the large thermal gradients close to the hot samples would crack glass windows. The steady-state temperature at which measurements are made is indicated by thermocouple leads which are fastened to the edge of the sample and fed out of the vacuum system. An optical pyrometer is used at temperatures above which platinum/platinum-rhodium thermocouples will perform. A glass lens below the sample focuses the center portion of the rear of the sample on a lead sulfide cell which measures the surface-temperature history over a range from 300 to 1800°C. The linearity of the lead sulfide cell is adequate, since the temperature change of the sample due to the pulse is not more than a few degrees. It should be noted that a knowledge of the detector sensitivity or the thermal input to the sample is not required because only $t_{1/2}$ is involved in Eq 2, and this time can be determined from the calibrated sweep of the oscilloscope.

The detector is connected differentially through a load selector and balance-control unit to the differential preamp of an oscilloscope. The use of differential detector circuitry is necessary to minimize the effects of the extremely high magnetic field which surrounds induction-heating coils. A trigger delay circuit is used to fire the flash lamp after the oscilloscope sweep has been triggered. This is necessary in order to have a base line on the print from which to measure the change in the detector output voltage.

Figure 7 is a Polaroid Land Camera print of the oscilloscopic display of the detector output. When the shape of the temperature rise is compared with Figure 5, the agreement indicates that the boundary requirements have been satisfied by the samples reported here. Since heat losses from the sample would show up as a decay in the detector output after the initial rise, it is evident from this print that the thermal pulse travels through the sample in a time which is extremely short compared with the time required for the sample to return by heat losses to the equilibrium temperature at which the measurement is made. Nonuniform illumination of the front surface could distort the knee of the curve.

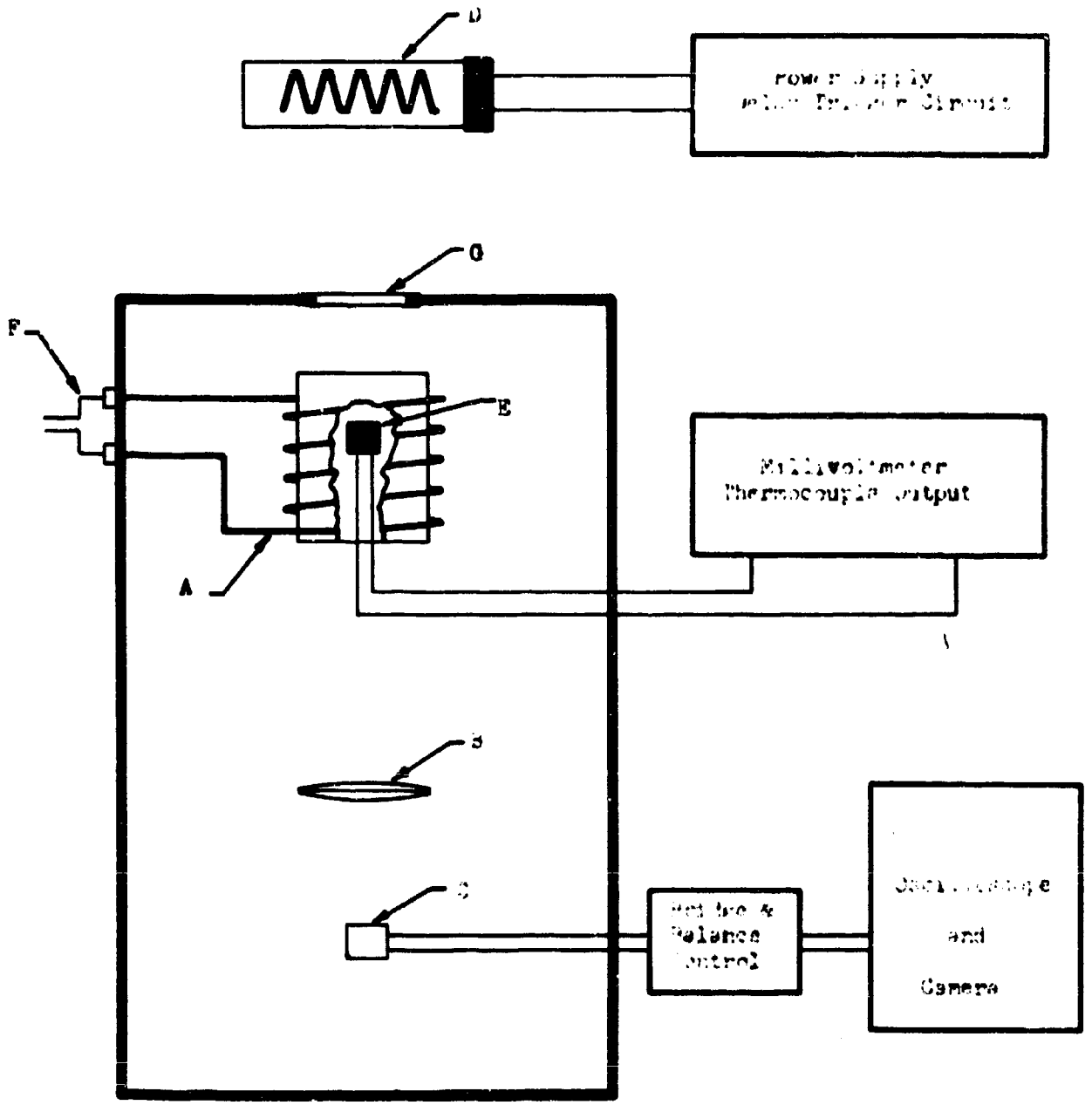

A - RF Induction Heater
B - Lens
C - Pbs Cell
D - [illegible] Flash Lamp GE 52A
E - [illegible]
F - To RF Generator
G - Window

Figure 6. Schematic Diagram of Experimental Arrangement

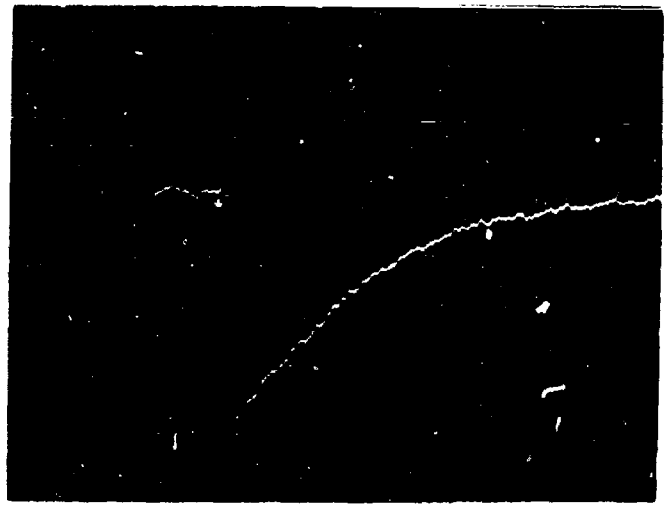

Virgin SMR 81-8 Material
at 150°F

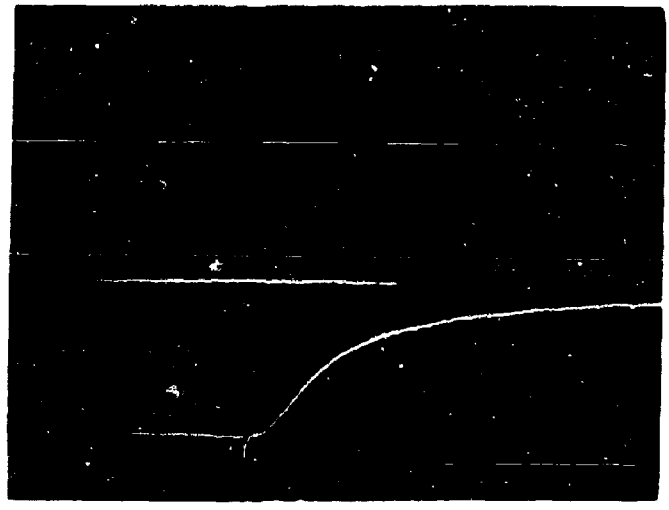

Charred 40SA40 Material
at 156°F

Figure 7. Examples of Temperature History of Elastomeric Insulation Specimens

II. DETERMINATION OF DECOMPOSITION PRODUCTS OF PYROLYZED MATERIALS

The insulation materials were pyrolyzed in a bomb shown in Figure 8. This bomb was leak proofed under vacuum, high-pressure, and high-temperature conditions. Also shown in Figure 8 is the adapter which was used to transfer gas samples directly into the mass spectrometer.

A temperature-pressure study was carried out to determine the best system which could be utilized for analytical purposes. A pressure of 349.3 psig at a pyrolytic temperature of 550°C were the conditions derived.

Gas samples were introduced directly from the pyrolysis bomb into a CEC21-103C mass spectrophotometer. A scan was made over the entire mass range from hydrogen up to a mass of 408 to ensure complete coverage of products. The bomb was then cooled with liquid nitrogen and the hydrogen, helium and other low molecular weight gases were removed under vacuum. Another scan was made of the remaining materials to aid in their qualitative identification.

Another sample was run in a Perkin-Elmer Vapor Fractometer to aid in the identification of the major components. After all of the major components were identified, standard mass spectrophotometric scans were made and all peaks calculated. A system of taking the highest molecular weight component and removing its contribution to the scan was used. By working down the scan and using simultaneous equations where necessary, it was possible to identify a minimum of 95 mole% of the constituents present.

After analysis of the gases evolved during sample pyrolysis, the bomb was opened and the char was removed. The chars were then analyzed using X-ray diffraction, emission spectrography, elemental analysis (C, H, N, O) and calorimetry techniques.

III. CHAR LAYERS

The charred specimens were formed in a high-pressure and high-temperature apparatus, a schematic of which is shown in Figure 9. It consists of an induction coil with either a tungsten or pyrolytic graphite susceptor as the heating source, a high pressure jacket housing the insulation coil, thermocouples to monitor sample temperature, a hydraulic ram to position sample, a graphite sample holder, and a cooldown zone within a graphite black body. Energy is furnished by a TOCCO power supply rated at 400 volts and 125 amps. The autoclave is capable of 800 psi pressure and vacuum operation. The tungsten susceptor has a higher surface temperature (4040°F) than the graphite susceptor (3540°F) but a lower heat flux capability (57 vs 119 Btu/ft^2-sec) because of a lower emissivity.

A. DENSITY

The bulk densities of the charred materials from both the correlation motors and high-pressure and high-temperature apparatus were obtained by first measuring machined rectangular specimens of the materials and then weighing same.

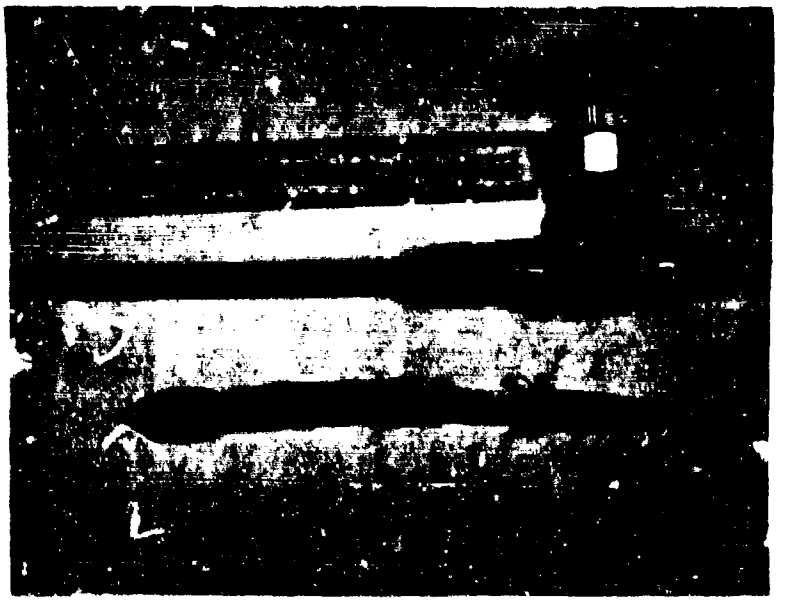

Figure 8. Pyrolysis Bomb

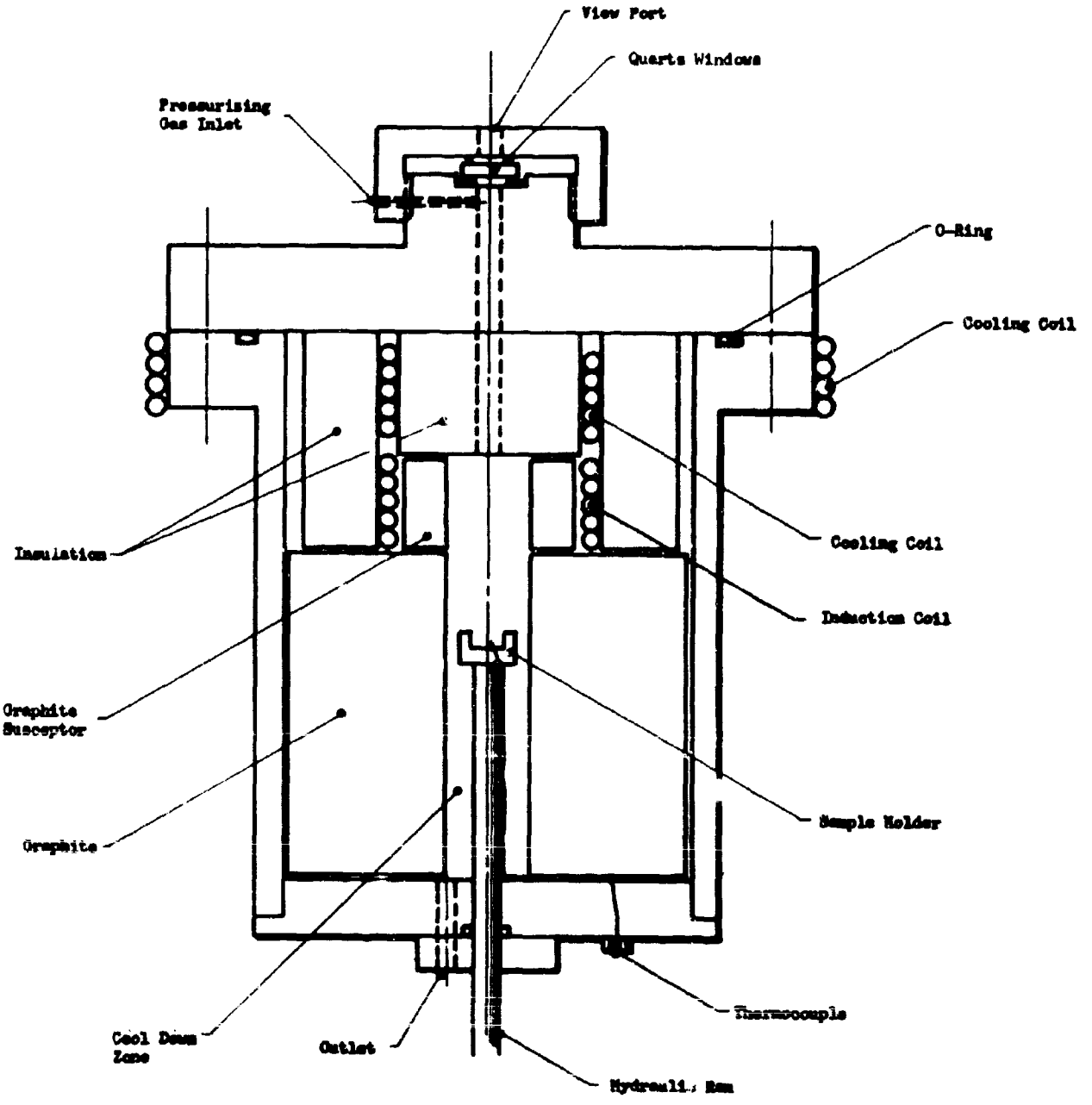

Figure 9. High Pressure-High Temperature Apparatus

III, Char Layers (cont.)

B. PERMEABILITY

The permeability of the charred specimens or the resistance to gas flow through the porous specimens was experimentally determined by use of the apparatus shown in Figure 10. The apparatus consists of two separate units: (1) an upper high-pressure chamber which connects to a high-pressure nitrogen gas supply and to a high-pressure calibrated Heise gage and (2) a lower unit which supports the sample and connects to a Fischer-Porter Flowrator. Nitrogen gas at room temperature was allowed to flow into the pressure chamber and through the specimen at various pressure levels. The ensuing nitrogen gas was metered by use of the calibrated Fischer-Porter Flowrator. Samples carefully machined to 0.75 in. in diameter and 0.25 in. in thickness were used in this determination. The samples were supported on a 0.030 in. wide ledge and sealed into place by a silicone rubber sealant. The silicone rubber sealant was placed around the lateral surface of the sample and on the support ledge to prevent gas flow through the lateral surface and gas leakage around the sample. The sealant was allowed to cure for 24 hr in each case before any measurements were obtained.

C. POROSITY AND PORE SPECTRA

The porosity and pore spectra of the charred specimens were determined on an Aminco-Winslow Porosimeter which employs the mercury intrusion technique. Open porosity measurements were made by forcing mercury into the pores of the specimen under pressures up to 5000 psi. At this pressure, mercury will flow into a pore as small as 0.035 microns in diameter. The volume of the mercury intruded is a direct measure of the volume of open porosity of the test sample. The pore size distribution can be determined from the relationships of pressure, surface tension of the mercury and contact angle between the mercury and the surface of the test material.

The method used consisted of placing a sample approximately one gram in size in the penetrometer and evacuating. Mercury was then admitted until the penetrometer was filled and the specimen covered. The mercury level was recorded at each pressure level. Isopropyl alcohol was used as the hydraulic fluid to pressures up to 5000 psi.

D. SHEAR STRENGTH

The shear strength of the charred specimens was determined in a single shear test fixture at room temperature. A 200 lb Instron tensile tester was used for this determination with a cross head speed of 0.05 in./min. Samples tested were approximately 0.500 in. in diameter and 0.75 in. in length.

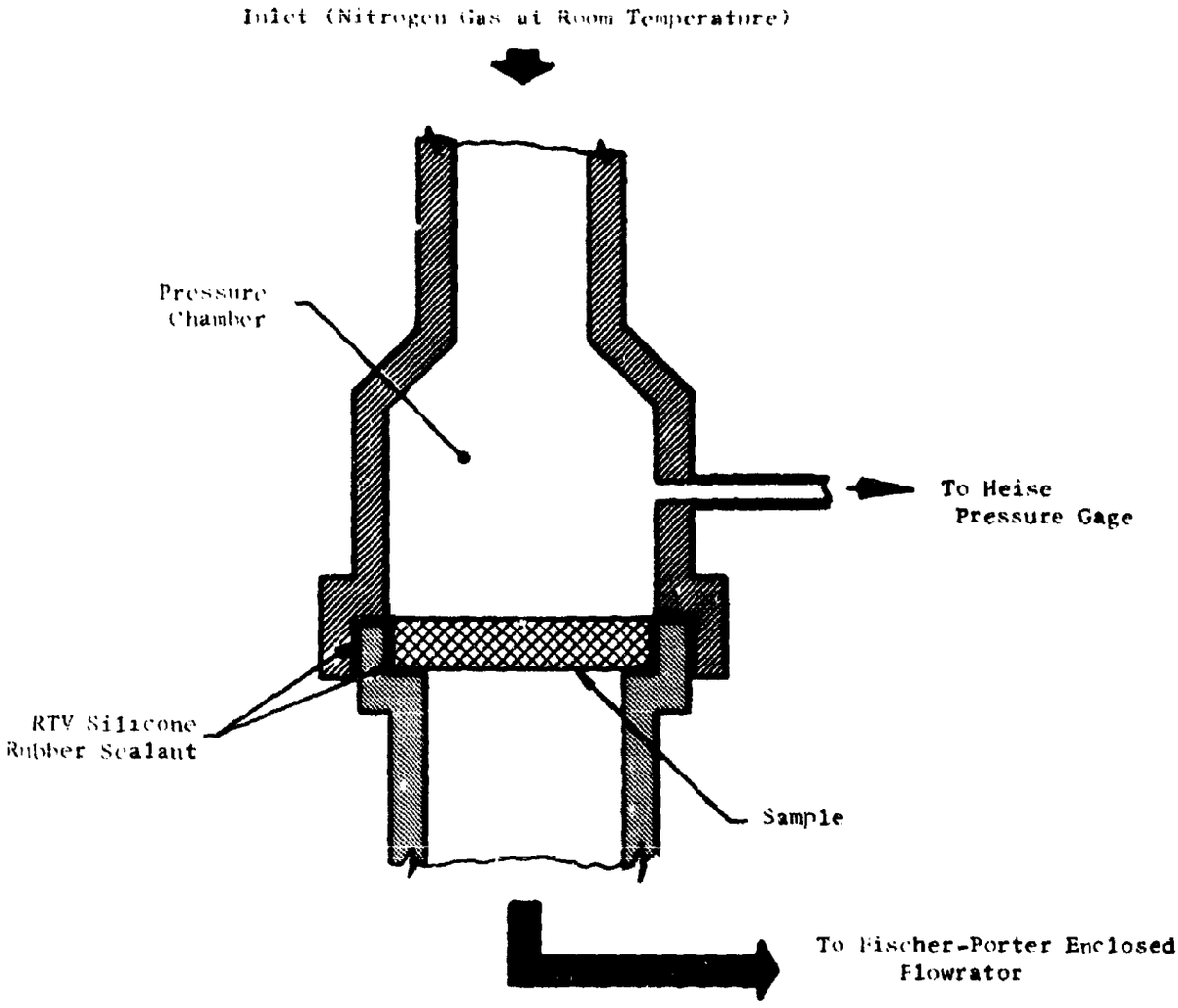

Figure 10. Permeability Apparatus

III, Char Layers (cont.)

E. COMPRESSIVE STRENGTH

The compressive strength of the charred specimen was obtained in a standard compressive fixture at room temperature in accordance with ASTM D695-54. A Tinius-Olsen Screw Driven Machine was used for this determination. The compressive load was applied to 0.500 in. diameter by approximately 0.75-in.-long specimens at a cross head speed of 0.50 in./min.

F. TENSILE STRENGTH

The tensile strength of the charred specimens was determined at room temperature in accordance with ASTM D638-527 using a Baldwin-Lima-Hamilton Universal Testing Machine. A load rate of 0.2 in./min was used in all tests. Since the charred specimens were very fragile and very flakey in nature, load grips for holding the specimens were modified from standard procedures somewhat in order to conduct the tests. The load grips in this case were made by potting both ends of a 0.500-in.-diameter sample, 0.75-in. long in epoxy-resin and then inserting small steel hooks into the resin at opposite ends of the sample.

G. EMISSIVITY

The emissivity of the charred specimens was determined by use of a total radiation pyrometer and the high-temperature, high-pressure heating apparatus. A 2-mm-diameter hole 0.375 in. deep was drilled into a charred specimen 0.500 in. in diameter and approximately 0.75 in. long. These particular specimens were not shrouded with RTV60 to allow uniform heating along the entire length. The specimens were placed into the hot zone of the charring apparatus and heated on all surfaces to incandescence. Data was taken at three temperature levels after obtaining thermal equilibrium in each case. A black-body temperature was obtained by sighting into the small drilled cavity. The surface temperatures were obtained by sighting around the periphery of the small hole on the surface of the specimen. The average temperature of the measured periphery values was used on the surface temperature.

The black-body temperatures and surface temperatures were obtained by sighting through a 90° angle prism which, in turn, was placed upon the quartz view-port of the high-pressure, high-temperature apparatus. Prior to the above measurements, "blank" temperature measurements were made on a graphite sample to determine the error associated with light absorption and light scattering from the quartz view-port and the 90° optical prism. It was found that in the temperature range of interest (2000 to 3500°F) only a 1% loss in total temperature occurred.

H. THERMAL CONDUCTIVITY

The same test procedures as used for thermal conductivity of virgin material were used.

III, Char Layers (cont.)

I. HEAT CAPACITY

The same test procedures as used for heat capacity of virgin materials were used.

J. THERMAL EXPANSION

A quartz-tube dilatometer was used to determine the thermal expansion of the charred specimens in accordance with ASTM D696-44. The instrument consists essentially of an outer tube of fused quartz (20 in. long, 0.5 in. inside diameter and a wall thickness of about 2 mm), and an inner tube, or extension rod, of fused quartz (18 in. long with an outside diameter such that this tube is allowed to fit snugly inside the outer tube without binding). The specimen is placed into the open trough (about 1.5 in. long) that is available at one end of the outer tube and the extension rod, with a hemispherical seat on one end, is allowed to rest against the top flat portion of the cylindrical specimen. The whole assembly of outer tube, specimen, and extension rod is then placed horizontally into a standard laboratory oven type heater. The extension rod connects to a strain-gage-galvonometer type arrangement which transmits the displacement as the sample expands. Samples 0.5 to 1.0 in. long by 0.25 in. in diameter and heating rates of 20°F/min were used in this determination. The maximum temperature obtained was 1652°F. The change in length of the specimen over a range of temperature on either side of the nominal test temperature was recorded at each temperature level.

IV. INSULATION-CASE BONDS

The effect of thermal cycling and long heat-soak periods on insulation-case bonds was determined by conducting lap shear tests in accordance with ASTM-D1002-535, at a rate of 0.05 in./min. The specimens were prepared with 0.125-in.-thick vulcanized insulation material and 4130 steel substrates, as follows:

1. All surfaces were abraded with 180 grit Al_2O_3, wiped with MEK and air dried for 15 minutes.

2. Primer was applied when required-air dried for 30 minutes.

3. Adhesive was applied and lap shear specimen assembled; a thermocouple was embedded in one specimen of each test group for monitoring the test environment.

IV, Insulation-Case Bonds (cont.)

4. Specimens were vacuum bagged and cured, as follows:

a. Thixon P4/1209, 2 hr at 300°F
b. Thixon XD9777/XD8394, 2 hr at 200°F
c. Multron R12/Mondur CB-75, 3 hr at 200°F
d. Chemlock 231/203, 2 hr at 250°F
e. Epon 921A/B, 1 hr at 180°F
f. Specimens were cooled under vacuum.

5. The temperature cycling specimens were alternately cooled by immersing in a dry ice-alcohol mixture and heated by means of an oven. The specimens were moved between the media as quickly as possible.

APPENDIX II

TEMPERATURE-TIME PLASMA ARC DATA

BLANK PAGE

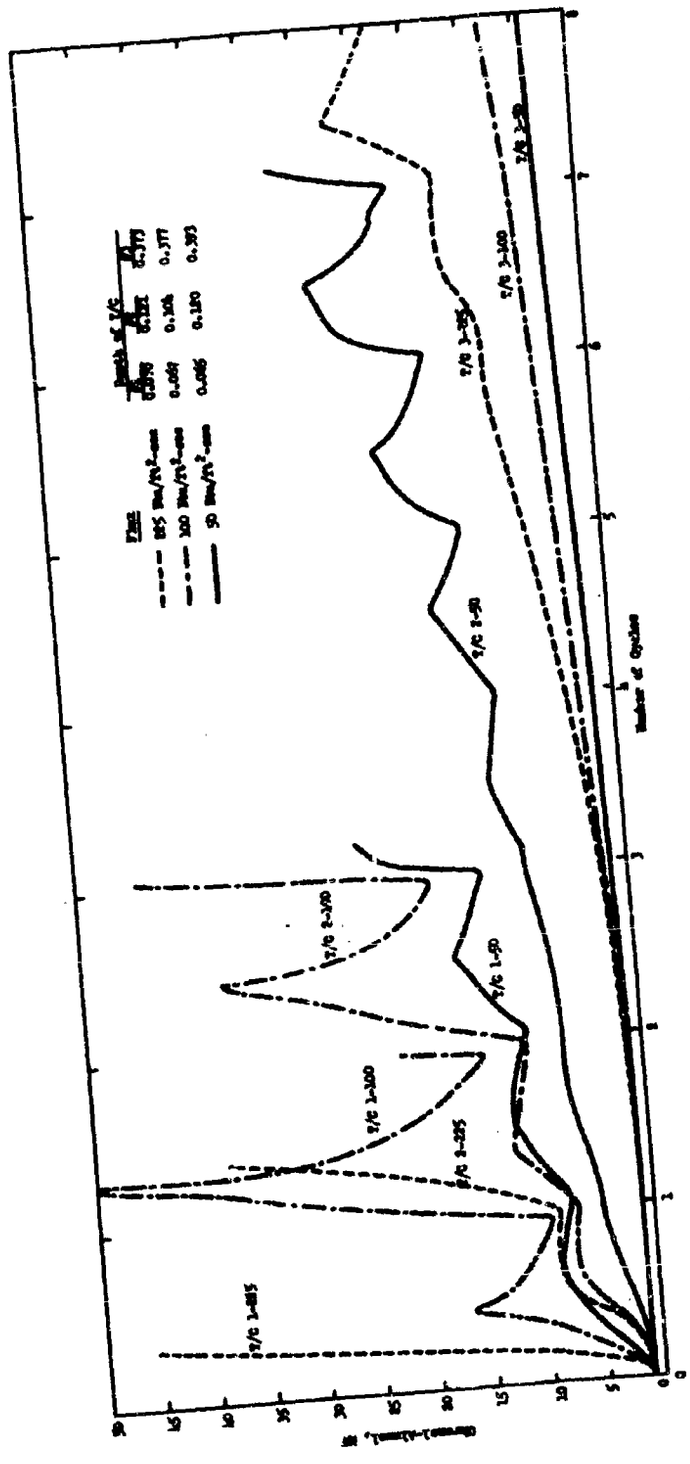

Figure 1. Temperature-Time Plasma Arc Data for V-62 Material

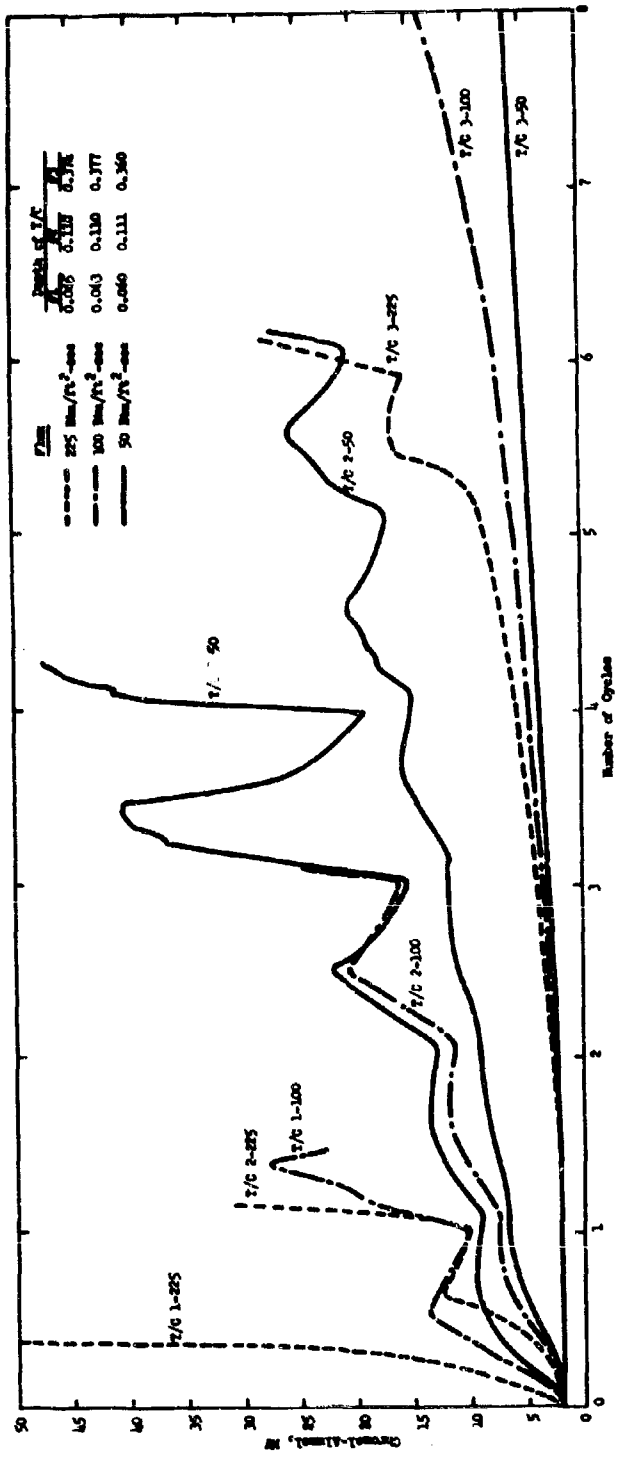

Figure 2. Temperature-Time Plasma Arc Data for V-44 Material

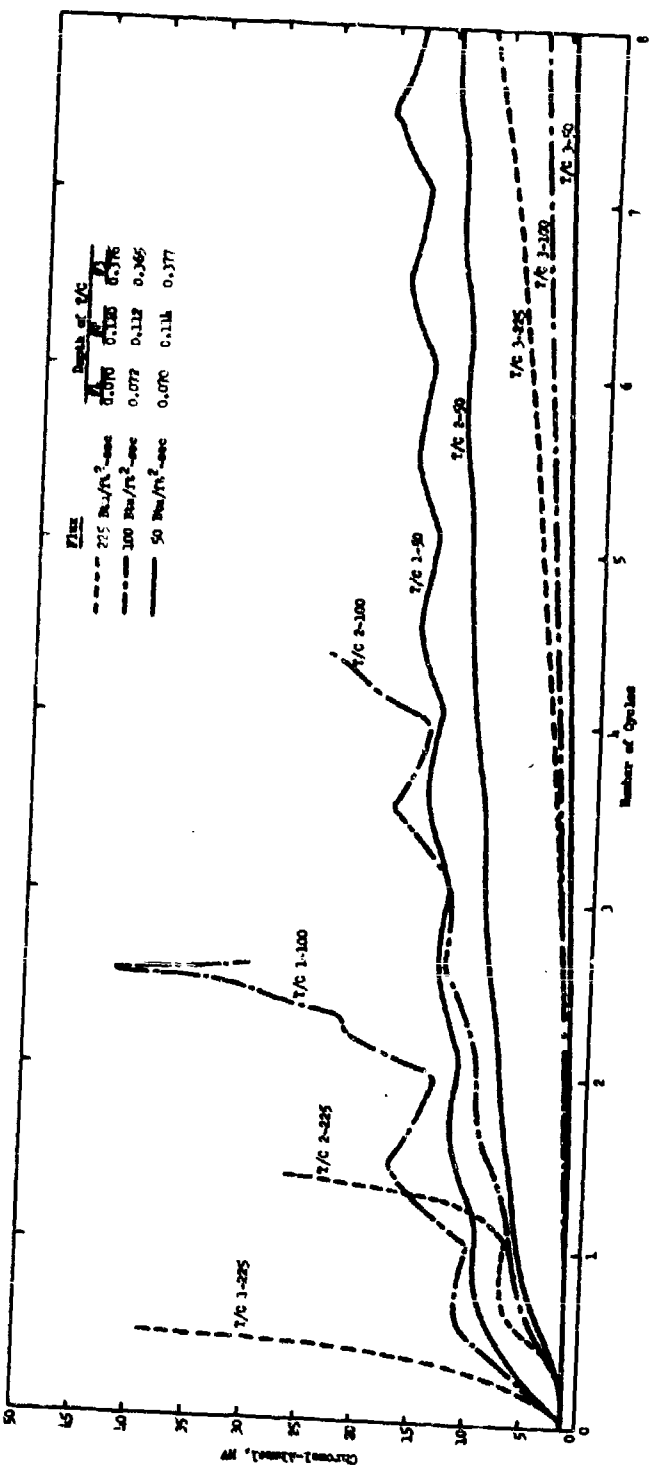

Figure 3. Temperature-Time Plasma Arc Data for 9790VI-126K Material

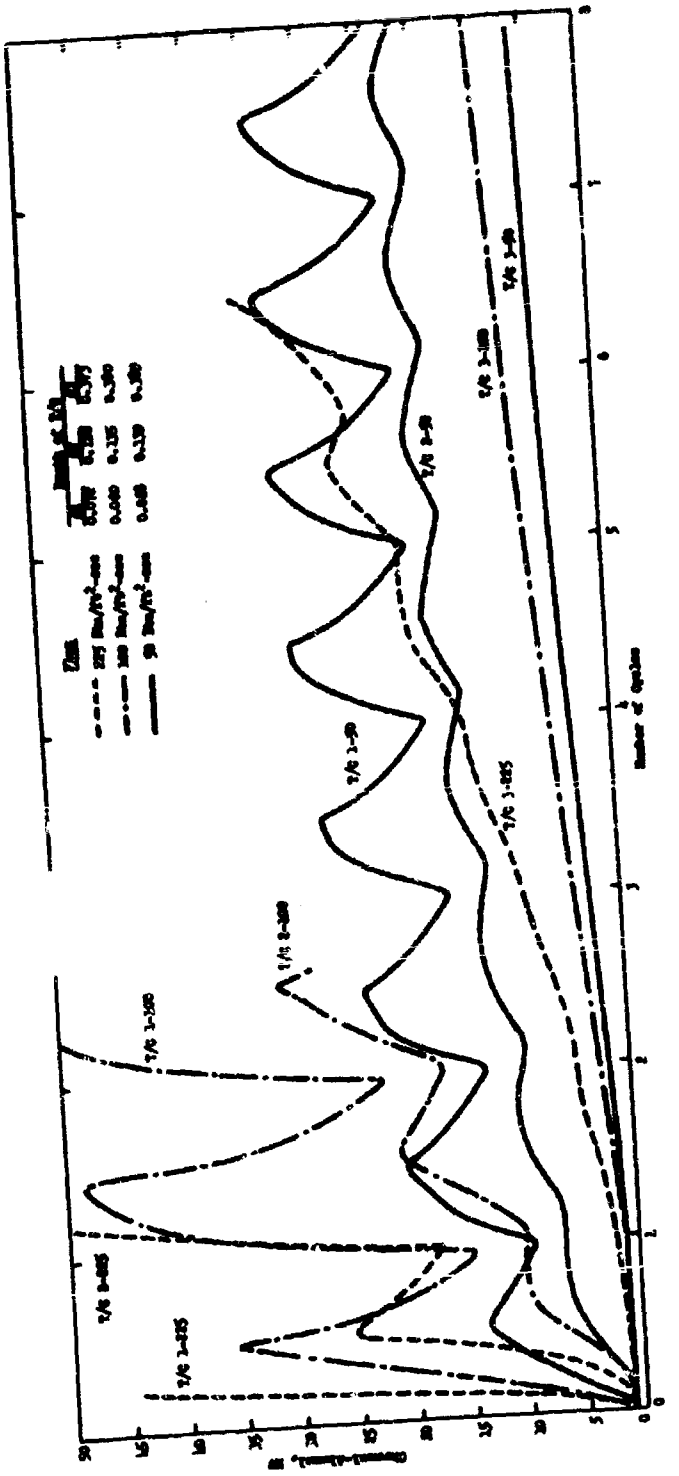

Figure 4. Temperature-Time Plasma Arc Data for MX-4737 Material

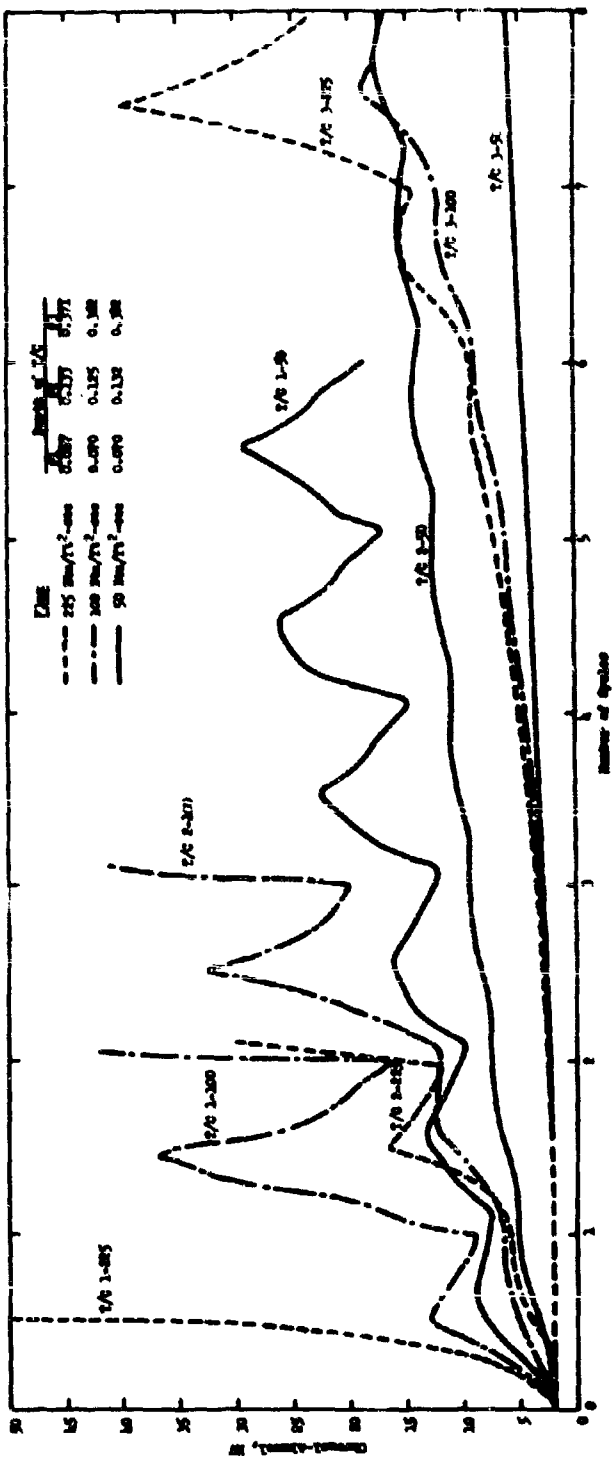

Figure 5. Temperature-Time Plasma Arc Data for V-61 Material

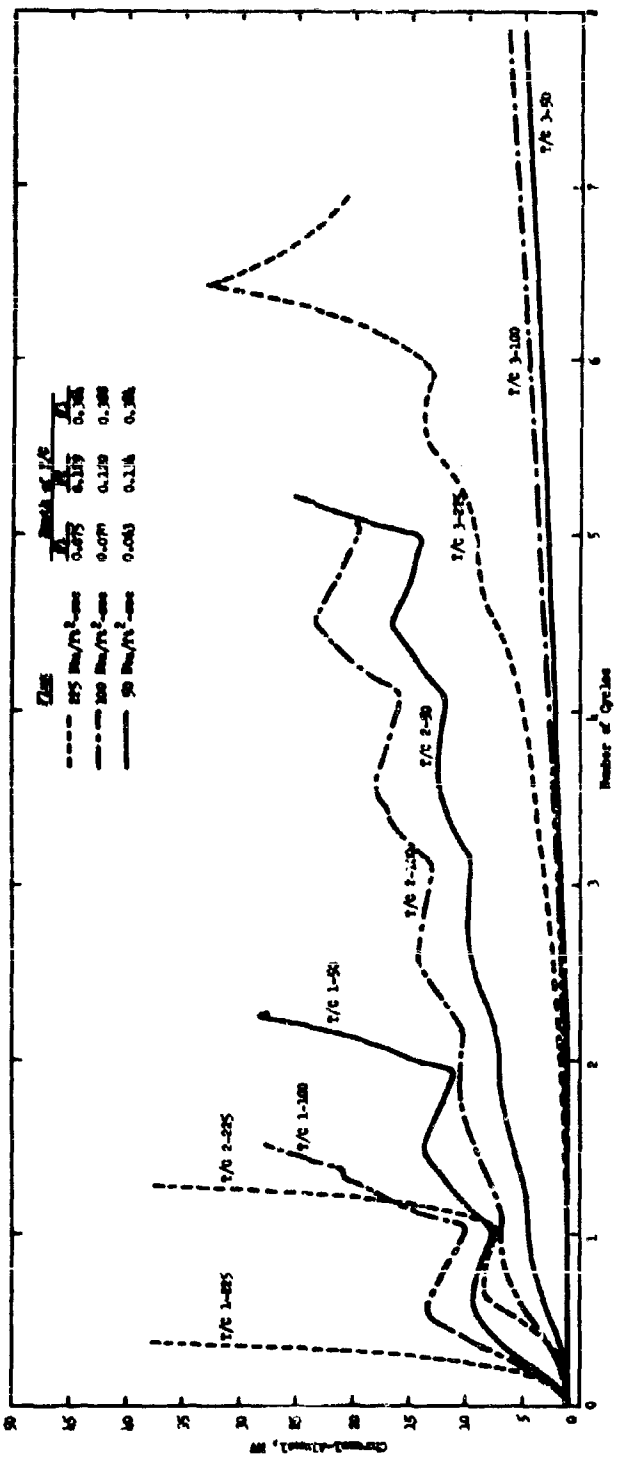

Figure 6. Temperature-Time Plasma Arc Data for V-51 Material

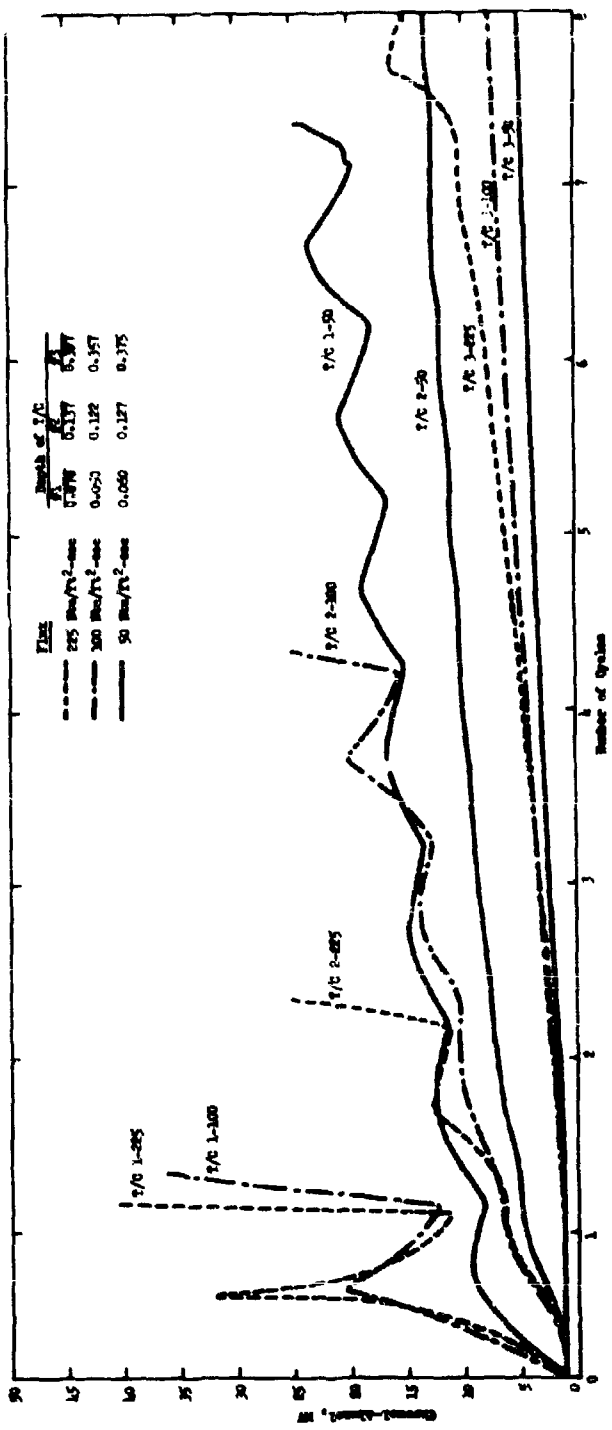

Figure 7. Temperature-Time Plasma Arc Data for V-50 Material

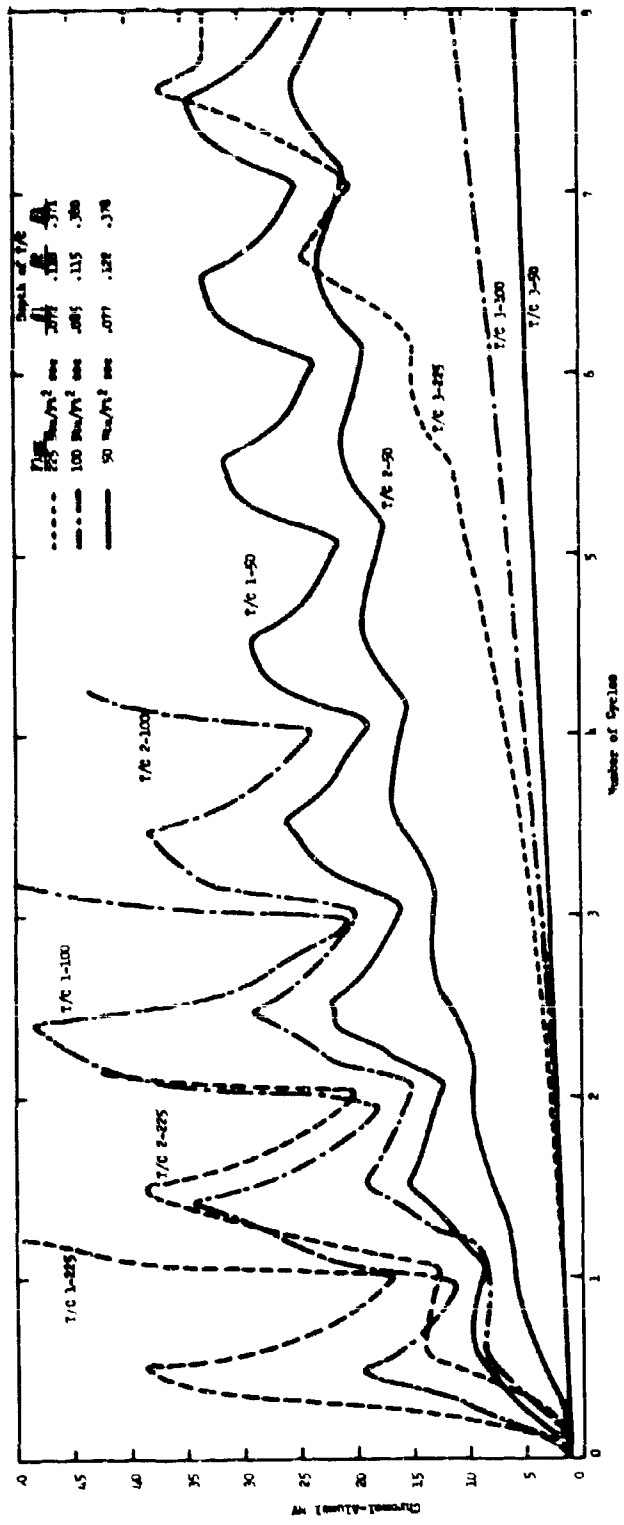

Figure 8. Temperature-Time Plasma Arc Data for SD 850-15C Material

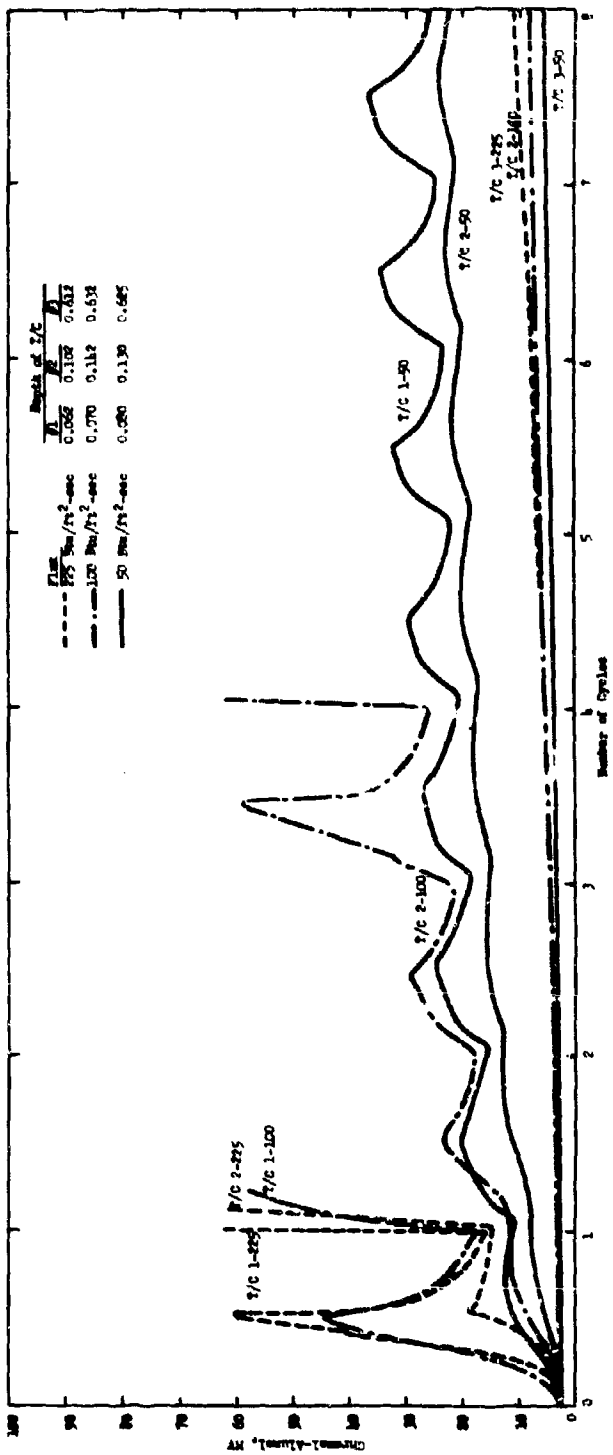

Figure 9. Temperature-Time Plasma Arc Data for 4OSA4O Material

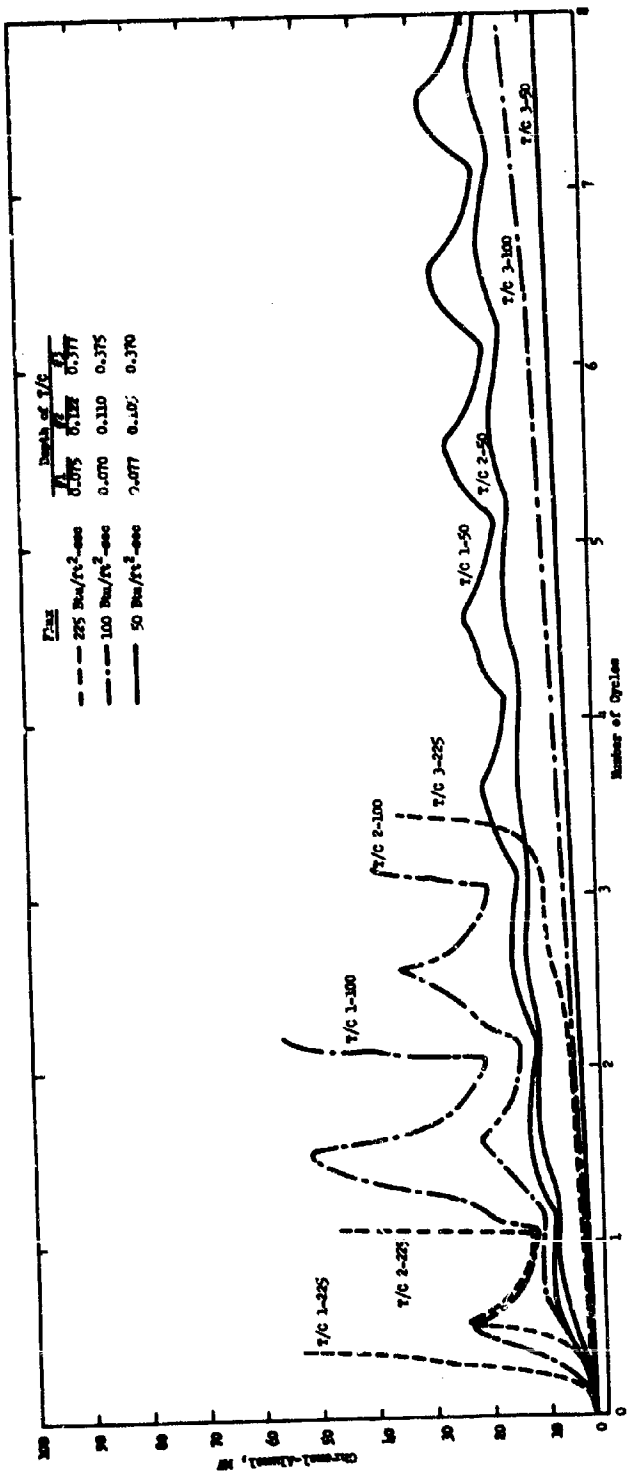

Figure 10. Temperature-Time Plasma Arc Data for 40SA2 Material

Figure 11. Temperature-Time Plasma Arc Data for USR-3800 Material

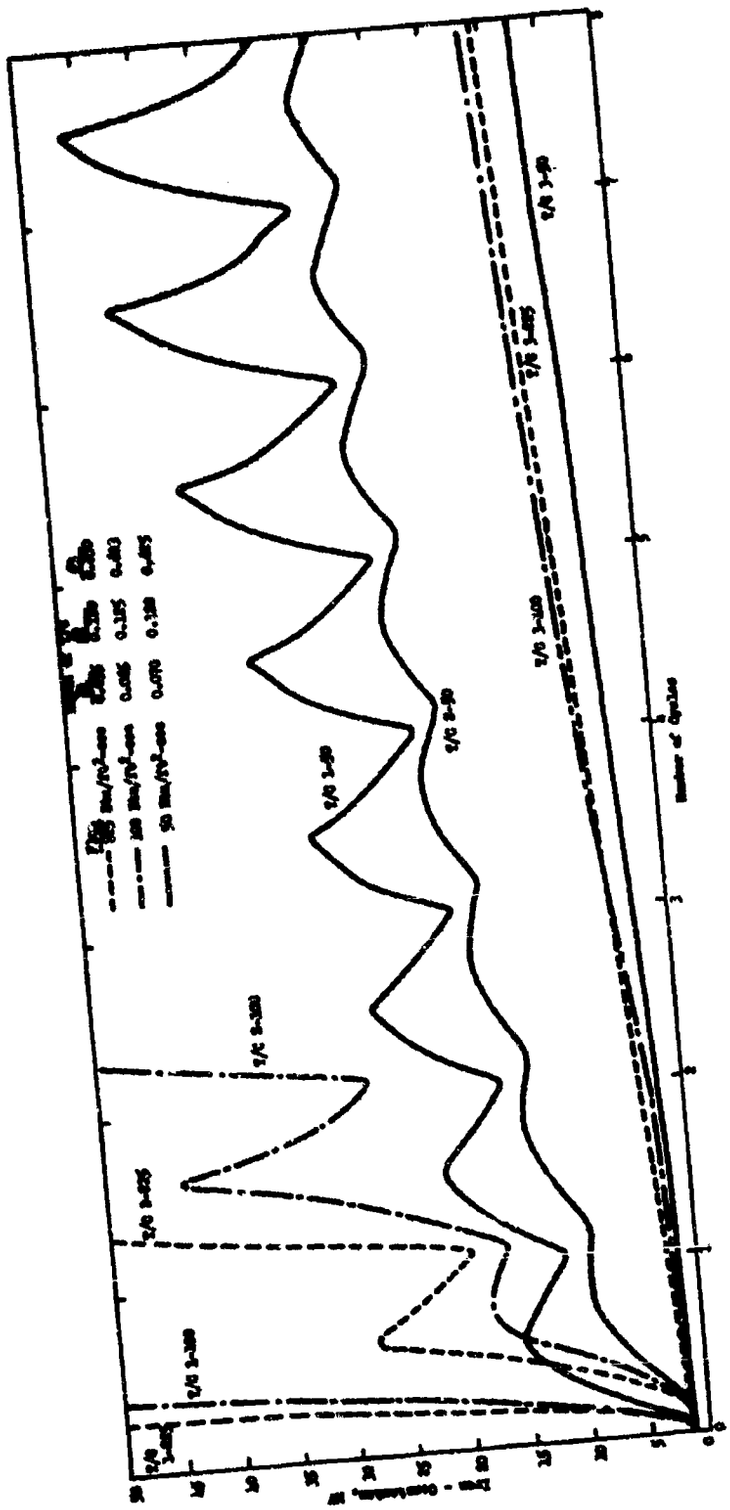

Figure 12. Temperature-Time Plasma Arc Data for USR-3804 Material

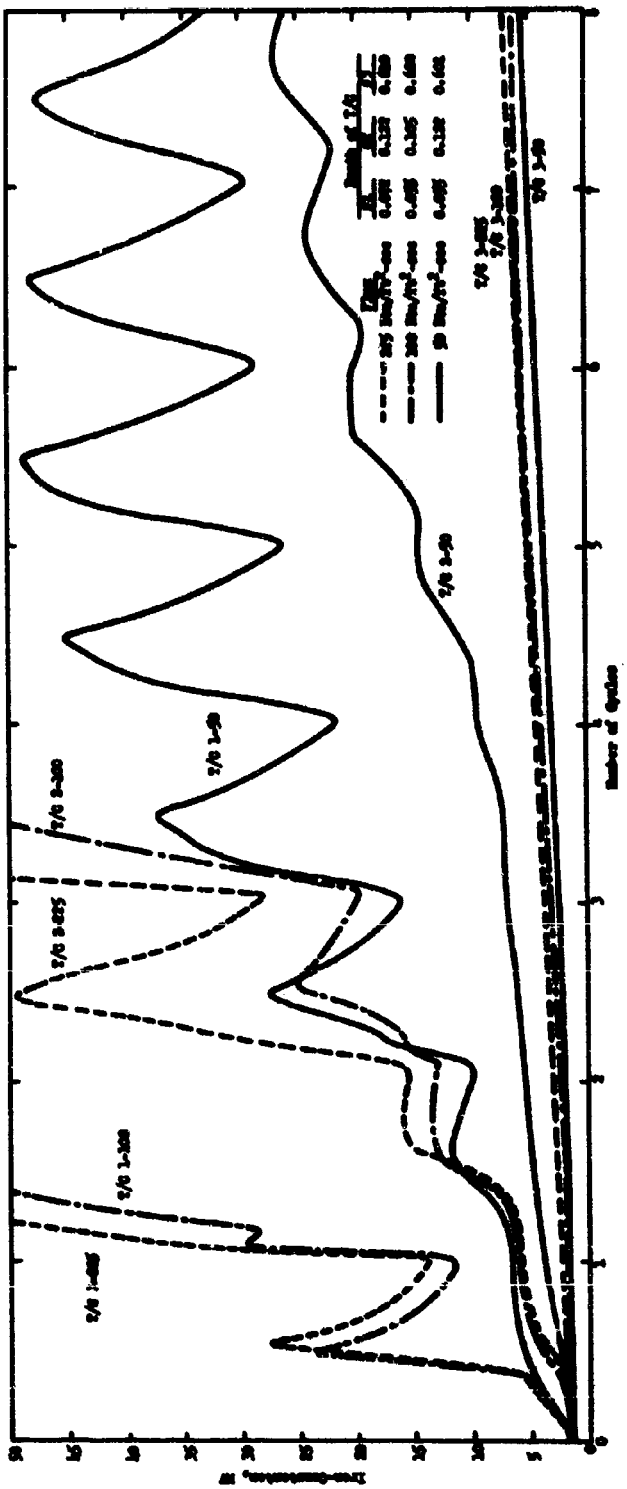

Figure 13. Temperature-Time Plasma Arc Data for H356 Material

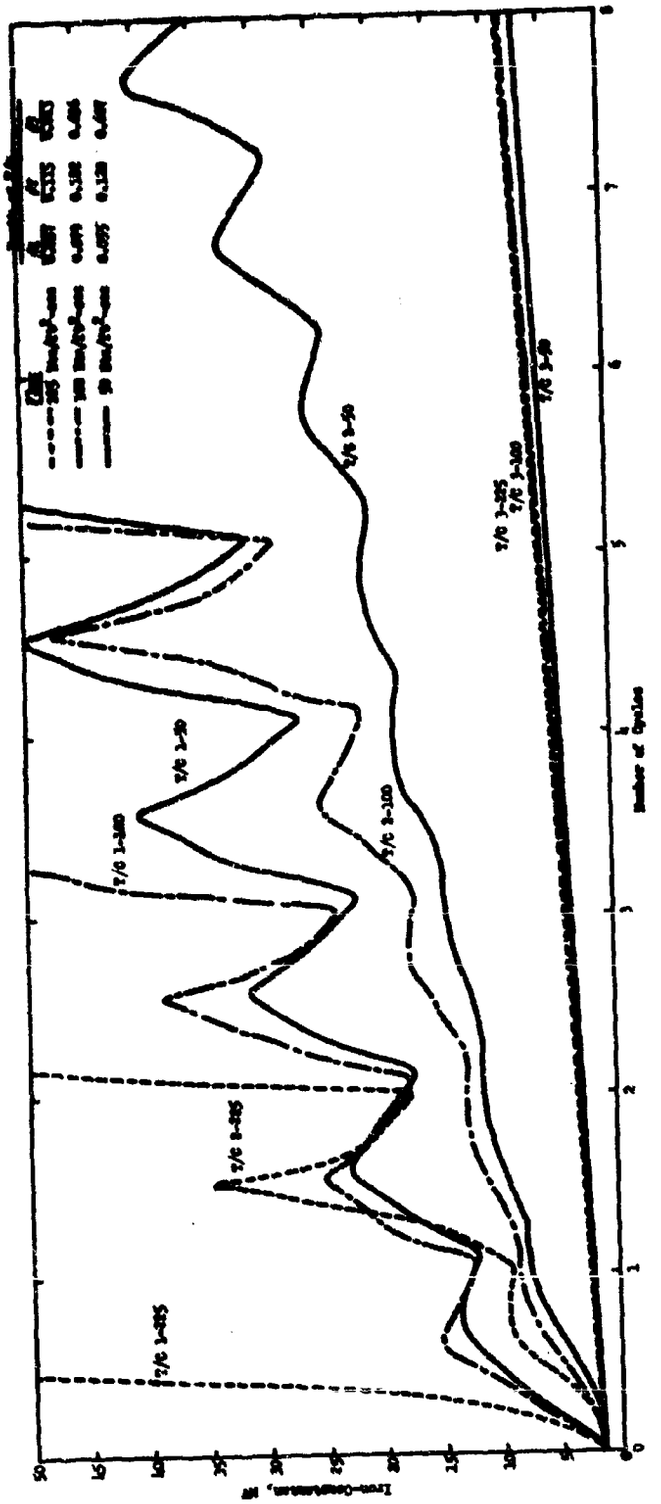

Figure 14. Temperature-Time Plasma Arc Data for SMR-81-15 Material

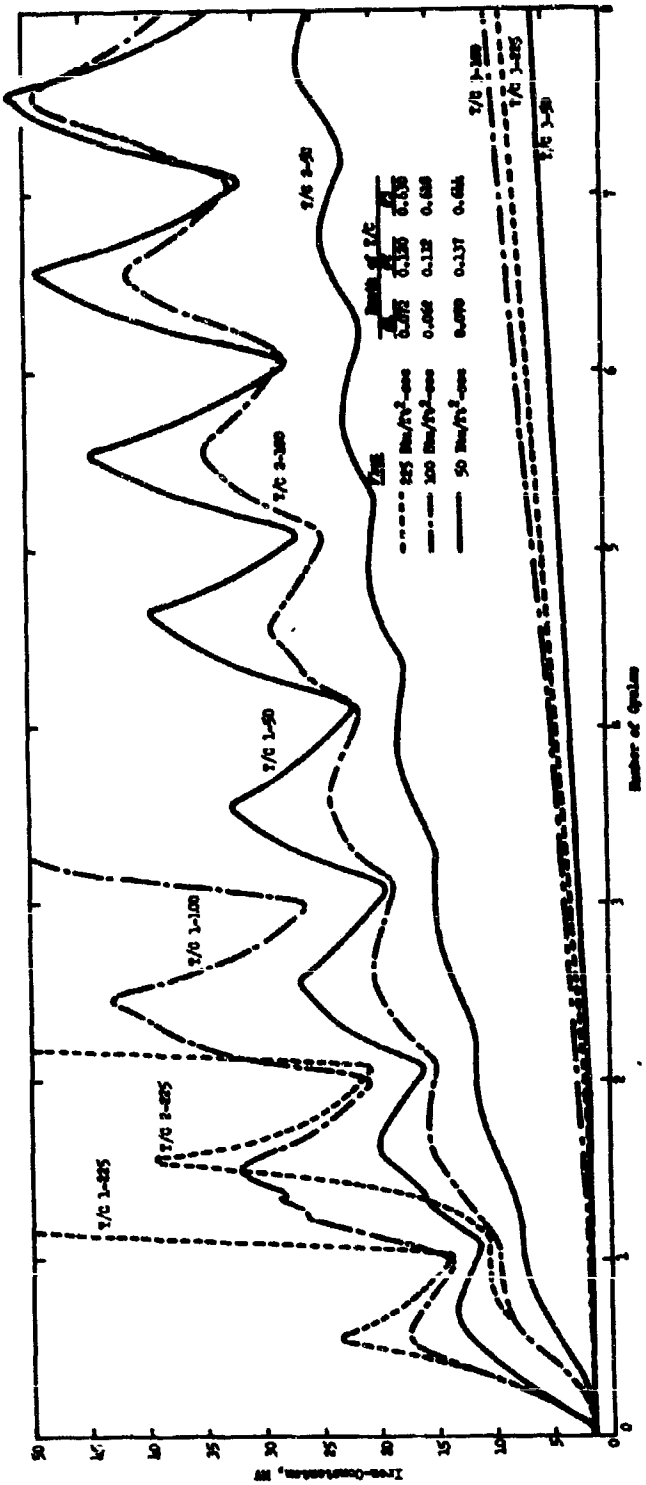

Figure 15. Temperature-Time Plasma Arc Data for SMR-81-8 Material

APPENDIX III

THROAT DIAMETER FOR CORRELATION MOTORS

I. THROAT DIAMETER REQUIRED FOR 700-psi NOMINAL OPERATING PRESSURE

$$A_t = \frac{\rho \times A_p \times r}{C_w \times P}$$

A_t - throat area

ρ - density = 0.0639 lb/cu in.

A_p - propellant area = 135.297 sq in. (13-1/8 in. dia)

r - burning rate = 0.365 in./sec at 700 psi

C_w - mass flow coefficient = 0.00626 l/sec

P - chamber pressure = 700 psi

$$A_t = \frac{0.0639 \times 135.297 \times 0.365}{0.00626 \times 700} = 0.720 \text{ sq in.}$$

Throat diameter = 0.960 in.

II. NOMINAL OPERATING PRESSURE WITH 1-in.-dia THROAT

$$P = \frac{\rho \times A_p \times r}{C_w \times A_t}$$

$$= \frac{0.0639 \times 135.297 \times 0.355}{0.00626 \times 0.785}$$

= 620 psi (too low, use 0.960-in. nominal throat diameter)

Report AFRPL-TR-67-33

UNCLASSIFIED

Security Classification

DOCUMENT CONTROL DATA - R&D

(Security classification of title, body of abstract and indexing annotation must be entered when the overall report is classified)

1 ORIGINATING ACTIVITY (Corporate author)
Aerojet-General Corporation
Sacramento, California 95809

2a REPORT SECURITY CLASSIFICATION
Unclassified

2b GROUP

3 REPORT TITLE
INVESTIGATION AND EVALUATION OF MOTOR INSULATION FOR MULTIPLE RESTART APPLICATION

4 DESCRIPTIVE NOTES (Type of report and inclusive dates)
First Phase Report 2 May 1966 to 15 January 1967

5 AUTHOR(S) (Last name, first name, initial)
Bradley, W.

6 REPORT DATE	7a TOTAL NO OF PAGES	7b NO OF REFS
January 1967	153	None

8a CONTRACT OR GRANT NO	9a ORIGINATOR'S REPORT NUMBER(S)
AF 04(611)-11609	AFRPL-TR-67-33
b PROJECT NO: N/A	9b OTHER REPORT NO(S) (Any other numbers that may be assigned this report)

10 AVAILABILITY/LIMITATION NOTICES
Foreign announcement and dissemination of this report by DDC is not authorized.

11 SUPPLEMENTARY NOTES	12 SPONSORING MILITARY ACTIVITY
None	Air Force Rocket Propulsion Laboratory Research and Technology Division Air Systems Command, Edwards, Calif.

13 ABSTRACT

The primary purpose of this program is to investigate the properties and behavior of elastomeric insulation materials during multiple restart conditions, and the influence of these properties on materials performance. During the first phase of work, tests were conducted to determine the five representative materials for correlation at a later date with motor performance. Designs, test firings, and performance analyses were completed for the three correlation motors (single-pulse, two-pulse, and three-pulse). The effects of heat soaking and thermal cycling on the lap shear strengths of insulation-case bonds were determined.

DD FORM 1473

UNCLASSIFIED

Security Classification

UNCLASSIFIED

Security Classification

14 KEY WORDS	LINK A		LINK B		LINK C	
	ROLE	WT	ROLE	WT	ROLE	WT
Insulation Candidates						
Multiple Restarts						
Properties of Insulation						
Motor Firings						
Heat Soak						
Thermal Cycling						

INSTRUCTIONS

1. ORIGINATING ACTIVITY: Enter the name and address of the contractor, subcontractor, grantee, Department of Defense activity or other organization (corporate author) issuing the report.

2a. REPORT SECURITY CLASSIFICATION: Enter the overall security classification of the report. Indicate whether "Restricted Data" is included. Marking is to be in accordance with appropriate security regulations.

2b. GROUP: Automatic downgrading is specified in DoD Directive 5200.10 and Armed Forces Industrial Manual. Enter the group number. Also, when applicable, show that optional markings have been used for Group 3 and Group 4 as authorized.

3. REPORT TITLE: Enter the complete report title in all capital letters. Titles in all cases should be unclassified. If a meaningful title cannot be selected without classification, show title classification in all capitals in parenthesis immediately following the title.

4. DESCRIPTIVE NOTES: If appropriate, enter the type of report, e.g., interim, progress, summary, annual, or final. Give the inclusive dates when a specific reporting period is covered.

5. AUTHOR(S): Enter the name(s) of author(s) as shown on or in the report. Enter last name, first name, middle initial. If military, show rank and branch of service. The name of the principal author is an absolute minimum requirement.

6. REPORT DATE: Enter the date of the report as day, month, year, or month, year. If more than one date appears on the report, use date of publication.

7a. TOTAL NUMBER OF PAGES: The total page count should follow normal pagination procedures, i.e., enter the number of pages containing information.

7b. NUMBER OF REFERENCES: Enter the total number of references cited in the report.

8a. CONTRACT OR GRANT NUMBER: If appropriate, enter the applicable number of the contract or grant under which the report was written.

8b, 8c, & 8d. PROJECT NUMBER: Enter the appropriate military department identification, such as project number, subproject number, system numbers, task number, etc.

9a. ORIGINATOR'S REPORT NUMBER(S): Enter the official report number by which the document will be identified and controlled by the originating activity. This number must be unique to this report.

9b. OTHER REPORT NUMBER(S): If the report has been assigned any other report numbers (either by the originator or by the sponsor), also enter this number(s).

10. AVAILABILITY/LIMITATION NOTICES: Enter any limitations on further dissemination of the report, other than those imposed by security classification, using standard statements such as:

(1) "Qualified requesters may obtain copies of this report from DDC."

(2) "Foreign announcement and dissemination of this report by DDC is not authorized."

(3) "U. S. Government agencies may obtain copies of this report directly from DDC. Other qualified DDC users shall request through _____."

(4) "U. S. military agencies may obtain copies of this report directly from DDC. Other qualified users shall request through _____."

(5) "All distribution of this report is controlled. Qualified DDC users shall request through _____."

If the report has been furnished to the Office of Technical Services, Department of Commerce, for sale to the public, indicate this fact and enter the price, if known.

11. SUPPLEMENTARY NOTES: Use for additional explanatory notes.

12. SPONSORING MILITARY ACTIVITY: Enter the name of the departmental project office or laboratory sponsoring (paying for) the research and development. Include address.

13. ABSTRACT: Enter an abstract giving a brief and factual summary of the document indicative of the report, even though it may also appear elsewhere in the body of the technical report. If additional space is required, a continuation sheet shall be attached.

It is highly desirable that the abstract of classified reports be unclassified. Each paragraph of the abstract shall end with an indication of the military security classification of the information in the paragraph, represented as (TS), (S), (C), or (U).

There is no limitation on the length of the abstract. However, the suggested length is from 150 to 225 words.

14. KEY WORDS: Key words are technically meaningful terms or short phrases that characterize a report and may be used as index entries for cataloging the report. Key words must be selected so that no security classification is required. Identifiers, such as equipment model designation, trade name, military project code name, geographic location, may be used as key words but will be followed by an indication of technical context. The assignment of links, rules, and weights is optional.

UNCLASSIFIED

Security Classification